New Light on Barrett's Esophagus

I.A. Boere

New Light on Barrett's Esophagus

I.A. Boere

New light on Barrett's esophagus.
Thesis, Erasmus University Rotterdam

Cover: Raman spectroscopic mapping of human Barrett's esophagus

New Light on Barrett's Esophagus

Nieuw Licht op Barrett Oesofagus

Proefschrift

ter verkrijging van de graad van doctor aan de

Erasmus Universiteit Rotterdam

Op gezag van de rector magnificus

Prof. dr. S. W. J. Lamberts

En volgens besluit van het College voor Promoties

De openbare verdediging zal plaatsvinden op

Vrijdag 15 september 2006 om 11.00 uur

door

Ingrid Alexandra Boere

geboren te Gouda

Promotiecommissie:

Promotor: Prof.dr. H.W. Tilanus

Overige leden: Prof.dr. E.J. Kuipers
Dr.ir. H.J.C.M. Sterenborg
Prof. J.H.P. Wilson

Co promotor: Dr. R.W.F. de Bruin

CONTENTS

Chapter 1

Introduction

Photodynamic therapy using 5-aminolevulinic acid for Barrett's esophagus

I.A. Boere, J. van den Boogert, R. van Hillegersberg, H.W. Tilanus, R.W.F. de Bruin

Department of Surgery, Erasmus Medical Center Rotterdam

ABSTRACT

The incidence of esophageal adenocarcinoma is steadily increasing in many western countries in the last 30 years. It is believed that the majority of the adenocarcinomas arise in Barrett's esophagus, following a sequence of metaplasia through dysplasia to carcinoma. At present, both endoscopic surveillance and esophageal resection are recommended for patients with Barrett's esophagus and high-grade dysplasia. Photodynamic therapy (PDT) with 5-aminolevulinic acid (ALA) is a new treatment option ideally leading to endoscopic ablation of the premalignant Barrett's mucosa. Administration of ALA, an endogenously occurring intermediary in the haem biosynthetic pathway, leads to accumulation of the photoactive agent protoporphyrin IX (PpIX) in the target tissue. Subsequent irradiation with light of a proper wavelength absorbed by the photosensitizer, results in a photochemical reaction that destroys the sensitized tissue. ALA induced PpIX accumulates in tumor tissue, glands and cells that line surfaces. Previously, we studied the pharmacokinetics of ALA administered orally and intravenously in rats, by protein and porphyrin measurements and fluorescence microscopy. ALA concentration was highest in the kidney, bladder and urine and in the jejunum. Porphyrins accumulated mainly in duodenal aspirate, jejunum, liver and kidney. In rats with Barrett's esophagus, the selectivity of ALA-induced PpIX accumulation lies in the difference between the epithelium and the muscle layers. The illumination and the position of the laser fiber further determine the selectivity of the treatment. The irradiation parameters determine to a great extent the results of ALA-PDT. The first important factor is the time interval between ALA administration and subsequent illumination. For the esophagus there is a narrow time interval in which illumination should be performed. Illumination at 2 h after oral administration of ALA resulted in maximal epithelial damage, whereas illumination at 4, 6 or 12 h resulted in esophageal dilatation, functional impairment and less epithelial damage. Second, the laser parameters wavelength, total light dose and power output need to be chosen accurately. A wavelength of 633 nm combined with a relatively low power output dramatically increased the induced epithelial damage in the esophagus, compared to a high power output or 532 nm light. The results from the presented studies cannot be translated directly to the human situation, since the irradiation parameters are different in man and rat. But important information regarding pharmacokinetics, mechanism, optimization and caveats of ALA-PDT can be obtained.

BARRETT'S ESOPHAGUS

Definition

Norman Barrett, a British surgeon published in 1950 a report in which he described ulcers in the distal part of the esophagus lined by columnar epithelium (1). He believed that this was a tubular segment of the stomach of patients with a congenitally short esophagus. Now, it is generally thought that he described the lower esophagus lined with columnar epithelium; an entity which is now called Barrett's esophagus (BE). BE is defined as the presence of metaplastic, intestinal columnar mucosa, characterized by goblet cells in the esophagus. In contrast, the normal esophagus is lined with squamous epithelium. BE is therefore diagnosed on biopsies obtained during endoscopy. BE is currently classified into three groups, depending on the length of the metaplastic segment: long-segment BE (LSBE; >3 cm), short-segment BE (SSBE; <3 cm) and intestinal metaplasia of the cardia or gastro-esophageal junction, which may be a different entity.

Origin

BE probably originates from a multipotent undifferentiated stem cell of esophageal origin (2). However the pathogenic stimuli that cause metaplasia in case of BE are not yet fully determined. Usually, BE is found in patients who are examined with endoscopy, because of gastro-esophageal reflux disease (GERD) on the basis of a defective lower esophageal sphincter or hiatal hernia. A long history of severe GERD predisposes to BE and usually males are affected (3, 4). Other risk factors include obesity and asthma (3, 5, 6).

Prevalence

The true prevalence of BE is difficult to determine, both in the general population as well as in patients with GERD, since BE itself does not cause any symptoms. There is a strong association of gastrointestinal reflux symptoms and presence of BE, but many patients with these symptoms don't enter the medical system nor are they screened for BE. In order to estimate the entire population prevalence of BE, autopsy findings were compared with clinical data in a study at the Mayo Clinic. It appeared that only one of 20 patients with BE was clinically diagnosed. On the basis of these findings, the estimated prevalence in the general population is 1% (7). The prevalence of BE in patients with GERD who underwent endoscopy, varies greatly among the different populations. In

Spain it was reported as low as 0.53%, in Germany 4.6%, in Taiwan 2%, in Brazil 3.5%. In different studies in the US it varied between 3.5 to 12.4% (3, 8-11).

Risk of esophageal cancer

There is a well-established association of BE and adenocarcinoma of the esophagus. It is believed that adenocarcinoma develops following a sequence of metaplasia through dysplasia (12). Many adenocarcinomas arise in a BE (13)and BE is detectable in 21-37% of adenocarcinomas (14). Over the past 20-30 years there has been an enormous increase in the incidence of adenocarcinoma of the esophagus as well as in the recognized prevalence of BE in the general population (15-17) This increase cannot only be explained by the fact that more endoscopies are performed today using well defined biopsy protocols. This development raises special interest in therapies with acceptable morbidity and mortality, which can eliminate the cancer risk sufficiently.

Management

Management of BE currently depends on the presence of dysplasia in biopsies. Dysplasia is defined as Barrett's epithelium with architectural or cytological abnormalities, such as increased numbers of mitosis and a high nucleus/ cytoplasm ratio (18). BE without dysplasia is treated with antireflux-surgery or with acid-inhibitors, usually an H-2 receptor blocker or a protonpump inhibitor. Only relief of the symptoms of GERD is achieved. Besides antireflux therapy, patients are advised to undergo endoscopy once every 2 years. Low-grade dysplasia (LGD) is monitored by endoscopy every ½ -2 years. Additionally in study protocols, ALA-PDT is currently performed for LGD (19). Management of high-grade dysplasia (HGD) is controversial. Many authors advise esophagectomy for HGD, because 10-70% of HGD harbor an invasive adenocarcinoma. In contrast, Schnell et al (20) advise an intensive endoscopy and biopsy protocol for HGD, as they found HGD harboring cancer in 12% of the cases and an incidence of adenocarcinoma of 16% for HGD during mean 7 years of follow up. Besides esophagectomy, HGD is a playing field of several experimental therapies, which aim at the ablation of the metaplastic and dysplastic epithelium and thereby eliminating the cancer risk with less invasive techniques. Among these experimental therapies are endoscopic mucosa ablation therapy using snare polypectomy, multipolar electrocoagulation, thermal therapy using Nd:YAG laser or Argon Plasma Beam laser and PDT (21).

ALA-PDT FOR BARRETT'S ESOPHAGUS

At present PDT for BE is performed in clinical trials on selective patient groups with Photofrin and ALA as photosensitizers (22-26). Additionally, PDT is performed in animal studies. In our centre, ALA-PDT is studied in rats with and without BE. The disadvantages of using a rat model for ALA-PDT and for BE are clearly that any results obtained from these studies cannot directly be translated into the clinical setting. Rat esophagus differs from human esophagus not only in size and thickness, but also in anatomy and histology. The rat esophagus is lined by keratinized squamous epithelium, whereas the human esophagus is lined by non-keratinized squamous epithelium. The rat esophagus lacks the submucosal glands that are found in the human esophagus and rats do not have a gall bladder. Most important, the optimal laser parameters are different in man and rat. However, using rat models has the advantages of an experimental setting, in which individual laser parameters can be evaluated in a homogenous group. Also, the entire esophagus can be examined, in contrast to the clinical setting, where biopsies are taken. Therefore, we will discuss ALA-PDT in a rat model.

ALA is a natural occurring intermediary in the haem biosynthetic pathway, in which the photoactive agent protoporphyrin IX (PpIX) is formed. When ALA is administered, the rate limiting enzyme in this pathway, ALA synthase is bypassed and thus intracellular accumulation of photosensitizing concentrations of PpIX are formed. Several mechanisms are thought to induce porphyrin accumulation: intracellular PpIX synthesis, uptake of PpIX produced in the liver after either absorption in the gastro-intestinal tract or direct entrance into the systemic circulation, and uptake of PpIX from production elsewhere. Ideally, ALA accumulates selectively in the target tissue, but the preferential accumulation of ALA-derived PpIX in tissues appears to be related to the tumor model used and the tissue characteristics, time, ALA dose and route of administration. ALA induced PpIX accumulates also in glands and tissues that line surfaces, such as gastrointestinal mucosa.

Knowledge about the pharmacokinetics of ALA and the preferential accumulation of PpIX is important. The pharmacokinetics of ALA and PpIX in the rat esophagus and other organs were investigated by biochemical analysis and fluorescence microscopy. These studies were also performed in rats with BE. Additionally, factors that may

influence porphyrin accumulation were studied. Figure 1 shows the formation and degradation of PpIX. Porphobilinogendeaminase (PBGD) is an enzyme that may be rate limiting in the PPIX synthesis, when ALA is administered exogenously. Ferrochelatase is the porphyrin-degrading enzyme, which converts the photochemically active PpIX into the photochemically inactive haem by incorporating ferrous iron. Thus, the accumulation of PpIX is also determined by the activities of PBGD and ferrochelatase and the availability of iron.
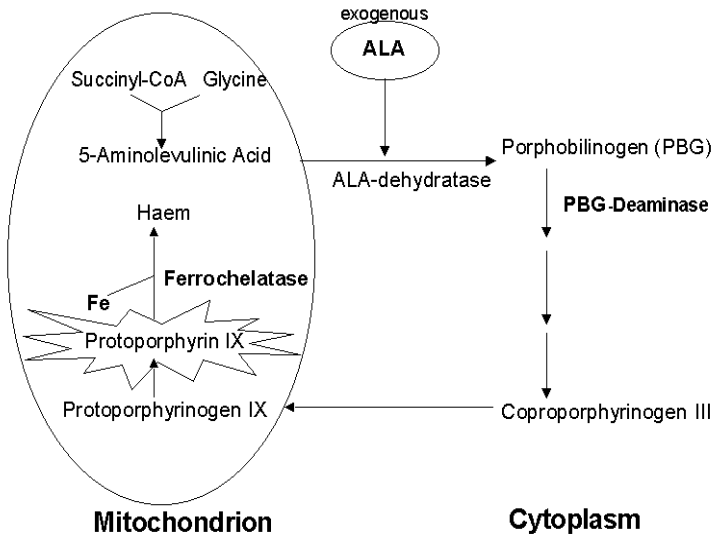
Figure 1 Haem biosynthetic pathway (27)

PDT induced damage depends on several parameters. They include the formation of PpIX from ALA, the timing of illumination after ALA administration, the wavelength of the light delivered, the output and total light dose, the blood flow and the availability of oxygen. The penetration depth of red light is deeper than the penetration depth of green light. Red light may therefore cause muscle damage to the esophagus besides epithelial damage. Fractionated illumination theoretically has some advantages over continuous light delivery. It permits the use of newly synthesized PpIX in the dark interval between the illuminations. Also, fractionation may have a positive influence on the oxygen supply needed for the PDT effect, by delaying vascular shutdown.

Pharmacokinetics of ALA and PPIX

In rats, the ALA and porphyrin concentrations after either oral (p.o.) or intravenous (i.v.) administration of ALA were measured in various organs (28). Porphyrin localization

within tissues was determined using laser scanning microscopy. Additionally, liver and renal function tests were performed to determine toxicity. The highest levels of ALA were reached in kidney, bladder and urine and after oral administration of ALA also in jejunum. In the stomach, duodenal aspirate, jejunum and kidney, ALA concentrations were higher after p.o. than after i.v. ALA administration. However, there was no difference in the porphyrin peak concentrations and total accumulation in these organs between the i.v. and the p.o. groups. Three hours after ALA administration, some ALA was still present in duodenal aspirate, jejunum, spleen, kidney and bladder and after p.o. ALA administration also in the stomach; therefore these organs may function as an ALA depot. After i.v. ALA administration, ALA is also found in duodenal aspirate and the peak concentration of ALA in jejunum was reached later than in other tissues, this suggests the possibility of an enterohepatic circulation as a source of ALA. ALA administration caused no elevation of ALAT and ASAT in the p.o. group and renal function tests showed only a mild transient elevation of creatinine. The photoactive porphyrins accumulated mainly in liver, jejunum, kidney and duodenal aspirate and were much lower in plasma, muscle, skin, fat and brain. Three hours after oral ALA administration, fluorescence by porphyrin accumulation was most pronounced in epithelial linings of the tongue, esophagus, jejunum, colon, bladder, prostate, and pancreatic duct. Control rats showed only autofluorescence on the luminal surface of the keratin layer of the tongue and esophagus and in the colic lumen. By evaluating the ALA and porphyrin concentrations during the given time course, it appeared that in situ synthesis of porphyrins is more likely than uptake of PpIX from the blood, since peak concentrations of porphyrins were found between 2 and 4 h in the p.o. group and between 1 and 3 h in the i.v. group, while porphyrins were detectable in urine after 4 h. Furthermore, the liver is unlikely to be the main supplier of PpIX, since peak porphyrin concentration in the liver appeared later than in other tissues. In conclusion, systemic and oral administration of ALA resulted in photosensitive concentrations of porphyrins in all tissues except muscle, fat, skin and brain. Fluorescence microscopy showed low porphyrin fluorescence in fat and muscle, while epithelial linings showed strong porphyrin fluorescence.

ALA kinetics and PPIX formation in normal and in Barrett's esophagus
The kinetics and localization of ALA induced porphyrin accumulation in the normal rat esophagus and BE were studied (29). Additionally, ALA and iron concentrations were

determined in the different layers of the normal esophagus. The localization and concentration of ALA-induced porphyrin accumulation in Barrett's and adjacent normal esophagus were studied using laser-scanning microscopy. Maximal ALA concentrations in mucosa (2 nmol mg^{-1} protein) and muscular layer (1 nmol mg^{-1} protein) were reached at 1 h after ALA administration. (Figure 2) In the mucosa, the peak ALA and porphyrin concentrations and fluorescence were higher than in muscularis. ALA concentration declined fast, with a half-life of approximately 1 h, and was at background levels at 4 h after administration. The maximal selectivity for mucosa was found at 2 h after ALA administration, when porphyrin levels were approximately 3.5 times higher in mucosa than in muscularis. At 6 h after administration of ALA, porphyrin levels had decreased to basal levels. No selectivity of PpIX accumulation in Barrett's epithelium over adjacent squamous epithelium could be detected.
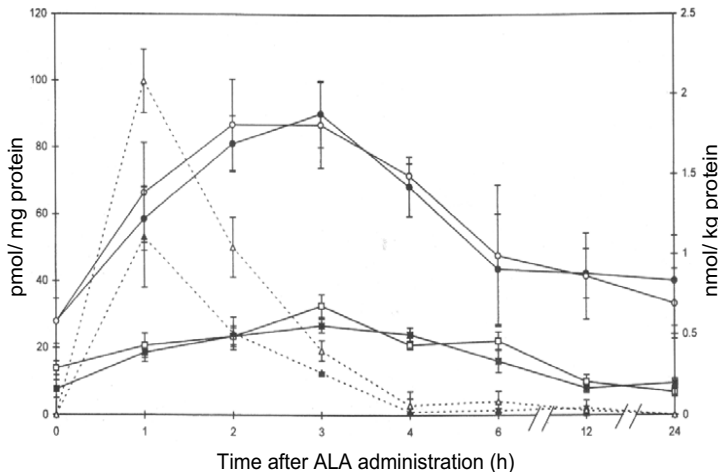
Figure 2 Extracted porphyrin levels (solid lines, left axis) and tissue ALA concentration (dashed lines, right axis) after administration of 200 mg kg^{-1} ALA by different routes. Each point indicates the mean level of 3 rats ± standard error of the mean. The ALA and porphyrin levels of control rats are given at 0 h. O = mucosa, i.v. ALA; ● = mucosa, oral gavage; □ = muscularis, i.v.; ■ = muscularis, oral gavage; Δ = ALA concentration in esophageal mucosa; ▲ = ALA concentration in esophageal muscularis.

Figure 3 shows fluorescence images with the corresponding haematoxylin and eosin (HE) sections. The activity of the porphyrin-converting enzyme ferrochelatase was equal in both the mucosa and muscular layer, but the activity of the porphyrin-forming enzyme

PBGD was 2-fold higher in mucosa than in muscularis. Iron concentration was significantly lower in the mucosa than in the muscularis. These experiments show that ALA-induced PpIX does not selectively occur in Barrett's mucosa. However, 3.5 times higher fluorescence levels were reached in the mucosa compared to the muscularis. Therefore, ALA seems a useful photosensitizer, which allows selective destruction of the mucosa rather than the muscularis, and which therefore may not cause esophageal stenosis as is seen with other photosensitizers. The possible underlying mechanisms of the selectivity of PDT for the mucosa may be the higher uptake of ALA in the mucosa compared to the muscularis, a higher PBGD/ ferrochelatase ratio in the mucosa, the lower iron storage of epithelium cells, and a high metabolic activity of endothelial cells.
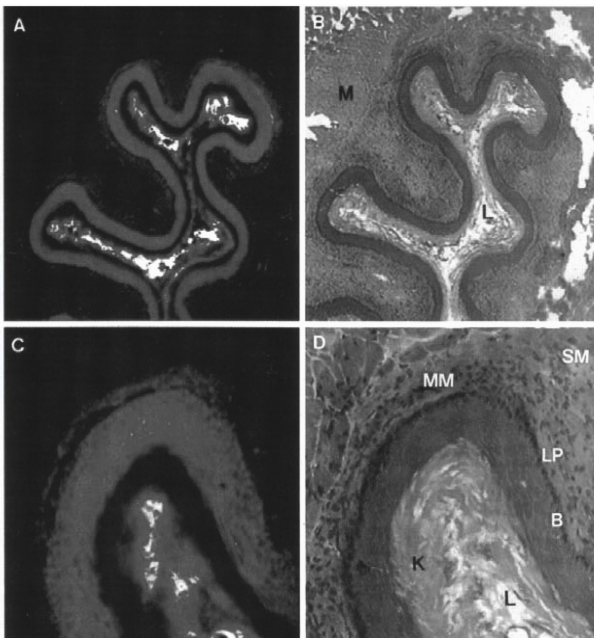
Figure 3 Fluorescence image (A) of a frozen section (10 µm) of a normal rat esophagus, 3 h after i.v. administration of ALA (200 mg kg^{-1}), together with corresponding section stained with HE (B). Fluorescence image (C) and corresponding HE section (D) of the same section at higher magnification. B, mucosal basal cell layer; K, keratin layer; L, lumen; LP, lamina propria; M, muscularis; MM, muscularis mucosae; SM, submucosa.

Timing of illumination

In this study the optimal timing of illumination after ALA-administration is determined, by evaluating the extent of mucosal ablation, damage to muscle layers and the impact on

esophageal healing (30). Illumination was performed at 1, 2, 3, 4, 6 or 12 h after ALA administration with 633 nm light. The output was 100 mW cm^{-1} diffuser, the total light dose 22.7 J cm^{-2} tissue. Almost complete ablation of epithelium in all animals was only found when rats were treated 2 h after oral administration of 200 mg kg^{-1} ALA. However, small areas of epithelial cells showing mitotic activity remained after treatment. When animals were illuminated at 1, 3, 4, 6 or 12 h after ALA, the esophageal epithelium was usually undamaged, whereas damage to the submucosa, muscularis and serosa was always present. Illumination at 4, 6 or 12 h resulted in esophageal dilatation, functional impairment and subsequent weight loss. Immunohistochemical staining in the latter groups showed a significant correlation between esophageal dilatation and loss of Schwann cells in the myenteric plexus in the muscularis propria, which suggests a PDT induced peripheral neuropathy causing dilatation at the treatment site. Both the effectiveness and the safety of ALA-PDT for esophageal lesions depend significantly on the time between ALA administration and illumination. The most selective effect was reached 2 h after ALA administration, when illumination resulted in a complete mucosal ablation without significant damage to the underlying muscle coat. The kinetics of ALA during time were also studied in man, Ackroyd et al showed that porphyrins reached maximal levels in the esophagus, preferentially in the mucosa, 4-6 h after oral administration of ALA (31).

Laser parameters

This study aimed to find the illumination parameters for selective and complete epithelial damage by varying the power output and total light dose applied in the normal rat esophagus (32). When PDT causes damage to the underlying muscle layer or nerve tissues, esophageal dilatation and functional impairment may be the result. Therefore we compared red light, 633 nm, with green light, 532 nm. Light with a shorter wavelength has a lesser penetration depth. Additionally, fluorescence of the esophageal wall was measured during illumination and light dosimetry was performed. Illumination was performed at 3 h after oral ALA administration with either 8.3 or 25 J applied with 33, 100 or 300 mW cm^{-1} diffuser. Animals were sacrificed at 48 h after PDT. Damage caused by PDT was scored semi-quantitatively on H&E stained sections on a scale from 0 to 3 for each separate esophageal layer. (Table 1) Given a fixed total light dose, most selective esophageal epithelial damage was achieved with 33 mW cm^{-1} illumination, while a higher output resulted in damage to the muscularis propria with less

damage to the epithelium. The most selective epithelial damage was found with 633 nm light and a light dose of 8.3 J with 33 mW cm^{-1} output, most complete epithelial damage was found after applying 25 J with 33 mW cm^{-1} output.

Lightdose (J)	Power (mW)	Epithelium	Submucosa		Muscularis propria		SF [^]
			edema	inflam	inflam	necrosis	
8.3	33	2.0±0.6	2.0±	1.4±0.5	0.8±0.4	0.4±0.2	3.7±0.7 *
	100	0.8±0.6	2.2±0.2	1.4±0.2	2.0±0.3	1.2±0.2	0.6±0.2
	300	0	0.8±0.4	0.8±0.2	0.6±0.2	0.6±0.2	0
25	33	2.8±0.2	2.6±0.2	2.2±0.4	3.0±0	2.4±0.2	1.1±0.1
	100	1.6±0.6	2.8±0.2	1.2±0.2	2.6±0.4	2.4±0.6	0.5±0.1
	300	0.8±0.6	0.8±0.6	1.2±0.2	2.0±0.3	2.2±0.3	0.4±0.1

Table 1 Histopathological changes of the esophageal wall 48 h after ALA-PDT in different groups, treated with 633 nm light. Mean damage scores of the layer ± standard error of the mean on a scale from 0 to 3 are shown (0: normal or no inflammation, 3: complete ablation, >2 inflammatory cells per grid or <25% vital muscle). ^SF = selectivity factor of epithelial damage; epithelial damage score / muscular damage score, expressed as mean ± standard error of the mean. *Selectivity factor is significantly higher ($P<0.05$) compared with all other 633 nm groups. (Inflam = inflammation)

Figure 4 shows the histologic characteristics of a rat esophagus at the PDT site after 633 nm illumination with 33 mW and 8.3 J (Figure 4A) and 25 J (B). Whereas red light resulted in some macroscopic liver damage, this was not seen using green light. Using the same parameters, light with a wavelength of 532 nm resulted in much less damage, both to the mucosa and to the muscularis. Application of 8.3 J did not cause any epithelial or muscular damage, but only caused edema and inflammation of the submucosa. Treatment with 25 J resulted in complete ablation of the mucosa only in a few animals.

When dosimetry was performed during optical irradiation, the measured true fluency rate (scattered plus non-scattered light) at the surface compared to the given output was 2 times higher in the 633 nm group than in the 532 nm group. Thus, when the damage in the 633 nm light group was compared with the damage in the 532 nm light group with a comparable true light dose, there were no differences in epithelial or muscular damage. Earlier studies by Van Staveren et al (33) showed that the true fluency rate in hollow organs is larger than the calculated incident fluency rate due to strong light scattering nature of the tissue. These tissue characteristics can be used for improving the therapeutic effect.
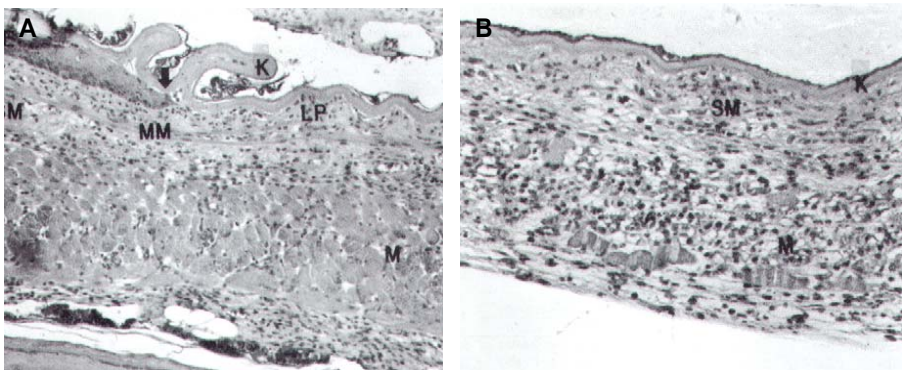
Figure 4 Histologic characteristics of a rat esophagus at the PDT site after 633 nm illumination with 33 mW cm^{-1} and 8.3 J (A) and 25 J (B). The arrow in panel A indicates the beginning of the illuminated area (from arrow to the right), showing very selective and complete loss of epithelium, whereas the muscular layer was not damaged. Long illumination (B) caused, besides loss of epithelium, severe damage to the muscularis propria. E = epithelium, K = keratin layer, LP = lamina propria, M = muscularis propria, MM = muscularis mucosae, SM = submucosa (x40, HE stain)

Fractionated Illumination

In an attempt to further increase the efficacy of ALA-PDT for the esophagus, fractionated light delivery was investigated (34). Various hypotheses support the assumption that fractionation increases the PDT effect. First, applying fractionated light doses as compared to continuous illumination may delay vascular shutdown and vasoconstriction (25, 35). Second, using longer fractionation intervals (1-3 h), new porphyrins can be synthesized from the ALA that is still present. Reappearance of porphyrin fluorescence has been demonstrated several hours after the first illumination,

resulting in a renewed photosensitization (36-39). Third, since exogenous ALA bypasses the negative feedback mechanism, resulting in the accumulation of PpIX in certain cells and tissues, one could assume a difference in the activity of certain enzymes of the haem biosynthetic pathway. Ferrochelatase may be the next rate limiting enzyme in the synthesis of haem and its activity may be lower, while PBGD activity may be higher in these tissues (27, 29, 40, 41). Inhibition of ferrochelatase could then increase the accumulation of PpIX. Ferrochelatase is temporarily bound to PpIX when converting PpIX into haem. A short period of illumination at this moment may selectively damage this enzyme and enhance the accumulation of PpIX, as it can no longer be converted into haem (42, 43). We found that illumination at 1 h after ALA administration with 12.5 J cm^{-1} caused a significant increase in the PBGD / ferrochelatase activity ratio at 4h, but not at 3 h following illumination. (Table 2)

Illumination		Damage		
Time after ALA	Light dose (J cm^{-1})	Epithelium	Muscularis propria	SF[^]
3 h	20	2.8±0.2	3.0±0	0.9±0.1
3 h	32.5	2.0±0.6	2.6±0.4	0.7±0.2
7 h	20	1.4±0.6	1.6±0.4	1.0±0.4
1 h+3 h	12.5+20	2.0±0.5	2.6±0.2	0.7±0.2
1 h+4 h	12.5+20	1.6±0.7	2.2±0.5	0.5±0.2
1 h+7 h	12.5+20	1.8±0.6	1.6±0.4	1.0±0.3

Table 2 Damage of the epithelium and muscularis propria of the normal rat esophagus induced by ALA-PDT. Three groups of rats were illuminated at 3 or 7 h after ALA. Three groups were illuminated at 1 h after ALA and additionally at 3, 4 or 7 h. Illumination at 1 h after ALA did not result in esophageal damage (34) nor in different tissue optical properties. Mean damage scores of the layer ± standard error of the mean were expressed on a scale from 0 to 3 (0: normal or no muscle necrosis, 3: complete ablation or <25% vital muscle). ^SF = selectivity factor of epithelial damage; epithelial damage score / muscular damage score, expressed as mean ± standard error of the mean.

However, this did not result in a higher production of porphyrins compared to non-illuminated animals. Moreover, a second illumination using 20 J cm^{-1} at various time intervals after the first illumination did not result in more or more selective damage to the esophageal mucosa. Also when a second dose of ALA at 4 h after the first dose was given, it did not result in more PpIX accumulation, or in more PDT-induced damage. Probably, maximal PpIX formation has already been achieved with an ALA dose of 200 mg/kg and this cannot be increased by administration of a second ALA dose. A more likely explanation is that the higher PBGD: ferrochelatase activity seen after the first illumination reflects PDT induced damage to the cells and decreased viability, which renders these cells incapable of synthesizing new PBGD. In this study fractionated illumination showed no beneficial effects, but in other studies the PDT effect increased when a fractionated light delivery was used, although they were not performed in a rat esophagus (25, 37, 39, 42-45). A beneficiary effect of a fractionated light delivery may depend on the organ or tissue irradiated, the initial light dose and the time interval between the illuminations.

DISCUSSION

Extensive studies in rats regarding the kinetics, timing of treatment, total light dose, power output and wavelength showed the importance of these parameters for success or failure of the treatment. Future experiments in rats, which aim to further increase the effectiveness of therapy, could include the use of ALA-esters, fractionated light delivery schedules, optimization of light delivery, the use of vaso-active drugs and immunomodulators. Although the outcomes from rat studies cannot be translated to humans, they provide important clues for the clinical setting.

Currently, PDT is used for Barrett's epithelium in small numbers of patients (19, 22-24, 46). Usually, patients with Barrett's esophagus with low or high grade dysplasia or mucosal cancer are treated. Overholt et al treated 100 patients with BE and HGD or superficial carcinoma with Photofrin-PDT and achieved in 75-80% of the patients mucosal ablation and squamous re-epithelialization with complete elimination in 43 cases. However, 34% of the patients developed esophageal stricture after the treatment (47). With ALA-PDT also partial and complete remission of the BE and small intramucosal cancers is achieved without formation of strictures and without prolonged skin sensitivity, but some small islands of Barrett's epithelium situated under the newly

generated squamous epithelium may remain (23). The importance of these residual islands of Barrett's epithelium is yet unknown and has to be determined during follow up. These cells are thought to be able to develop to BE and adenocarcinoma, but they may also be silenced under the normal squamous epithelium and not develop to adenocarcinoma. However, a case report of Van Laethem et al (48), showed an adenocarcinoma arising in residual submucosal Barrett's epithelium after ablation of BE with Argon Plasma Beam coagulation. Therefore, the efficacy of ALA-PDT for BE has to be improved to eliminate all Barrett's epithelium.

REFERENCES

1. Barrett, N. (1950) Chronic peptic ulcer of the oesophagus and "oesophagitis". *Br J Surg.* **38**, 175-182.

2. Spechler, S. J. and R. K. Goyal (1986) Barrett's esophagus. *N Engl J Med.* **315**, 362-71.

3. Lieberman, D. A., M. Oehlke and M. Helfand (1997) Risk factors for Barrett's esophagus in community-based practice. GORGE consortium. Gastroenterology Outcomes Research Group in Endoscopy. *Am J Gastroenterol.* **92**, 1293-7.

4. Oberg, S., T. R. DeMeester, J. H. Peters, J. A. Hagen, J. J. Nigro, S. R. DeMeester, J. Theisen, G. M. Campos and P. F. Crookes (1999) The extent of Barrett's esophagus depends on the status of the lower esophageal sphincter and the degree of esophageal acid exposure. *J Thorac Cardiovasc Surg JID - 0376343.* **117**, 572-580.

5. El-Serag, H. B., P. Kvapil, J. Hacken-Bitar and J. R. Kramer (2005) Abdominal obesity and the risk of Barrett's esophagus. *Am J Gastroenterol.* **100**, 2151-6.

6. Sontag, S. J., T. G. Schnell, T. Q. Miller, S. Khandelwal, S. O'Connell, G. Chejfec, H. Greenlee, U. J. Seidel and L. Brand (1992) Prevalence of oesophagitis in asthmatics. *Gut.* **33**, 872-6.

7. Cameron, A. J., A. R. Zinsmeister, D. J. Ballard and J. A. Carney (1990) Prevalence of columnar-lined (Barrett's) esophagus. Comparison of population-based clinical and autopsy findings. *Gastroenterology.* **99**, 918-22.

8. Yeh, C., C. T. Hsu, A. S. Ho, R. E. Sampliner and R. Fass (1997) Erosive esophagitis and Barrett's esophagus in Taiwan: a higher frequency than expected. *Dig Dis Sci.* **42**, 702-6.

9. Andreollo, N. A., M. U. Michelino, N. A. Brandalise, L. R. Lopes, M. A. Trevisan and L. S. Leonardi (1997) [Incidence and epidemiology of Barrett's epithelium at the Gastrocentro-UNICAMP]. *Arq Gastroenterol.* **34**, 22-6.

10. de Mas, C. R., M. Kramer, E. Seifert, G. Rippin, M. Vieth and M. Stolte (1999) Short Barrett: prevalence and risk factors. *Scand J Gastroenterol.* **34**, 1065-70.

11. Conio, M., A. J. Cameron, Y. Romero, C. D. Branch, C. D. Schleck, L. J. Burgart, A. R. Zinsmeister, L. J. r. Melton and G. R. r. Locke (2001) Secular trends in the epidemiology and outcome of Barrett's oesophagus in Olmsted County, Minnesota. *Gut.* **48**, 304-9.

12. Spechler, S. J. and R. K. Goyal (1996) The columnar-lined esophagus, intestinal metaplasia, and Norman Barrett. *Gastroenterology.* **110**, 614-621.

13. Cameron, A. J., C. T. Lomboy, M. Pera and H. A. Carpenter (1995) Adenocarcinoma of the esophagogastric junction and Barrett's esophagus. *Gastroenterology.* **109**, 1541-6.

14. Sabel, M. S., K. Pastore, H. Toon and J. L. Smith (2000) Adenocarcinoma of the esophagus with and without Barrett mucosa. *Arch Surg.* **135**, 831-5.

15. Blot, W. J., S. S. Devesa, R. W. Kneller and J. F. Fraumeni, Jr. (1991) Rising incidence of adenocarcinoma of the esophagus and gastric cardia. *JAMA.* **265**, 1287-9.

16. Pera, M., V. F. Trastek, P. C. Pairolero, A. Cardesa, M. S. Allen and C. Deschamps (1993) Barrett's disease: pathophysiology of metaplasia and adenocarcinoma. *Ann Thorac Surg.* **56**, 1191-7.

17. Devesa, S. S., W. J. Blot and J. F. Fraumeni, Jr. (1998) Changing patterns in the incidence of esophageal and gastric carcinoma in the United States. *Cancer.* **83**, 2049-53.

18. Goldblum, J. R. (2003) Barrett's esophagus and Barrett's-related dysplasia. *Mod Pathol.* **16**, 316-24.

19. Ackroyd, R., N. J. Brown, M. F. Davis, T. J. Stephenson, S. L. Marcus, C. J. Stoddard, A. G. Johnson and M. W. Reed (2000) Photodynamic therapy for dysplastic Barrett's oesophagus: a prospective, double blind, randomised, placebo controlled trial. *Gut.* **47**, 612-617.

20. Schnell, T. G., S. J. Sontag, G. Chejfec, G. Aranha, A. Metz, S. O'Connell, U. J. Seidel and A. Sonnenberg (2001) Long-term nonsurgical management of Barrett's esophagus with high-grade dysplasia. *Gastroenterology.* **120**, 1607-19.

21. Boogert, J. v. d., R. v. Hillegersberg, P. D. Siersema, R. W. d. Bruin and H. W. Tilanus (1999) Endoscopic ablation therapy for Barrett's esophagus with high-grade dysplasia: a review. *Am J Gastroenterol.* **94**, 1153-60.

22. Ackroyd, R., N. J. Brown, M. F. Davis, T. J. Stephenson, C. J. Stoddard and M. W. Reed (2000) Aminolevulinic acid-induced photodynamic therapy: safe and effective ablation of dysplasia in Barrett's esophagus. *Dis Esophagus.* **13**, 18-22.

23. Barr, H., N. A. Shepherd, A. Dix, D. J. Roberts, W. C. Tan and N. Krasner (1996) Eradication of high-grade dysplasia in columnar-lined (Barrett's) oesophagus by photodynamic therapy with endogenously generated protoporphyrin IX. *Lancet.* **348**, 584-585.

24. Gossner, L., M. Stolte, R. Sroka, K. Rick, A. May, E. G. Hahn and C. Ell (1998) Photodynamic ablation of high-grade dysplasia and early cancer in Barrett's esophagus by means of 5-aminolevulinic acid. *Gastroenterology.* **114**, 448-55.

25. Messmann, H., R. M. Szeimies, W. Baumler, R. Knuchel, H. Zirngibl, J. Scholmerich and A. Holstege (1997) Enhanced effectiveness of photodynamic therapy with laser light fractionation in patients with esophageal cancer. *Endoscopy.* **29**, 275-80.

26. Orth, K., A. Stanescu, A. Ruck, D. Russ and H. G. Beger (1999) [Photodynamic ablation and argon-plasma coagulation of premalignant and early-stage malignant lesions of the oesophagus--an alternative to surgery?]. *Chirurg.* **70**, 431-8.

27. Van Hillegersberg, R., J. W. Van den Berg, W. J. Kort, O. T. Terpstra and J. H. Wilson (1992) Selective accumulation of endogenously produced porphyrins in a liver metastasis model in rats. *Gastroenterology.* **103**, 647-51.

28. Boogert, J. v. d., R. v. Hillegersberg, F. W. d. Rooij, R. W. d. Bruin, A. Edixhoven-Bosdijk, A. B. Houtsmuller, P. D. Siersema, J. H. Wilson and H. W. Tilanus (1998) 5-Aminolaevulinic acid-induced protoporphyrin IX accumulation in tissues: pharmacokinetics after oral or intravenous administration. *J Photochem Photobiol B.* **44**, 29-38.

29. Boogert, J. v. d., A. B. Houtsmuller, F. W. d. Rooij, R. W. d. Bruin, P. D. Siersema and R. v. van Hillegersberg (1999) Kinetics, localization, and mechanism of 5-aminolevulinic acid-induced porphyrin accumulation in normal and Barrett's-like rat esophagus. *Lasers Surg Med.* **24**, 3-13.

30. Boogert, J. v. d., R. v. Hillegersberg, H. J. v. Staveren, R. W. d. Bruin, H. v. Dekken, P. D. Siersema and H. W. Tilanus (1999) Timing of illumination is essential for effective and safe photodynamic therapy: a study in the normal rat oesophagus. *Br J Cancer.* **79**, 825-830.

31. Ackroyd, R., N. Brown, D. Vernon, D. Roberts, T. Stephenson, S. Marcus, C. Stoddard and M. Reed (1999) 5-Aminolevulinic acid photosensitization of dysplastic Barrett's esophagus: a pharmacokinetic study. *Photochem Photobiol.* **70**, 656-662.

32. Boogert, J. v. d., H. J. v. Staveren, R. W. d. Bruin, J. H. Eikelaar, P. D. Siersema and R. v. Hillegersberg (1999) Photodynamic therapy for esophageal lesions: selectivity depends on wavelength, power, and light dose. *Ann Thorac Surg.* **68**, 1763-1769.

33. Staveren, H. J. v., M. Keijzer, T. Keesmaat, H. Jansen, W. J. Kirkels, J. F. Beek and W. M. Star (1996) Integrating sphere effect in whole-bladder wall photodynamic therapy: III. Fluence multiplication, optical penetration and light distribution with an eccentric source for human bladder optical properties. *Phys Med Biol.* **41**, 579-90.

34. Boogert, J. v. d., H. J. v. Staveren, R. W. F. d. Bruin, F. W. M. d. Rooij, A. Edixhoven-Bosdijk, P. D. Siersema and R. v. Hillegersberg (2000) Fractionated illumination in oesophageal ALA-PDT: effect on ferrochelatase activity. *J Photochem Photobiol B.* **56**, 53-60.

35. Hua, Z., S. L. Gibson, T. H. Foster and R. Hilf (1995) Effectiveness of delta-aminolevulinic acid-induced protoporphyrin as a photosensitizer for photodynamic therapy in vivo. *Cancer Res.* **55**, 1723-31.

36. Veen, N. v. d., K. M. Hebeda, H. S. d. Bruijn and W. M. Star (1999) Photodynamic effectiveness and vasoconstriction in hairless mouse skin after topical 5-aminolevulinic acid and single- or two-fold illumination. *Photochem Photobiol.* **70**, 921-9.

37. Robinson, D. J., H. S. de Bruijn, N. van der Veen, M. R. Stringer, S. B. Brown and W. M. Star (1999) Protoporphyrin IX fluorescence photobleaching during ALA-mediated photodynamic therapy of UVB-induced tumors in hairless mouse skin. *Photochem Photobiol.* **69**, 61-70.

38. Veen, N. v. d., H. S. d. Bruijn and W. M. Star (1997) Photobleaching during and re-appearance after photodynamic therapy of topical ALA-induced fluorescence in UVB-treated mouse skin. *Int J Cancer.* **72**, 110-8.

39. Bruijn, H. S. d., N. v. d. Veen, D. J. Robinson and W. M. Star (1999) Improvement of systemic 5-aminolevulinic acid-based photodynamic therapy in vivo using light fractionation with a 75-minute interval. *Cancer Res.* **59**, 901-904.

40. Hinnen, P., F. W. de Rooij, M. L. van Velthuysen, A. Edixhoven, R. van Hillegersberg, H. W. Tilanus, J. H. Wilson and P. D. Siersema (1998) Biochemical basis of 5-aminolaevulinic acid-induced protoporphyrin IX accumulation: a study in patients with (pre)malignant lesions of the oesophagus. *Br J Cancer.* **78**, 679-82.

41. el-Sharabasy, M. M., A. M. el-Waseef, M. M. Hafez and S. A. Salim (1992) Porphyrin metabolism in some malignant diseases. *Br J Cancer.* **65**, 409-12.

42. He, D., S. Behar, N. Nomura, S. Sassa, S. Taketani and H. W. Lim (1995) The effect of porphyrin and radiation on ferrochelatase and 5-aminolevulinic acid synthase in epidermal cells. *Photodermatol Photoimmunol Photomed.* **11**, 25-30.

43. Lim, H. W., S. Behar and D. He (1994) Effect of porphyrin and irradiation on heme biosynthetic pathway in endothelial cells. *Photodermatol Photoimmunol Photomed.* **10**, 17-21.

44. Curnow, A., J. C. Haller and S. G. Bown (2000) Oxygen monitoring during 5-aminolaevulinic acid induced photodynamic therapy in normal rat colon. Comparison of continuous and fractionated light regimes. *J Photochem Photobiol B.* **58**, 149-155.

45. Geel, I. P. v., H. Oppelaar, J. P. Marijnissen and F. A. Stewart (1996) Influence of fractionation and fluence rate in photodynamic therapy with Photofrin or mTHPC. *Radiat Res.* **145**, 602-609.

46. Gossner, L., A. May, R. Sroka, M. Stolte, E. G. Hahn and C. Ell (1999) Photodynamic destruction of high grade dysplasia and early carcinoma of the esophagus after the oral administration of 5-aminolevulinic acid. *Cancer.* **86**, 1921-8.

47. Overholt, B. F. (1999) Results of photodynamic therapy in Barrett's esophagus: A review. *Can J Gastroenterol.* **13**, 393-6.

48. Van Laethem, J. L., M. O. Peny, I. Salmon, M. Cremer and J. Deviere (2000) Intramucosal adenocarcinoma arising under squamous re-epithelialisation of Barrett's oesophagus. *Gut.* **46**, 574-7.

Chapter 2

Aim of the thesis

I.A. Boere, J. Kluin, R.W.F. de Bruin

Department of Surgery, Erasmus Medical Center Rotterdam

AIM OF THE THESIS

Barrett's esophagus is a premalignant condition of the esophagus in which pathogenesis and therapy are still subject of research. Since photodynamic therapy with 5-aminolevulinic acid (ALA-PDT) is a relatively new method to ablate premalignant Barrett's mucosa, many caveats need to be solved. ALA-PDT for Barrett's esophagus is not effective enough to ablate all the premalignant epithelium. Furthermore, the results of ALA-PDT vary between patients. There are a number of laser parameters that influence the results of ALA-PDT, such as time interval, light dose or fluence, and intensity or fluence rate of the laser light applied. However, optimization of these parameters is still subject of research. The photosensitizer PpIX is consumed during ALA-PDT, and an indirect parameter, PpIX fluorescence is decreased. In the present thesis, standardization of the laser parameters in vivo is applied and studied in the normal and Barrett's rat esophagus. Additionally, during therapy, PpIX fluorescence was measured and investigated.

The pathogenesis of Barrett's esophagus has not yet been fully elucidated. Questions remain concerning risk factors, the malignant potential, the need for therapy, and which therapy to use. Whereas Barrett's esophagus has been histologically defined as intestinal metaplasia with goblet cells, diagnosing Barrett's esophagus with dysplasia is not as clear. There is a considerable interobserver variation, even between experienced pathologists. Therefore reliable animal models are needed to study the pathogenesis, the effects of therapy, and to develop diagnostic tools. Ideally, a diagnostic tool would be able to help define the difference between Barrett's esophagus with or without dysplasia in vivo, during endoscopy. In this thesis, the rat model for Barrett's esophagus was compared to a model in the opossum, a species that has an esophagus with more resemblance to man. Subsequently, the rat model was used to study photodynamic therapy and Raman spectroscopy. Raman spectroscopy is studied as a potential diagnostic tool for in-vivo detection and discrimination between Barrett's esophagus and dysplasia.

Chapter 3

Duodeno-esophageal reflux induced columnar lined esophagus in rats but not in opossums is comparable to human Barrett's esophagus

I.A. Boere, J. Kluin , R.R. Sital, H. van Dekken, P.D. Siersema, H.W. Tilanus, R.W.F. de Bruin

Departments of Surgery, Gastroenterology & Hepatology and Clinical Pathology, Erasmus MC Rotterdam

ABSTRACT

In search of a useful animal model for BE, the effects of duodenal reflux were examined both in rat and opossum *(Monodelphis domestica)* esophagus. Unlike rats, opossums have a gastrointestinal tract that resembles more that in man, with non-keratinitized squamous epithelium in the esophagus, esophageal gland ducts and a gall bladder. An esophagojejunostomy, which induces duodeno-esophageal reflux, was performed in 20 rats and 32 opossums. They were sacrificed at 8 or 12 months thereafter. Twelve months after the esophagojejunostomy all rats showed microscopic and macroscopic specialised intestinal metaplasia (length 16.5 ± 1.6 mm), whereas only microscopic foci could be found in 25% of the opossums (length 0.4 ± 0.3 mm). In rats, the duration of the reflux correlated well with the length of specialised intestinal metaplasia. The microscopic appearance well resembled human Barrett's esophagus. In conclusion, this study confirms that duodenal reflux in the rat reproducibly induces Barrett's esophagus. In the opossum however, BE was not induced by longstanding gastro-esophageal reflux.

INTRODUCTION

Barrett's esophagus (BE) is defined as the presence of intestinal metaplasia with goblet cells in the esophagus, which has replaced the normal squamous epithelium (1). The presence of BE increases the risk of esophageal adenocarcinoma 30-125 fold, with an estimated incidence of 0.5% per year, through a sequence of metaplasia, dysplasia and carcinoma (2, 3). The pathogenesis of intestinal metaplasia is still subject of research. Acid reflux and gastro-esophageal reflux disease (GERD) are considered to be the cause of BE, but in animal studies reflux of alkaline duodenal contents and bile has also shown to be implicated in the pathogenesis of BE (4-6). Animal models have been used in search of the pathogenesis and treatment of BE, but there still is a need for an animal model in which a considerable length of BE develops and that is comparable to human BE.

Surgery with or without the administration of a carcinogen has been used to induce reflux in dogs and rats (7-20). Only small areas (a few millimeters maximum) or small islands of Barrett's epithelium, some even beneath the squamous epithelium are described in rat models (14-16, 21). In the different rat models (gastro-) duodenal reflux induces microscopic foci of columnar lined epithelium (CLE) in the esophagus, which is morphologically similar to BE in man. Also, mutations in the p53 gene and Ki67 expression, similar to human BE, have been described (22). It is hypothesized that BE originates in pluripotent stem cells in the esophageal (sub-) mucosa in rat and man.

Although the current rat models with duodenal or gastroduodenal reflux have proven their usefulness to study the development of BE, there are substantial differences in size, anatomy, and histology of the upper gastrointestinal tract, between rat and man. First, the rat esophagus is lined by keratinized squamous epithelium, whereas the human esophagus is lined by non-keratinized squamous epithelium. Second, as the rat has a squamous fore-stomach, the squamo-columnar junction is located within the stomach, not at the gastro-esophageal junction. Third, the rat esophagus lacks submucosal glands that are found in the human esophagus and which have been thought of as the location of the pluripotent stem cell from which BE may develop. Fourth, rats do not have a gallbladder. Besides these anatomical differences, there may also be differences in the pathogenesis of BE in rat and man, as there is only a

relatively short period necessary to induce CLE in the rat esophagus, as compared to the longstanding history of GERD in BE in man. Furthermore, the rat model has shown to be dependent on duodenal reflux, gastric reflux alone was not sufficient to develop CLE.

In view of these limitations, we have sought a new animal species that possesses a gastro-intestinal tract that more resembles the human gastrointestinal tract. The opossum esophagus is lined by non-keratinized epithelium, it contains submucosal glands and the opossum has a gallbladder. The opossum has therefore previously been used as an animal model for studying the physiology of the esophagus (23) and inflammatory changes after resection of the cardia (24, 25), but studies on BE have not been reported in this species. The aim of the study is to develop a reliable animal model for BE to study its pathogenesis and therapeutic options.

For that purpose, the development of BE by induction of duodeno-esophageal reflux was studied both in the rat and in the opossum. Both species underwent an esophagojejunostomy to study the development of BE and its application as an animal model for BE. In addition, to obtain more insight in the role of bile acids in BE, opossums with or without gallbladder, after cholecystectomy, were studied, and bile composition of both species was analysed.

MATERIALS AND METHODS

Design of the study and animals. Twenty-three male inbred WAG/Rij rats (Harlan CPB, Austerlitz, The Netherlands), weighing 200-275 grams were used. The animals had free access to rat chow (AM II, Hope Farms, Woerden, The Netherlands) and tap water. Twenty-three female grey short tailed opossums *(Monodelphis domestica),* weighing approximately 90 grams, were used. The animals were housed individually in plastic rat cages containing wooden shavings and nesting material. Animals were fed commercial cat food (Rokus meat chunks, De Haan, Nieuwkoop, The Netherlands, and Catfood 2572, Hope Farm B.V., Woerden, The Netherlands), pieces of apple, and orange and water ad libitum. Three rats and 3 opossums served as unoperated controls. The remaining animals underwent an esophagojejunostomy (EJ) to induce reflux of duodenal (pancreatic and biliary) juice. Ten animals of each species were sacrificed at 8 and 12 months after surgery.

Another 12 opossums underwent EJ with resection of their gallbladder and were followed for 8 months. Table 1 summarizes the different groups.

Group (n)		Sacrifice
1 (3)	Control WAG rats	12 months
2 (20)	WAG rats with EJ	8 & 12 months
3 (3)	Control opossums	12 months
4 (20)	Opossum with EJ, gallbladder preserved	8 & 12 months
3 (12)	Opossum with EJ and cholecystectomy	8 months

Table 1 Animals used for each treatment and time point.

Surgical technique. Ether anaesthesia was used for rats. A combination of intramuscular ketamin, xylazin, and midazolam (4, 0.2 and 0.2 mg/ animal respectively) was used for the opossums. An esophagojejunostomy according to the model of Levrat was performed through a median laparotomy (26). The esophagus was dissected from the stomach and anastomosed in an end-to-side manner to the jejunum (continuous 7/0 silk sutures) approximately 3 cm distally from the entry of the common bile duct. In 12 opossums the gallbladder was also removed. The abdominal wall of the rats was closed in one layer, the abdominal wall of the opossums in two layers (2/0 silk sutures). After surgery, the animals received buprenorphin as analgesic and 2 ml glucose 10% subcutaneously. Water was provided directly and chow after 24 hours.

Handling of the specimens. Animals were weighed before sacrifice by exsanguination under ether or isoflurane anaesthesia. The thoracic and abdominal cavities were inspected and the esophagus, the anastomosis and the proximal jejunum were excised en bloc. The esophagus was opened longitudinally, the circumference was measured and the specimen was rolled up from distal to proximal in a swiss roll manner and fixed in formalin (27).

Histological examination. Specimens were embedded in paraffin wax, cut in 5 μm sections and stained with haematoxylin and eosin (H&E), periodic acid Schiff

(PAS) and alcian blue. A pathologist (H.v.D.) blinded for the species and the treatment microscopically evaluated the sections. The esophagus was examined for hyperkeratosis, squamous hyperplasia, erosions, metaplastic columnar epithelium, dysplasia, benign papillomas and carcinoma. A specimen was defined as having squamous hyperplasia when there was papillary elongation or basal cell hyperplasia, occasionally resulting in the formation of intramural cysts. Dysplasia was diagnosed according to standard criteria and included dysplasia arising in either glandular or squamous epithelium (28). Barrett's esophagus was defined as esophageal mucosa lined by columnar epithelium with the presence of goblet cells, verified with alcian blue staining.

Composition of bile. Bile was collected in 5 opossums by aspirating bile from the gall bladder directly after sacrifice. In 5 rats the common bile duct was cannulated and bile was collected for one hour under ether anaesthesia, after which they were sacrificed. Total bile acids were analysed enzymatically according to Mashige (29). Individual bile acid concentrations in bile samples were then determined by gas-chromatography using 23-nordeoxycholic acid (Steraloids Inc. Wilton, N.H., USA) after hydrolysis with Cholylglycinhydrolase (Sigma Aldrich Chemical B.V., Zwijndrecht, The Netherlands) and derivatization to their methylesteracetate derivatives (30, 31). The ratio glycine/ taurine was determined according to Blom (32).

Statistical analysis. The length of BE and the weight of the animals are expressed as mean ± standard error of the mean (SEM). Comparisons were made using Student's t-test. A difference was considered to be significant if P values were < 0.05.

RESULTS

General observations and histology

Eight opossums died or were sacrificed before the end of the study due to surgical complications due to gnawing through sutures. The 24 remaining animals recovered quickly from surgery. They ate and drank normally and did not loose weight. Sixteen opossums were sacrificed at 8 months, and 8 animals one year after EJ. In contrast to the opossums, the rats did not thrive well and lost weight following EJ. Two

animals were euthanized because of stenosis of the anastomosis and 7 for
complications of reflux esophagitis such as malnutrition and pneumonia.
Postoperatively, rats lost weight within a limit of 25% of the preoperative weight, and
they regained less than control animals (p<0.01). After follow up, 7 rats were
sacrificed at 8 months and four at 12 months after surgery. In control animals, the
differences between the opossum and rat esophagus are clearly visible (figure 1).
The opossum esophagus is lined by non-keratinised squamous epithelium and has
submucosal glands, whereas the rat esophagus is lined by a keratinised squamous
epithelium and lacks these glands.
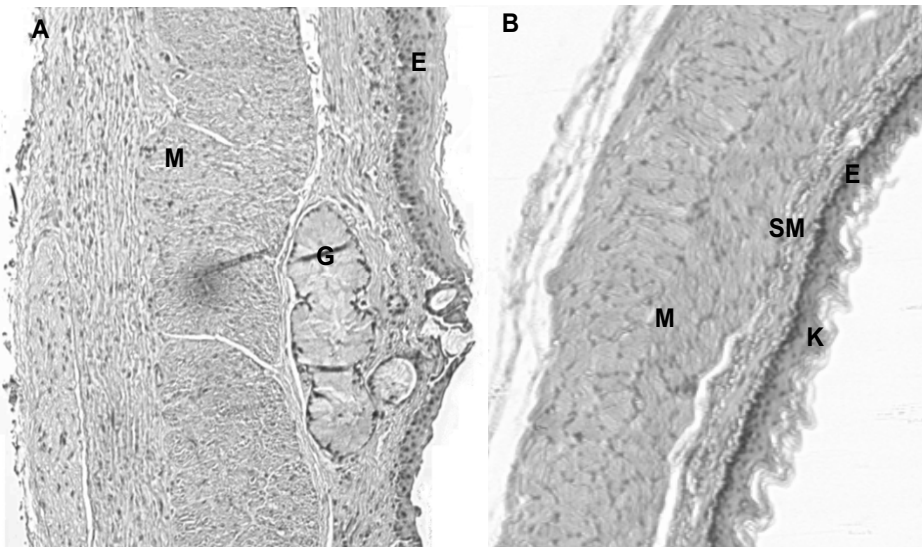
Figure 1A: Section of the distal esophagus of a control opossum, lined by non-keratinised
squamous epithelium. Esophageal glands, staining positively with PAS and alcian blue, are
visible in the submucosa (x40, H&E staining) E = epithelium, G = submucosal gland, M =
muscularis propria. **B**: Section of the distal esophagus of a control rat, lined by keratinised
squamous epithelium. The rat esophagus shows no submucosal glands (x20, H&E staining)
E = epithelium, K = keratin layer, M = muscularis propria, SB = submucosa.

Eight and 12 months after EJ, opossums showed macroscopical marginal thickening
of the longitudinal white folds in the distal esophagus. No other abnormalities to the
esophagus were noticed. In rats exposed to reflux, the distal and middle part of the
esophagus was thickened and dilated. Distally, the esophagus had a smooth pink

aspect, separated from the white squamous lining of the proximal esophagus by a zone with erosions. In opossums with EJ with or without gall bladder resection, no evidence of BE was found at histological examination. In two opossums with 12 months of reflux and in the opossums with EJ and gall bladder resection, the submucosal glands showed hyperplasia. Also, foci of cardiac type epithelium were found in the distal esophagus (figure 2). The squamous epithelium showed mild regenerative thickening and was sparsely infiltrated by neutrophils. In one of the opossums with EJ and gall bladder resection, an esophageal squamous cell carcinoma was observed at 8 months.
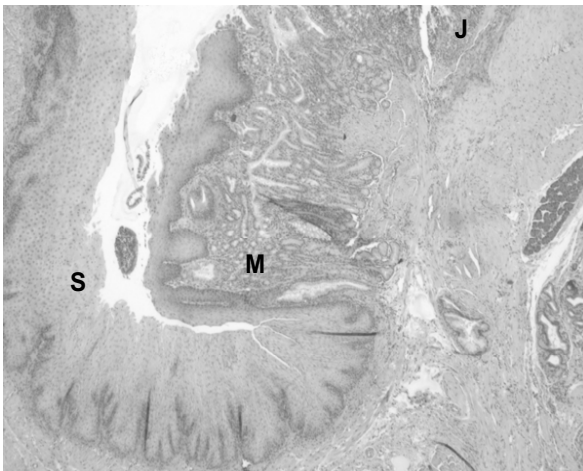
Figure 2 Distal esophagus of the opossum 1 year after EJ. The section shows microscopic foci of cardiac type intestinal metaplasia (length 1 mm) (x20 HE staining) J = jejunum, M = foci of cardiac type metaplasia, S = squamous epithelium.

In contrast, in rats BE was found in the distal esophagus from the anastomosis to 6.1 ± 1.4 mm (8-month group) and 16.5 ± 1.6 mm (12-month group) cranial from the sutures (table 2, figure 3). H&E, PAS and alcian blue stained sections showed columnar epithelium with intestinal metaplasia and goblet cells. This glandular epithelium was markedly different from the adjacent jejunal epithelium. The villi are less well organized and shorter with glands and foveolae instead of crypts and villi as found in the jejunum. No dysplasia was found. Proximal from the intestinal metaplasia, an area of erosion and inflammation with eosinophils and an area of

hyperplastic squamous epithelium were observed. The proximal esophagus was lined by normal squamous epithelium.
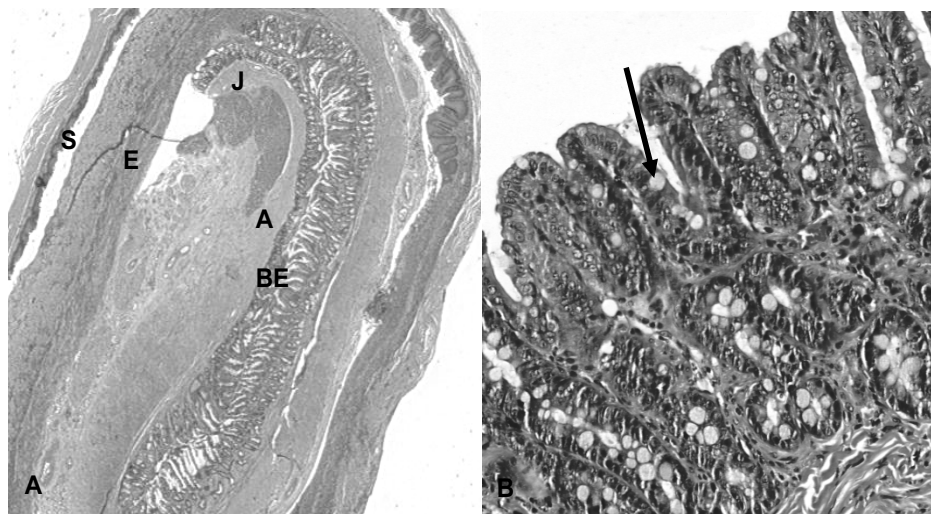
Figure 3A: Rat esophagus after 1 year of gastroduodeno-esophageal reflux, showing macroscopic BE (x10, H&E staining). (A = site of anastomosis, BE = Barrett's esophagus, E = erosion, J = jejunum, S= squamous epithelium). **B**: Distal rat esophagus exposed to gastroduodenal reflux during 1 year. Cranial from the anastomosis, the esophagus was lined by columnar epithelium with intestinal metaplasia and goblet cells (arrow) (x40, H&E staining).

Group (n)	BE (n)	Length of BE (mm)	Weight (g)
Opossums			
Controls (3) 12 months	0	0	96 ± 4
8 months (7)	0	0	93 ± 4§
12 months (8)	0	Microscopic foci	97 ± 5§
Rats			
Controls (3)	0	0	386 ± 21
8 months (6)	6	6.1 ± 1.4	274 ± 46*
12 months (4)	4	16.5 ± 1.6	255 ± 34*

Table 2 Incidence and length of BE and weight of opossums before and after esophagojejunostomy. § not significant versus control, * P < 0.05 versus control.

Composition of bile

In table 3, the bile acid concentration and its relative composition in opossum, rat and man are shown. Total bile acid concentration in bile in the gall bladder of opossums was comparable to the reported bile acid concentration in human gall bladder (33). The total bile acid concentration in opossum gall bladder was 4-5 times higher than the bile acid concentration in the common bile duct in rats. The chemical composition of opossum bile resembled the human situation, whereas rat bile contained more cholic acid (86% compared to 42%) and less chenodeoxycholic acid (10% compared to 27%) and deoxycholic acid (4% compared to 28%). The ratio glycine: taurine was higher in man (2:1 to 3:1) than in rats (1:2 to 1:5). In opossums, the ratio glycine: taurine was very low (1:48 to 1:117).

	Rat	Opossum	Man
Total bile acid concentration (mmol/l)	39±3	166±28	50-200
Cholic acid (%)	86±2	42±7	35
Chenodeoxycholic acid (%)	10±2	27±4	35
Deoxycholic acid (%)	4±2	28±7	24
Lithocholic acid (%)	0	4±4	6
Glycin: taurin	1:2 -1:5	1:48-1:118	2:1-3:1

Table 3 Total bile acid concentration and percentage of individual bile acids in rat bile (collected in the common bile duct) and opossum bile (collected in the gall bladder). Values are expressed as mean ± SEM (n=5 in both groups). The data on human bile (in the gall bladder) are taken from the literature [33].

DISCUSSION

In our animal model chronic reflux of duodenal juice induced macroscopic BE in rats. In line with other experimental rat models for BE, duodenal contents induced inflammation, ulceration and intestinal metaplasia in rats. Intestinal metaplasia developed first at the site of the anastomosis between jejunum and esophagus and progressed cranially. Histology demonstrated the similarity of rat BE to that found in man. The duration of the period of reflux correlated with the extent of BE that developed, which is unique compared to other studies (9, 12-16, 21). In contrast to

rats, opossums did not develop macroscopic or microscopic BE after long term duodenal reflux. Even when the gall bladder was resected to induce more continuous biliary flow, opossums did not develop intestinal metaplasia. In the opossums subjected to EJ with gall bladder resection, one animal showed a squamous cell carcinoma in the esophagus at 8 months.

Both human and animal studies have investigated and debated the exact nature of the pathogenic stimuli in the refluxate that cause BE, with special interest in the roles of acid and biliary or duodenal reflux (34-40). Acid reflux is essential for development of BE in the canine esophagus. Columnar re-epithelialization of the denuded lower esophagus occurred in the presence of acid or acid plus bile reflux, whereas squamous re-epithelialization occurred in the absence of (acid) reflux (7, 8). In rat studies there is evidence that duodenal reflux is more important in the pathogenesis of BE, gastric-, and esophageal cancer (4, 12-14, 16, 18, 21, 41-47). Columnar metaplasia of the rat esophagus can be induced by reflux of duodenal contents into the esophagus, without the administration of carcinogens (9, 12, 14-16, 21, 48). In man there is a clear relationship between BE and GERD (49), but the relative influences of duodenal and bile reflux are not clear. Gastric surgery, inducing duodenal reflux, did not lead to a higher prevalence of BE (50). In contrast, other studies have shown that bile acid concentrations in the esophagus are elevated in patients with BE, compared to patients with GERD but without BE (5, 51). Current consensus is that both gastric and duodenal reflux contribute to the pathogenesis of BE (37, 52).

In the present study, duodenal reflux was induced in rats and opossums, but only rats developed BE. There are differences between the GI tracts of opossum and rat, and differences in their bile acid contents that may explain the fact that opossums did not develop BE. The opossum has a gall bladder, which stores and concentrates bile and releases it into the small intestine after a food stimulus. Additionally, the activity of the sphincter of Oddi regulates the flow of bile and pancreatic secretions into the duodenum (53). The tone of this sphincter between meals is high and consequently pancreaticobiliary reflux is confined to the time of food intake. This mechanism may still have been intact after gall bladder resection in opossums. In contrast, rats do not have a gallbladder and only a low tonic activity of the sphincter of Oddi, which results

in a continuous flow of bile through the common bile duct into the duodenum (54). When the composition of bile is compared between rats and opossums, opossum bile contained a higher percentage of the (cheno-) deoxycholic bile acids than rat bile, which contained more cholic bile acids. Opossum bile acids were almost exclusively conjugated with taurine, whereas rat bile acids were also conjugated with glycine. Bile acids have previously been shown to induce mucosal damage in the isolated esophagus (55). In the colon, bile acids have been shown to increase epithelial cell proliferation and tumor promotion by chemical carcinogens (56). The pH and conjugation state determine the toxicity of the different bile acids. In an acidic environment, cholic acid and chenodexoycholic acid are nonionized and therefore more toxic (55, 57, 58). The presence of pancreatic juice and pepsin can further enhance erosive effects of bile acids on the esophagus (59-61). Since rats developed BE and opossums did not, glycine conjugated bile acids or cholic acid may exert erosive or carcinogenic effects on the esophageal epithelium, but further studies are warranted to determine the role of bile acid composition on the development of BE.

It is tempting to identify bile acids and the amount of refluxed bile as the causal factors in this animal model, but many other factors may also be involved. In recent studies, expression of the pro-inflammatory enzyme cyclooxygenase-2 (COX-2) was increased in BE (62, 63) and inhibition of COX-2 led to prevention of esophageal carcinomas in rats (48). However, we did not determine COX-2 expression in the different animals. In addition, it has been shown that administration of free radical scavengers inhibited the development reflux esophagitis in rats (64-66). Therefore oxygen radicals, produced by infiltrating neutrophils and macrophages, may be important factors. In this study, the distal segment of the rat esophagus lined by columnar epithelium showed marginal inflammatory infiltration and more proximally, the area of erosion showed severe inflammation with extensive infiltration of neutrophils and eosinophils. In contrast, the opossum esophagus showed no signs of severe inflammation. It is unclear why the esophagus of the opossum showed only very mild signs of inflammation and no erosion after EJ.

In conclusion, we describe an animal model, in which macroscopic BE develops in a reproducible manner, over a length of 1.6 cm, after one year of duodeno-esophageal reflux, in contrast to other studies in which microscopic BE developed. However, in

opossums with duodeno-esophageal reflux with or without cholecystectomy, no BE could be observed. This implies that other factors, such as bile acid composition, the presence of submucosal glands that excrete bicarbonate or genetic susceptibility are essential for the development of BE.

REFERENCES

1. Spechler, S. J. (2002) Columnar-lined esophagus. Definitions. *Chest Surg Clin N Am.* **12**, 1-13, vii.

2. Shaheen, N. J., M. A. Crosby, E. M. Bozymski and R. S. Sandler (2000) Is there publication bias in the reporting of cancer risk in Barrett's esophagus? *Gastroenterology.* **119**, 333-8.

3. Jankowski, J. A., N. A. Wright, S. J. Meltzer, G. Triadafilopoulos, K. Geboes, A. G. Casson, D. Kerr and L. S. Young (1999) Molecular evolution of the metaplasia-dysplasia-adenocarcinoma sequence in the esophagus. *Am J Pathol.* **154**, 965-73.

4. Marshall, R. E., A. Anggiansah and W. J. Owen (1997) Bile in the oesophagus: clinical relevance and ambulatory detection. *Br J Surg.* **84**, 21-8.

5. Nehra, D., P. Howell, C. P. Williams, J. K. Pye and J. Beynon (1999) Toxic bile acids in gastro-oesophageal reflux disease: influence of gastric acidity. *Gut.* **44**, 598-602.

6. Vaezi, M. F. and J. E. Richter (1999) Importance of duodeno-gastro-esophageal reflux in the medical outpatient practice. *Hepatogastroenterology.* **46**, 40-7.

7. Bremner, C. G., V. P. Lynch and F. H. Ellis, Jr. (1970) Barrett's esophagus: congenital or acquired? An experimental study of esophageal mucosal regeneration in the dog. *Surgery.* **68**, 209-16.

8. Gillen, P., P. Keeling, P. J. Byrne, A. B. West and T. P. Hennessy (1988) Experimental columnar metaplasia in the canine oesophagus. *Br J Surg.* **75**, 113-5.

9. Seto, Y. and O. Kobori (1993) Role of reflux oesophagitis and acid in the development of columnar epithelium in the rat oesophagus. *Br J Surg.* **80**, 467-70.

10. Kawaura, Y., Y. Tatsuzawa, T. Wakabayashi, N. Ikeda, M. Matsuda and S. Nishihara (2001) Immunohistochemical study of p53, c-erbB-2, and PCNA in barrett's esophagus with dysplasia and adenocarcinoma arising from experimental acid or alkaline reflux model. *J Gastroenterol.* **36**, 595-600.

11. Li, H., T. N. Walsh, G. O'Dowd, P. Gillen, P. J. Byrne and T. P. Hennessy (1994) Mechanisms of columnar metaplasia and squamous regeneration in experimental Barrett's esophagus. *Surgery.* **115**, 176-81.

12. Clark, G. W., T. C. Smyrk, S. S. Mirvish, M. Anselmino, Y. Yamashita, R. A. Hinder, T. R. DeMeester and D. F. Birt (1994) Effect of gastroduodenal juice and dietary fat on the development of Barrett's esophagus and esophageal neoplasia: an experimental rat model. *Ann Surg Oncol.* **1**, 252-61.

13. Ireland, A. P., J. H. Peters, T. C. Smyrk, T. R. DeMeester, G. W. Clark, S. S. Mirvish and T. E. Adrian (1996) Gastric juice protects against the development of esophageal adenocarcinoma in the rat. *Ann Surg.* **224**, 358-70.

14. Miwa, K., H. Sahara, M. Segawa, S. Kinami, T. Sato, I. Miyazaki and T. Hattori (1996) Reflux of duodenal or gastro-duodenal contents induces esophageal carcinoma in rats. *Int J Cancer.* **67**, 269-74.

15. Goldstein, S. R., G. Y. Yang, S. K. Curtis, K. R. Reuhl, B. C. Liu, S. S. Mirvish, H. L. Newmark and C. S. Yang (1997) Development of esophageal metaplasia and adenocarcinoma in a rat surgical model without the use of a carcinogen. *Carcinogenesis.* **18**, 2265-70.

16. Chen, X., G. Yang, W. Y. Ding, F. Bondoc, S. K. Curtis and C. S. Yang (1999) An esophagogastroduodenal anastomosis model for esophageal adenocarcinogenesis in rats and enhancement by iron overload. *Carcinogenesis.* **20**, 1801-8.

17. Pera, M., M. J. Brito, R. Poulsom, E. Riera, L. Grande, A. Hanby and N. A. Wright (2000) Duodenal-content reflux esophagitis induces the development of glandular metaplasia and adenosquamous carcinoma in rats. *Carcinogenesis.* **21**, 1587-91.

18. Sato, T., K. Miwa, H. Sahara, M. Segawa and T. Hattori (2002) The sequential model of Barrett's esophagus and adenocarcinoma induced by duodeno-esophageal reflux without exogenous carcinogens. *Anticancer Res.* **22**, 39-44.

19. Kumagai, H., K. Mukaisho, H. Sugihara, M. Bamba, T. Miyashita, K. Miwa and T. Hattori (2003) Cell kinetic study on histogenesis of Barrett's esophagus using rat reflux model. *Scand J Gastroenterol.* **38**, 687-92.

20. Nishijima, K., K. Miwa, T. Miyashita, S. Kinami, I. Ninomiya, S. Fushida, T. Fujimura and T. Hattori (2004) Impact of the biliary diversion procedure on carcinogenesis in Barrett's esophagus surgically induced by duodenoesophageal reflux in rats. *Ann Surg.* **240**, 57-67.

21. Pera, M., A. Cardesa, J. A. Bombi, H. Ernst, C. Pera and U. Mohr (1989) Influence of esophagojejunostomy on the induction of adenocarcinoma of the distal esophagus in Sprague-Dawley rats by subcutaneous injection of 2,6-dimethylnitrosomorpholine. *Cancer Res.* **49**, 6803-8.

22. Su, Y., X. Chen, M. Klein, M. Fang, S. Wang, C. S. Yang and R. K. Goyal (2004) Phenotype of columnar-lined esophagus in rats with esophagogastroduodenal anastomosis: similarity to human Barrett's esophagus. *Lab Invest.* **84**, 753-65.

23. Marklin, G. F., W. J. Krause and J. H. Cutts (1979) Structure of the esophagus in the adult opossum, Didelphis virginiana. *Anat Anz.* **145**, 249-61.

24. De Carle, D. J. (1975) Experimental gastroesophageal reflux in the Australian brush-tailed possum. *Gastroenterology.* **69**, 625-9.

25. Schulze-Delrieu, K., F. A. Mitros and S. Shirazi (1982) Inflammatory and structural changes in the opossum esophagus after resection of the cardia. *Gastroenterology.* **82**, 276-83.

26. Levrat, M., R. Lambert, G. Kirschbaum (1962) Esophagitis produced by reflux of duodenal contents in rats. *Am J Dig Dis.* **7**, 564-573.

27. Park, C. M., P. E. Reid, D. C. Walker and B. R. MacPherson (1987) A simple, practical 'swiss roll' method of preparing tissues for paraffin or methacrylate embedding. *J Microsc.* **145 (Pt 1)**, 115-20.

28. Riddell, R. H. (1996) The biopsy diagnosis of gastroesophageal reflux disease, "carditis," and Barrett's esophagus, and sequelae of therapy. *Am J Surg Pathol.* **20 Suppl 1**, S31-50.

29. Mashige, F., K. Imai and T. Osuga (1976) A simple and sensitive assay of total serum bile acids. *Clin Chim Acta.* **70**, 79-86.

30. Lillington, J. M., D. J. Trafford and H. L. Makin (1981) A rapid and simple method for the esterification of fatty acids and steroid carboxylic acids prior to gas-liquid chromatography. *Clin Chim Acta.* **111**, 91-8.

31. Karlaganis, G. and G. Paumgartner (1979) Determination of bile acids in serum by capillary gas-liquid chromatography. *Clin Chim Acta.* **92**, 19-26.

32. Blom, W. and H. J.G.M. (1992) Differential diagnosis of (inherited) amino acid metabolism or transport disorders. *Amino Acids.* **2**, 25-67.

33. Carey, M. C. (1982) The liver; biology and pathobiology. In Vol. (Edited by I. Arias, H. Popper, D. Schachter and D. A. Shafritz), pp. 429-265. Raven Press, New York.

34. Kauer, W. K. and H. J. Stein (2002) Role of acid and bile in the genesis of Barrett's esophagus. *Chest Surg Clin N Am.* **12**, 39-45.

35. Guillem, P. G., J. F. Flejou, P. Sharma, E. I. Sidorenko and R. C. Fitzgerald (2005) How to make a Barrett esophagus: pathophysiology of columnar metaplasia of the esophagus. *Dig Dis Sci.* **50**, 415-24.

36. Fitzgerald, R. C. (2005) Barrett's oesophagus and oesophageal adenocarcinoma: how does acid interfere with cell proliferation and differentiation? *Gut.* **54 Suppl 1**, i21-6.

37. Richter, J. E. (2000) Importance of bile reflux in Barrett's esophagus. *Dig Dis.* **18**, 208-16.

38. Pera, M. (2002) Experimental Barrett's esophagus and the origin of intestinal metaplasia. *Chest Surg Clin N Am.* **12**, 25-37.

39. Vaezi, M. F., S. Singh and J. E. Richter (1995) Role of acid and duodenogastric reflux in esophageal mucosal injury: a review of animal and human studies. *Gastroenterology.* **108**, 1897-907.

40. Mirvish, S. S. (1997) Studies on experimental animals involving surgical procedures and/or nitrosamine treatment related to the etiology of esophageal adenocarcinoma. *Cancer Lett.* **117**, 161-74.

41. Attwood, S. E., T. C. Smyrk, T. R. DeMeester, S. S. Mirvish, H. J. Stein and R. A. Hinder (1992) Duodenoesophageal reflux and the development of esophageal adenocarcinoma in rats. *Surgery.* **111**, 503-10.

42. Miwa, K., T. Fujimura, H. Hasegawa, T. Kosaka, R. Miyata, I. Miyazaki and T. Hattori (1992) Is bile or are pancreaticoduodenal secretions related to gastric carcinogenesis in rats with reflux through the pylorus? *J Cancer Res Clin Oncol.* **118**, 570-4.

43. Pera, M., V. F. Trastek, H. A. Carpenter, P. L. Fernandez, A. Cardesa, U. Mohr and P. C. Pairolero (1993) Influence of pancreatic and biliary reflux on the development of esophageal carcinoma. *Ann Thorac Surg.* **55**, 1386-92.

44. Goldstein, S. R., G. Y. Yang, X. Chen, S. K. Curtis and C. S. Yang (1998) Studies of iron deposits, inducible nitric oxide synthase and nitrotyrosine in a rat model for esophageal adenocarcinoma. *Carcinogenesis.* **19**, 1445-9.

45. Melo, L. L., C. D. Kruel, L. M. Kliemann, L. T. Cavazzola, L. Boeno Rda, P. C. Silber and R. S. Grossi (1999) Influence of surgically induced gastric and gastroduodenal content reflux on esophageal carcinogenesis--experimental model in Wistar female rats. *Dis Esophagus.* **12**, 106-15.

46. Chen, X., Y. W. Ding, G. Yang, F. Bondoc, M. J. Lee and C. S. Yang (2000) Oxidative damage in an esophageal adenocarcinoma model with rats. *Carcinogenesis.* **21**, 257-63.

47. Fein, M., K. H. Fuchs, H. Stopper, S. Diem and M. Herderich (2000) Duodenogastric reflux and foregut carcinogenesis: analysis of duodenal juice in a rodent model of cancer. *Carcinogenesis.* **21**, 2079-84.

48. Buttar, N. S., K. K. Wang, O. Leontovich, J. Y. Westcott, R. J. Pacifico, M. A. Anderson, K. K. Krishnadath, L. S. Lutzke and L. J. Burgart (2002) Chemoprevention of esophageal adenocarcinoma by COX-2 inhibitors in an animal model of Barrett's esophagus. *Gastroenterology.* **122**, 1101-12.

49. Lagergren, J., R. Bergstrom, A. Lindgren and O. Nyren (1999) Symptomatic gastroesophageal reflux as a risk factor for esophageal adenocarcinoma. *N Engl J Med.* **340**, 825-31.

50. Parrilla, P., R. Liron, L. F. Martinez de Haro, A. Ortiz, J. Molina and B. De Andres (1997) Gastric surgery does not increase the risk of developing Barrett's esophagus. *Am J Gastroenterol.* **92**, 960-3.

51. Vaezi, M. F. and J. E. Richter (1996) Role of acid and duodenogastroesophageal reflux in gastroesophageal reflux disease. *Gastroenterology.* **111**, 1192-9.

52. Triadafilopoulos, G. (2001) Acid and bile reflux in Barrett's esophagus: a tale of two evils. *Gastroenterology.* **121**, 1502-6.

53. Becker, J. M. (1993) Physiology of motor function of the sphincter of Oddi. *Surg Clin North Am.* **73**, 1291-309.

54. Shorter, R. G., J. L. Bollman and A. H. Baggenstoss (1959) Pressures in the common bile duct of the rat. *Proc Soc Exp Biol Med.* **102**, 682-686.

55. Salo, J. A. and E. Kivilaakso (1983) Role of bile salts and trypsin in the pathogenesis of experimental alkaline esophagitis. *Surgery.* **93**, 525-32.

56. Hori, T., K. Matsumoto, Y. Sakaitani, M. Sato and M. Morotomi (1998) Effect of dietary deoxycholic acid and cholesterol on fecal steroid concentration and its impact on the colonic crypt cell proliferation in azoxymethane-treated rats. *Cancer Lett.* **124**, 79-84.

57. Martinez-Diez, M. C., M. A. Serrano, M. J. Monte and J. J. Marin (2000) Comparison of the effects of bile acids on cell viability and DNA synthesis by rat hepatocytes in primary culture. *Biochim Biophys Acta.* **1500**, 153-60.

58. Zheng, Z. Y. and C. Bernstein (1992) Bile salt/acid induction of DNA damage in bacterial cells: effect of taurine conjugation. *Nutr Cancer.* **18**, 157-64.

59. Salo, J. A. and E. Kivilaakso (1984) Contribution of trypsin and cholate to the pathogenesis of experimental alkaline reflux esophagitis. *Scand J Gastroenterol.* **19**, 875-81.

60. Lillemoe, K. D., L. F. Johnson and J. W. Harmon (1985) Taurodeoxycholate modulates the effects of pepsin and trypsin in experimental esophagitis. *Surgery.* **97**, 662-7.

61. Kivilaakso, E., D. Fromm and W. Silen (1981) Effect of bile salts and related compounds on esophageal mucosa. *Scand J Gastroenterol Suppl.* **67**, 119-21.

62. Zhang, F., N. K. Altorki, Y. C. Wu, R. A. Soslow, K. Subbaramaiah and A. J. Dannenberg (2001) Duodenal reflux induces cyclooxygenase-2 in the esophageal mucosa of rats: evidence for involvement of bile acids. *Gastroenterology.* **121**, 1391-9.

63. Morris, C. D., G. R. Armstrong, G. Bigley, H. Green and S. E. Attwood (2001) Cyclooxygenase-2 expression in the Barrett's metaplasia-dysplasia-adenocarcinoma sequence. *Am J Gastroenterol.* **96**, 990-6.

64. Wetscher, G. J., P. R. Hinder, D. Bagchi, G. Perdikis, E. J. Redmond, K. Glaser, T. E. Adrian and R. A. Hinder (1995) Free radical scavengers prevent reflux esophagitis in rats. *Dig Dis Sci.* **40**, 1292-6.

65. Oh, T. Y., J. S. Lee, B. O. Ahn, H. Cho, W. B. Kim, Y. B. Kim, Y. J. Surh, S. W. Cho and K. B. Hahm (2001) Oxidative damages are critical in pathogenesis of reflux esophagitis: implication of antioxidants in its treatment. *Free Radic Biol Med.* **30**, 905-15.

66. Oh, T. Y., J. S. Lee, B. O. Ahn, H. Cho, W. B. Kim, Y. B. Kim, Y. J. Surh, S. W. Cho, K. M. Lee and K. B. Hahm (2001) Oxidative stress is more important than acid in the pathogenesis of reflux oesophagitis in rats. *Gut.* **49**, 364-71.

Chapter 4

Increased deoxycholic acid concentration due to bacterial overgrowth in the proximal jejunum is associated with the development of Barrett's epithelium in rat esophagus

R.R. Sital, I.A. Boere, F.W.M. de Rooij, L.H. van Damme, J.L.D. Wattimena, R.W.F. de Bruin, A.H.M. van Vliet, H. van Dekken, J.G. Kusters, E.J. Kuipers and P.D. Siersema

Departments of Gastroenterology & Hepatology, Internal Medicine, Surgery, Medical Microbiology and Pathology, Erasmus Medical Center Rotterdam

ABSTRACT

Barrett's esophagus (BE) is a precursor of esophageal adenocarcinoma. Bile reflux is considered to contribute to the development of BE, however the role of the primary and secondary bile acids in the pathogenesis of BE has not yet been elucidated. The aim of the study was to determine whether the development of BE in a rat model is associated with altered bile acid composition and bacterial overgrowth in the small intestine. Male Wistar rats were either sham-operated (controls, n=30) or received a gastrectomy with esophagojejunostomy (GEJ, n=24). BE length, bile acid composition and bacterial colonization of jejunum, ileum, caecum and colon were determined after 6 months. BE developed in 23/24 rats of the GEJ-group, whereas none of the controls developed BE. The presence of BE was associated with a fivefold increased concentration of the secondary bile acid deoxycholic acid (DCA) in the EJ-group compared to the control group (2.69 and 0.51 mmol/L, p<0.001). The length of BE correlated with the increase in DCA concentration (r=0.473, p=0.041). Only the small intestine of EJ-operated rats was colonized by *Clostridium perfringens* and *Bacteroides* spp. In conclusion, the development of experimental BE is associated with a changed bile acid composition and overgrowth of the small intestine with bacteria capable of metabolizing bile acids. This implies that in humans bacterial overgrowth, as a result of chronic use of proton pump inhibitors (PPI's), also may change bile acid composition and contribute to the development of BE in patients with reflux disease.

INTRODUCTION

Barrett's esophagus (BE) is a condition of the esophagus in which the normal squamous epithelium is replaced by columnar epithelium. BE is found in approximately 10% of patients with gastro-esophageal reflux disease (GERD) (1). The symptoms of GERD are believed to be caused by the retrograde flow of gastric and/or duodenal contents into the esophagus. Likewise, duodenogastro-esophageal reflux contributes to the development of esophagitis and BE (2, 3).

BE, as a complication of GERD, predisposes to the development of esophageal adenocarcinoma (1, 4). Recently, Lagergren et al. have reported a strong correlation between long-lasting and severely symptomatic GERD and esophageal adenocarcinoma (5). Esophageal adenocarcinoma develops in approximately 0.5 percent of patients with BE annually (6). Since 1970, the incidence of adenocarcinoma of the esophagus and esophago-gastric junction has increased dramatically in western countries, at a rate that exceeds far that of any other malignancy (7).

Presently, no therapies are known to prevent the development of adenocarcinoma in BE, Most patients are treated with antireflux therapy, either with medication or surgical intervention. Anti-reflux therapy is mainly used for the alleviation of co-existing GERD symptoms in BE patients, but has little or no effect on the length of the Barrett's epithelium or the risk of malignant degeneration in BE (8-10). Nowadays, proton pump inhibitors (PPI's) are most commonly used as anti-reflux medication. However, it has been demonstrated that the use of PPI's, particularly omeprazole, by means of a reduced gastric acid secretion, may result in bacterial overgrowth in the normally sterile stomach (11-13), and subsequently in bacterial colonization of the jejunum (14). It is also known that gastric hypochlorhydria induces bacterial overgrowth (15) and in that way can lead to an altered bile metabolism (14, 16). The implications of an altered bile metabolism for patients with GERD treated with PPI's are unknown.

The pathogenesis of Barrett's metaplasia is not fully understood, although gastroduodeno-esophageal reflux seems to play a key role. Acid and pepsin are major constituents of the gastric refluxate and studies have shown that patients with

various grades of esophagitis and BE, have an increased frequency and duration of esophageal exposure to a pH < 4 (17, 18). Recently, attention has been focused on the role of the duodenal juice in the refluxate in the pathogenesis of BE. The proposed predominant cytotoxic components of duodenal juice are bile acids and pancreatic enzymes. Of these two, bile acids are thought to be the most important factor in the pathogenesis of BE. The primary bile acids cholic acid (CA) and chenodeoxycholic acid (CDCA) are synthesized in the liver and can be dehydroxylated into the secondary bile acids deoxycholic acid (DCA) and lithocholic acid (LCA), respectively, by the bacterial flora of the colon.

In the present study, we investigated the role of bile acids in the development of BE in a rat model. Previously, it was demonstrated that BE was induced in rats by reflux of duodenal juice into the esophagus (19-21). These rat models provide a reliable tool to investigate the role of duodenal components, such as bile acids, involved in the pathogenesis of BE. In this study, a model for BE was created by performing a gastrectomy with esophagojejunostomy, which ensures the regurgitation of only duodenal juice into the esophagus, excluding any gastric factors involved in the pathogenesis of BE. Furthermore a gastrectomy mimics the effect of total suppression of gastric acid secretion, a desired effect of PPI's when administered to patients with symptoms of GERD. Therefore, we were also able to study the effect of achlorhydria on bacterial colonization and bacterial dehydroxylation of bile acids in this BE model in rats.

MATERIALS AND METHODS

Animals Sixty-six male Wistar rats (Harlan CPB, Austerlitz, the Netherlands), weighing 200-250 grams, were housed three animals per cage under standard laboratory conditions. The animals had free access to commercial semi-synthetic rat chow (Hope Farms, Woerden, the Netherlands) and tap water before surgical intervention. The rats were allowed to acclimatize for two weeks before the surgical intervention. This study was approved by the Animal Care Committee of the Erasmus Medical Center Rotterdam, the Netherlands.

Surgical technique Surgery was performed under anesthesia with ether inhalation. Rats were either sham operated or a gastrectomy with

esophagojejunostomy (EJ) was performed (Figure 1). A sham operation was performed through a median laparotomy. The abdominal wall was closed in one layer (2/0 silk sutures). The esophagojejunostomy was also performed through a median laparotomy (22). After dissection of the esophagus from the stomach, a gastrectomy was performed as described by Santini et al. (23). The esophagus was anastomized end-to-site (uninterrupted 7/0 silk sutures) to the jejunum approximately 3 cm distal from the ligament of Treitz. The abdominal wall was closed in one layer (2/0 silk sutures). After surgery, the animals received drinking water ad libitum and had access to rat chow 24 hours after the operation.
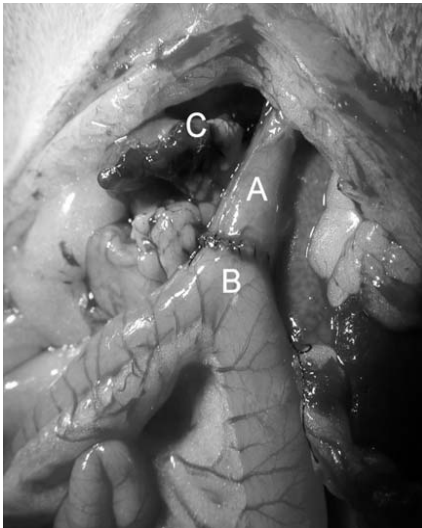
Figure 1: Total gastrectomy with esophagojejunostomy in EJ-operated rats. (A: Esophagus, B: Proximal Jejunum, and C: Duodenum)

Design of the study One week after the operation, sham-operated animals (n=30, group I) and EJ-operated animals (n=36, group II) received drinking water, which was acidified to pH 1.8 (19), supplemented with pepsin to a final concentration of 500 U/ml (Sigma, Steinheim, Germany). Rats in the EJ-group received the equivalent of 5 mg iron sorbitol (Jectofer; AstraZeneca, Zoetermeer, the Netherlands) and 0.5 mg/kg Hydrocobamine® (hydroxycobalamine HCL; Byk, Zwanenburg, the Netherlands), administered intramuscularly once every 6 weeks, until the end of the experiment.

Histological examination Animals were weighed just before sacrifice. The esophagus, the anastomosis and the proximal jejunum were inspected and excised *en bloc*. The esophagus was then opened longitudinally and inspected. Subsequently, the specimen was rolled up from distal to proximal, as a Swiss roll (24) and preserved by formalin fixation. The formalin fixed specimens were embedded in paraffin, sectioned (5 μm) and stained with haematoxylin and eosin (H&E). Six slices from each esophageal specimen representing the entire length of the esophagus were used for histopathological examination. Histopathological examination was performed independently by 3 investigators (RRS, IAB and HvD). Barrett's epithelium was defined as the presence of intestinal metaplasia (with goblet cells) in the esophagus (25). The longest segment of Barrett's epithelium (if present) was measured in each of the six H&E slides for each individual rat. Subsequently, the mean length of Barrett's epithelium with standard deviation was then calculated from the six H&E slices for each rat.

Bacterial colonization Bacterial colonization was determined in 3 EJ- and 3 sham-operated rats. Before sacrifice, three samples for culture were taken from the jejunum, ileum, caecum and ascending colon from each rat. The samples were immediately plated on blood agar, MacConkey agar, Brucella blood agar, Bacteroides bile esculine agar, and kanamycin/vancomycine agar (Becton Dickinson, Alphen aan de Rijn, the Netherlands). The plates were then transferred to a 37°C incubator and cultured under aerobic (24 and 48 hours) and anaerobic (48 and 120 hours) conditions. After incubation, pure cultures were isolated from the cultured bacteria and these were morphologically reviewed. The Vitek system (BioMerieux) was subsequently used for final identification of the cultured bacteria (26).

Composition of rat bile

Bile was collected by cannulating the common bile duct for approximately 1 hour under anesthesia before the rats were sacrificed. Total concentration of bile acids were analyzed enzymatically, according to Mashige (27). Concentrations of CA, CDCA, DCA and LCA in bile samples were determined. This was performed on a HP 5880 gaschromatograph equipped with a split/ Splitless injector (Hewlett Packard, Amsterdam, the Netherlands) and a 15 m, 0.22 mm ID fused silica capillary column coated with 0.2 μm CP-Sil19CB (Chrompack, Middelburg, the Netherlands). Ten μl

23-Nordeoxycholic acid (5.3 mmol/L) (Steraloids Inc. Wilton, N.H. USA) was added as an internal standard to 100 μl of rat bile. Bile acids were enzymatically hydrolyzed with cholylglycinehydrolase (Sigma, Aldrich Chemie, Zwijndrecht, the Netherlands) over 16 hours at 37°C (28). Subsequently, bile acids were extracted twice with chloroform and the extract dried under nitrogen. The unconjugated bile acids were then derivatisized to their methylesteracetate derivatives according to Lillington et al (29). Gaschromatographic conditions were as follows: carrier gas (Helium) 2 ml min^{-1}; injector and detector temperature 300°C; oven temperature 250°C during 2 minutes and increased to 290°C at 8°C min^{-1}. One μl split injection was done with a split ratio of 30:1.

Statistical analysis The animal weight and the length of Barrett's epithelium in rats were expressed as mean ± standard deviation (SD). Comparisons were made using the Wilcoxon-test. A difference was considered significant at *P* values of $<$ 0.05. The correlation between bile acid concentrations and length of Barrett's epithelium was calculated using the Pearson test.

RESULTS

General observations

In the sham operated group, all rats completed the study. In the 36 EJ operated group, 12 (33%) rats died before the endpoint of the study (6 months) and these animals were not included in the final statistical analysis. Of these rats, 8 died or were killed in a moribund condition from reflux-related complications, such as malnutrition and pneumonia. Furthermore, one rat died from an anastomotic stenosis, one of pneumonia and two from unknown causes. The animals of the sham group gained weight until the end of the experiment (from 272 ± 11 to 605 ± 62 grams) and their weight was significantly higher than in the experimental group (weight 277 ± 70 grams) at the time of sacrifice (p<0.001).

### Concentration of different bile acids in the bile pool

The concentrations of the primary bile acids (CA and CDCA) and the secondary bile acids (DCA and LCA) were determined in the bile samples of all rats (Table 1). The concentration of CA was not significantly affected when EJ-rats were compared with

sham operated animals (p=0.100). The CDCA concentration in the EJ-group was increased by almost two-fold compared with sham-operated rats (p=0.021).

	sham	GEJ	p-value
CA	10.55 ± 4.72	13.55 ± 5.33	p=0.1
CDCA	0.59 ± 0.34	1.01 ± 0.74	p=0.02
DCA	0.51 ± 0.29	2.69 ± 1.69	p<0.001
LCA	n.d.*	n.d.*	

Table 1 Cholic acid (CA), chenodeoxycholic acid (CDCA), deoxycholic acid (DCA) and lithocholic acid (LCA) concentrations (mmol/l (mean ± SD)) in sham- and EJ-operated animals. *not detectable

In contrast to CA, its bacterial product DCA showed a five-fold increase in the EJ-operated group when compared with the sham-operated group (p< 0.001) (Figure 2). LCA concentration in bile was below detection levels.
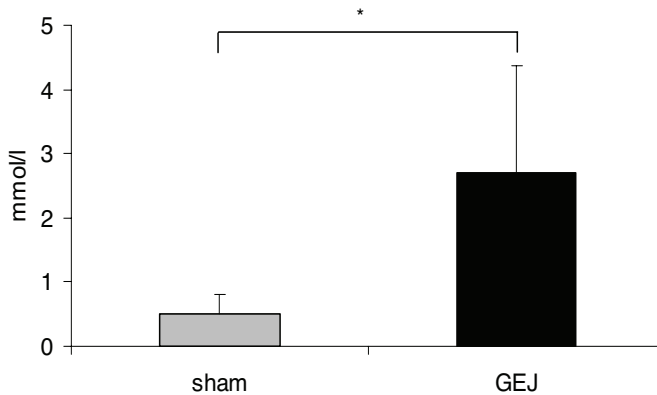
Figure 2 Deoxycholic acid (DCA) concentration in bile of sham-operated (▢) and EJ-operated rats (■) 6 months after operation.
* P<0.001 sham- vs. EJ-operated rats using the Wilcoxon-test.

Development of Barrett's epithelium in EJ-rats

After a period of 6 months, none of the 30 sham-operated animals had developed Barrett's epithelium. However in the EJ-group, 23 of the 24 rats had developed Barrett's epithelium (Figure 3). The mean length (± SD) of Barrett's epithelium in the

EJ-group was 3.73 ± 1.72 mm (range: 0- 6.49 mm). The length of the Barrett's epithelium correlated with the DCA concentration in bile (r=0.473, p=0.041) (Figure 4), whereas no significant correlation between the length of BE and the CA or the CDCA concentration was found (r=0.246 (p=0.310) and r=0.165 (p=0.499), respectively).
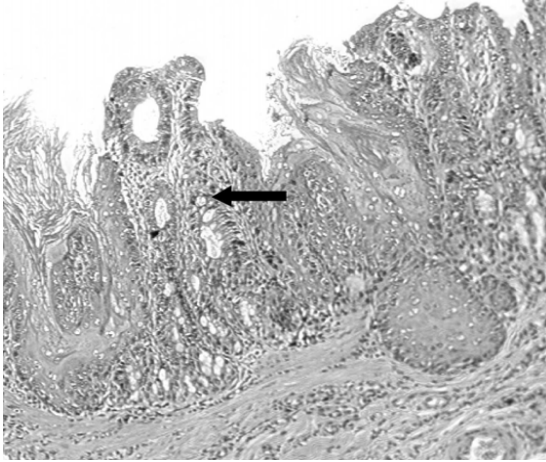
Figure 3 Light microscopical view of columnar epithelium with intestinal metaplasia and characteristic goblet cells (arrow) in the distal esophagus of a EJ-operated rat 6 months after operation (x40, H&E staining).
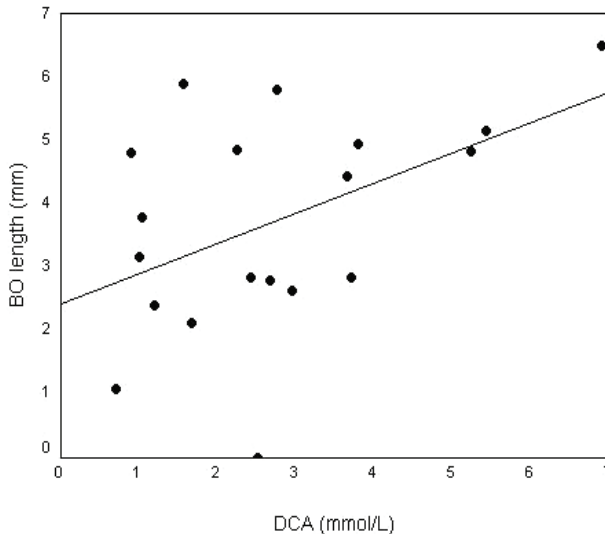
Figure 4 Correlation between deoxycholic acid (DCA) concentration and the length of Barrett's epithelium. R=0.473 (P=0.041) using the Pearson test.

Bacterial overgrowth in the jejunum of achlorhydric rats

All three EJ-operated rats were colonized with aerobic and anaerobic bacteria in the jejunum, whereas in the jejunum of the sham-operated animals only aerobic were present. *Clostridium perfringens* and *Bacteroides* species were the only anaerobic bacteria present in the cultures of the jejunum of the EJ-rats. The jejunum was colonized by *C. perfringens* in all three EJ-operated rats, whereas *Bacteroides* spp*.* were present in two EJ-rats. Samples taken from the ileum, caecum and colon yielded both aerobic and anaerobic in the sham- and EJ-operated animals. In all three EJ-rats, anaerobic cultures of the ileum revealed the presence of *C. perfringens* and *Bacteroides* spp. In the sham-operated group, the ileum of two rats were colonized by *Bacteroides* spp., whereas no *C. perfringens* was present in the ileum of this group. No single predominant bacterium species were found in the aerobic cultures from the jejunum and ileum in the sham or EJ-operated rats. The caecum and colon of both sham-operated and EJ-rats were colonized with a variety of aerobic and anaerobic bacterial species (Table 2).

organ	sham (n=3)	EJ (n=3)
jejunum		Clostridium perfringens
		Bacteroides spp.
ileum		Clostridium perfringens
	Bacteroides spp.	Bacteroides spp.
caecum	Bacteroides spp.	Bacteroides spp.
	Prevotella corporis	Prevotella corporis
	Fusobacterium varium	Clostridium perfringens
		Fusobacterium nucleatum
ascend. colon	*	*

Table 2 Bacterium species identified from the anaerobic cultures. Samples were taken from the jejunum, ileum, caecum and ascending colon in sham- and EJ-operated rats. *mixed flora

DISCUSSION

Since the incidence of adenocarcinoma of the esophagus has increased dramatically over the past two decades, its precursor BE has become the focus of several studies.

Although duodenogastro-esophageal reflux is a recognized risk factor in the pathogenesis of BE, it remains unclear which component of the refluxate is responsible for the induction of BE.

In the present study, induction of chronic reflux of duodenal juice resulted in the development of BE in rats. Furthermore, the concentration of DCA correlated with the length of BE that was induced in EJ-operated rats. This suggests that in duodenal juice, the secondary bile acid DCA is involved in the pathogenesis of BE. In animal studies, it has been shown that exposure of colonic mucosa to bile acids, including DCA, resulted in increased epithelial cell proliferation. In addition, bile acids promoted the development of colonic tumors by chemical carcinogens (30, 31). In the colon, the secondary bile acid DCA has been associated with DNA damage and DCA has been shown to negatively influence apoptotic mechanisms. It has been proposed that DCA in that way acts as a tumor promotor (32). Furthermore, cyclooxygenase-2, which is implicated in colorectal, gastric and esophageal carcinogenesis could be induced by CDCA or DCA in human esophageal carcinoma cell lines (33, 34). Moreover, in BE organ cultures, a bile acid mixture enhanced cell proliferation of Barrett's epithelial cells (35). More importantly, in an aspiration study by Nehra et al. it was found that patients with Barrett's esophagus or a stricture in the esophagus had significantly higher concentrations of DCA in esophageal aspirates compared to asymptomatic subjects (36) indicating the possible role that DCA plays in the pathogenesis of BE.

Normally the colon is the only site where the secondary bile acids DCA and LCA are formed from the primary bile acids CA and CDCA, respectively. The conversion of primary bile acids to secondary bile acids is mediated by anaerobic bacteria. In our study, a profound increase of DCA concentration in the bile pool was seen in all EJ-operated rats that developed Barrett's epithelium. It is known that the loss of gastric acid production, by means of a gastrectomy, results in bacterial overgrowth. Cultures from the jejunum of EJ-operated rats revealed the presence of *C. perfringens* and *Bacteroides* spp, which are both capable of bile acid dehydroxylation (37, 38). Therefore, bacterial overgrowth of the normally sterile jejunum by *C. perfringens* and *Bacteriodes* spp. most likely resulted in the increased concentration of DCA found in bile of EJ-operated rats.

If loss of gastric acid production can lead to an altered bile metabolism in man, this could have major implications for patients who use PPI's. The use of PPI's has been demonstrated to be associated with bacterial overgrowth of the small intestine. Both Shindo et al. and Theisen et al. have reported that the use of PPI's resulted in bacterial overgrowth with an increased concentration of unconjugated bile acids in patients (14, 16). However in those studies the concentrations of the more toxic secondary bile acids were not determined.

In conclusion, our finding that the loss of acid production leads to the formation of increased DCA levels in rats may have important implications for individuals with a decreased acid production, e.g., as induced by long term use of PPI's. Especially since the incidence of BE in the Western world has increased in the last two decades, concomitant with the introduction of acid inhibiting drugs, such as H_2-receptor antagonists initially, and PPI's more recently. If bile acids really are the pathogenetic stimuli which cause metaplasia in the esophagus and if reduced acid production, by use of PPI's or gastric atrophy, leads to bacterial overgrowth and thus increased dehydroxylation of bile acids, then the safety of PPI's prescribed to these patients should be reconsidered. Further studies are needed to investigate the role of PPI's on bile acid metabolism, especially in patients who chronically receive PPI's as a treatment for gastro-esophageal reflux disease.

REFERENCES

1. Spechler, S. J. and R. K. Goyal (1996) The columnar-lined esophagus, intestinal metaplasia, and Norman Barrett. *Gastroenterology.* **110**, 614-21.

2. Kauer, W. K., J. H. Peters, T. R. DeMeester, A. P. Ireland, C. G. Bremner and J. A. Hagen (1995) Mixed reflux of gastric and duodenal juices is more harmful to the esophagus than gastric juice alone. The need for surgical therapy re- emphasized. *Ann Surg.* **222**, 525-31; discussion 531-3.

3. Gillen, P., P. Keeling, P. J. Byrne, M. Healy, R. R. O'Moore and T. P. Hennessy (1988) Implication of duodenogastric reflux in the pathogenesis of Barrett's oesophagus. *Br J Surg.* **75**, 540-3.

4. Spechler, S. J. (2002) Clinical practice. Barrett's Esophagus. *N Engl J Med.* **346**, 836-42.

5. Lagergren, J., R. Bergstrom, A. Lindgren and O. Nyren (1999) Symptomatic gastroesophageal reflux as a risk factor for esophageal adenocarcinoma. *N Engl J Med.* **340**, 825-31.

6. Shaheen, N. J., M. A. Crosby, E. M. Bozymski and R. S. Sandler (2000) Is there publication bias in the reporting of cancer risk in Barrett's esophagus? *Gastroenterology.* **119**, 333-8.

7. Blot, W. J., S. S. Devesa, R. W. Kneller and J. F. Fraumeni, Jr. (1991) Rising incidence of adenocarcinoma of the esophagus and gastric cardia. *Jama.* **265**, 1287-9.

8. Sampliner, R. E., H. S. Garewal, M. B. Fennerty and M. Aickin (1990) Lack of impact of therapy on extent of Barrett's esophagus in 67 patients. *Dig Dis Sci.* **35**, 93-6.

9. Sagar, P. M., R. Ackroyd, K. B. Hosie, J. E. Patterson, C. J. Stoddard and A. N. Kingsnorth (1995) Regression and progression of Barrett's oesophagus after antireflux surgery. *Br J Surg.* **82**, 806-10.

10. Ortiz, A., L. F. Martinez de Haro, P. Parrilla, G. Morales, J. Molina, J. Bermejo, R. Liron and J. Aguilar (1996) Conservative treatment versus antireflux surgery in Barrett's oesophagus: long-term results of a prospective study. *Br J Surg.* **83**, 274-8.

11. Thorens, J., F. Froehlich, W. Schwizer, E. Saraga, J. Bille, K. Gyr, P. Duroux, M. Nicolet, B. Pignatelli, A. L. Blum, J. J. Gonvers and M. Fried (1996) Bacterial overgrowth during treatment with omeprazole compared with cimetidine: a prospective randomised double blind study. *Gut.* **39**, 54-9.

12. Karmeli, Y., R. Stalnikowitz, R. Eliakim and G. Rahav (1995) Conventional dose of omeprazole alters gastric flora. *Dig Dis Sci.* **40**, 2070-3.

13. Freston, J. W. (1997) Long-term acid control and proton pump inhibitors: interactions and safety issues in perspective. *Am J Gastroenterol.* **92**, 51S-55S; discussion 55S-57S.

14. Shindo, K., M. Machida, M. Fukumura, K. Koide and R. Yamazaki (1998) Omeprazole induces altered bile acid metabolism. *Gut.* **42**, 266-71.

15. Sanduleanu, S., D. Jonkers, A. De Bruine, W. Hameeteman and R. W. Stockbrugger (2001) Non-Helicobacter pylori bacterial flora during acid-suppressive therapy: differential findings in gastric juice and gastric mucosa. *Aliment Pharmacol Ther.* **15**, 379-88.

16. Theisen, J., D. Nehra, D. Citron, J. Johansson, J. A. Hagen, P. F. Crookes, S. R. DeMeester, C. G. Bremner, T. R. DeMeester and J. H. Peters (2000) Suppression of gastric acid secretion in patients with gastroesophageal reflux disease results in gastric bacterial overgrowth and deconjugation of bile acids. *J Gastrointest Surg.* **4**, 50-4.

17. Stein, H. J., A. P. Barlow, T. R. DeMeester and R. A. Hinder (1992) Complications of gastroesophageal reflux disease. Role of the lower esophageal sphincter, esophageal acid and acid/alkaline exposure, and duodenogastric reflux. *Ann Surg.* **216**, 35-43.

18. Gillen, P., P. Keeling, P. J. Byrne and T. P. Hennessy (1987) Barrett's oesophagus: pH profile. *Br J Surg.* **74**, 774-6.

19. Seto, Y. and O. Kobori (1993) Role of reflux oesophagitis and acid in the development of columnar epithelium in the rat oesophagus. *Br J Surg.* **80**, 467-70.

20. Clark, G. W., T. C. Smyrk, S. S. Mirvish, M. Anselmino, Y. Yamashita, R. A. Hinder, T. R. DeMeester and D. F. Birt (1994) Effect of gastroduodenal juice and dietary fat on the development of Barrett's esophagus and esophageal neoplasia: an experimental rat model. *Ann Surg Oncol.* **1**, 252-61.

21. Ireland, A. P., J. H. Peters, T. C. Smyrk, T. R. DeMeester, G. W. Clark, S. S. Mirvish and T. E. Adrian (1996) Gastric juice protects against the development of esophageal adenocarcinoma in the rat. *Ann Surg.* **224**, 358-70; discussion 370-1.

22. M Levrat, L. R., Kirschbaum G. (1962) Esophagitis produced by reflux of duodenal contents in rats. *Am J Dig Dis.* **7**, 564-573.

23. Santini A, M. E., Baccarini M. (1984) Jejunal transposition after total or partial gastrectomy - an experimental model in the rat. In Handbook of microsurgery Vol. II. (Edited by W. Olszewski), pp. CRC press, Boca Raton, Florida.

24. Moolenbeek, C. and E. J. Ruitenberg (1981) The "Swiss roll": a simple technique for histological studies of the rodent intestine. *Lab Anim.* **15**, 57-9.

25. Buttar, N. S., K. K. Wang, O. Leontovich, J. Y. Westcott, R. J. Pacifico, M. A. Anderson, K. K. Krishnadath, L. S. Lutzke and L. J. Burgart (2002) Chemoprevention of esophageal adenocarcinoma by COX-2 inhibitors in an animal model of Barrett's esophagus. *Gastroenterology.* **122**, 1101-12.

26. Reisner BS, Woods GL, Thomson RB jr., Larone DH, Garcia LS and S. RY (1999) General issues in clinical microbiology: General processing. In Manual of clinical microbiology Vol. (Edited by T. FC), pp. 64-104. ASM Press, Washington.

27. Mashige, F., K. Imai and T. Osuga (1976) A simple and sensitive assay of total serum bile acids. *Clin Chim Acta.* **70**, 79-86.

28. Karlaganis G, B. G. (1979) Determination of bile acids in serum by capillary gas-liquid chromatography. *Clin Chim Acta.* **92**, 19-26.

29. Lillington, J. M., D. J. Trafford and H. L. Makin (1981) A rapid and simple method for the esterification of fatty acids and steroid carboxylic acids prior to gas-liquid chromatography. *Clin Chim Acta.* **111**, 91-8.

30. Deschner, E. E., B. I. Cohen and R. F. Raicht (1981) Acute and chronic effect of dietary cholic acid on colonic epithelial cell proliferation. *Digestion.* **21**, 290-6.

31. Hori, T., K. Matsumoto, Y. Sakaitani, M. Sato and M. Morotomi (1998) Effect of dietary deoxycholic acid and cholesterol on fecal steroid concentration and its impact on the colonic crypt cell proliferation in azoxymethane-treated rats. *Cancer Lett.* **124**, 79-84.

32. Glinghammar, B., H. Inoue and J. J. Rafter (2002) Deoxycholic acid causes DNA damage in colonic cells with subsequent induction of caspases, COX-2 promoter activity and the transcription factors NF-kB and AP-1. *Carcinogenesis.* **23**, 839-45.

33. Zhang, F., K. Subbaramaiah, N. Altorki and A. J. Dannenberg (1998) Dihydroxy bile acids activate the transcription of cyclooxygenase-2. *J Biol Chem.* **273**, 2424-8.

34. Zhang, F., N. K. Altorki, Y. C. Wu, R. A. Soslow, K. Subbaramaiah and A. J. Dannenberg (2001) Duodenal reflux induces cyclooxygenase-2 in the esophageal mucosa of rats: evidence for involvement of bile acids. *Gastroenterology.* **121**, 1391-9.

35. Kaur, B. S., R. Ouatu-Lascar, M. B. Omary and G. Triadafilopoulos (2000) Bile salts induce or blunt cell proliferation in Barrett's esophagus in an acid-dependent fashion. *Am J Physiol Gastrointest Liver Physiol.* **278**, G1000-9.

36. Nehra, D., P. Howell, C. P. Williams, J. K. Pye and J. Beynon (1999) Toxic bile acids in gastro-oesophageal reflux disease: influence of gastric acidity. *Gut.* **44**, 598-602.

37. Uchida, K., T. Satoh, S. Narushima, K. Itoh, H. Takase, K. Kuruma, H. Nakao, N. Yamaga and K. Yamada (1999) Transformation of bile acids and sterols by clostridia (fusiform bacteria) in Wistar rats. *Lipids.* **34**, 269-73.
38. Lewis, R. and S. Gorbach (1972) Modification of bile acids by intestinal bacteria. *Arch Intern Med.* **130**, 545-9.

Chapter 5

Monitoring in situ dosimetry and PpIX fluorescence photobleaching in the normal rat esophagus during 5-aminolevulinic acid photodynamic therapy

I.A. Boere, D.J. Robinson, H.S. de Bruijn, J. van den Boogert, H.W. Tilanus, H.J.C.M. Sterenborg, R.W.F. de Bruin

Departments of Surgery and Radiation Oncology, Photodynamic Therapy & Optical Spectroscopy Research Program, Erasmus Medical Center Rotterdam

ABSTRACT

Experimental therapies for Barrett's esophagus like 5-aminolevulinic acid based photodynamic therapy aim to ablate the premalignant Barrett's epithelium. However, the reproducibility of the effects should be improved to optimize treatment. Accurate irradiation with light of a proper wavelength (633 nm), fluence and fluence rate, has shown to be critical for successful ALA-PDT. We have used in-situ light dosimetry to adjust the fluence rate measured within the esophagus for individual animals and monitored PpIX fluorescence photobleaching simultaneously. Rats were administered 200 mg kg^{-1} ALA (n=14) or served as control (n=7). Animals were irradiated with an in-situ measured fluence rate of 75 mW cm^{-2} and a fluence of 54 J cm^{-2}. This more accurate method of light dosimetry did not decrease the variation in tissue response. Large differences were also observed in the dynamics of PpIX fluorescence photobleaching in animals that received the same measured illumination parameters. We found that higher PpIX fluorescence photobleaching rates corresponded with more epithelial damage, whereas lower rates corresponded with no response. A two-phased decay in PpIX fluorescence could be identified in the response group, with a rapid initial phase followed by a slower rate of photobleaching. Non-responders did not show the rapid initial decay and had a significantly lower rate of photobleaching during the second phase of the decay (p=0.012).

INTRODUCTION

In the past two decades the incidence of esophageal adenocarcinoma has increased dramatically, while survival rates have remained poor (1, 2). The majority of these esophageal carcinomas are thought to originate from Barrett's esophagus, which is defined as intestinal metaplasia of the epithelium (3). Therefore, patients with Barrett's esophagus undergo regular endoscopic follow up. Esophageal resection is the treatment of choice for esophageal cancer, but an experimental alternative to surgery for intraepithelial carcinomas or precursor lesions is 5-aminolevulinic acid photodynamic therapy (ALA-PDT). Prior to treatment, 5-aminolevulinic acid (ALA) is administered, which induces the accumulation of the endogenous photosensitizer protoporphyrin IX (PpIX) (4). Subsequently, the esophagus is illuminated with light of a suitable wavelength (633 nm) at a defined fluence and fluence rate. Activated oxygen species, generated by ALA-PDT, notably singlet oxygen, act on critical cellular components resulting in epithelial ablation (5-9). Since 1996, when the first clinical study with ALA-PDT for Barrett's esophagus was published (10), complete eradication of dysplastic cells has been accomplished (11), but in the majority of patients some Barrett's epithelium remains. Re-epithelization with normal squamous epithelium is observed in 68-89% of patients with a median reduction in area of only 30% (12-15). Therefore, treatment of Barrett's esophagus by ALA-PDT should be improved. The efficacy of ALA-PDT is determined by a variety of parameters: the distribution and concentration of the photosensitizer at the time of treatment, the wavelength of the light, the fluence and irradiance, the availability of oxygen within the illuminated volume and the optical properties of the tissue at the treatment wavelength. Using standardized treatment parameters, results of ALA-PDT should be subject to minimal variation, but in a previous study on ALA-PDT for the normal rat esophagus, large variations in outcome were seen using fixed *ex-vivo* laser settings (data not shown). Both no response and complete ablation of the epithelium were found, using the same drug and light parameters (200 mg kg^{-1} ALA, 633 nm wavelength, 7.5 J cm^{-2} and 30 mW cm^{-2}). A major consideration during PDT of hollow organs such as the esophagus is the contribution of tissue back-scattered light to the true fluence rate within the target tissue. This phenomenon has been denoted as the integrating sphere effect (16, 17). Its magnitude is determined by the optical properties of the tissue and is expressed by build up factor beta (β). However, β can vary significantly between tissues and individuals and therefore lead to wide

variations in true fluence rate, which may be an explanation for the dramatic differences in response observed. Since the response of tissues to ALA-PDT has previously been shown to be highly dependent on the fluence rate, it is important to accurately standardize this illumination parameter (18). The aims of the present study therefore were to determine if the reproducibility of the PDT response could be improved by: standardizing the *in-situ* fluence rate and thus the fluence delivered and by monitoring PpIX fluorescence photobleaching during ALA-PDT. Monitoring the fluence rate in-situ and adjusting the intensity of the source fiber accordingly should compensate for variations in optical properties of the esophageal epithelium between individual animals.

MATERIALS AND METHODS

Study design. A total of 21 normal male Wistar rats (Harlan, The Netherlands) were included in this study and used for ALA-PDT of the esophagus. The "Committee on Animal Research" of the Erasmus MC Rotterdam approved the experimental design. Prior to treatment, rats were fed on a diet free of chlorophyll (Hope farms, The Netherlands) for two weeks in order to minimize the autofluorescence emission from the esophagus centered on 675 nm, attributed to a breakdown product of chlorophyll, pheophorbide-α (19, 20). This fluorescence emission overlaps with the fluorescence of PpIX and its photoproducts; moreover pheophorbide-α itself is a photosensitizer. Animals were randomized to 3 groups; treatment groups A (n=9) and B (n=6) received ALA and were illuminated 2 h hereafter. Control group C (n=6) received no ALA. ALA (Sigma Chemical Company, Zwijndrecht, The Netherlands, purity 98%) was dissolved in phosphate buffered saline (pH 7.0) and administered to all animals by oral gavage 2 h before illumination (200 mg kg^{-1}). The esophagus was irradiated with a measured fluence rate of 75 mW cm^{-2} and a total measured fluence of 54 J cm^{-2}, comparable to previous experiments using ex-situ laser settings (30 mW cm^{-2} and 22.7 J cm^{-2}, with mean β 2.4) (21, 22). The control group and treatment group A were sacrificed after 48 h to measure PDT damage, treatment group B was sacrificed after 3 weeks to study the recovery of the esophageal tissue. Fluorescence spectroscopy was performed before and during ALA-PDT. Rats were anaesthetized with ether inhalation during measurement of the autofluorescence spectrum and with a combination of ketamin and xylazin (50 and 5 mg kg^{-1} im) during treatment. After

treatment a single dose of buprenorphin (0.05 mg kg^{-1} im) was administered as analgesic.

Illumination set up. A balloon catheter was used to illuminate the circumference of the esophagus homogeneously. The device consisted of an inflatable cylindrical balloon attached to one end of a semi-flexible catheter (Cordis, Roden, The Netherlands). The optically clear balloon measured 3 mm in diameter and was 40 mm long when inflated with 0.6 ml of air. A 200 micron fiber with a 10 mm cylindrically diffusing tip (uniformity ± 6.57%) (Cardiofocus (formerly Rare Earth Medical), Norton, MA, USA) was placed in the center of the balloon and thus centrally in the esophagus. The illumination was performed using 633 nm light (600 Series Dye Module pumped by a KTP/532 laser, Laserscope, San Jose, CA, USA) interrupted for a period of 3 s 405 nm light (0.5 mW cm^{-2}) (LG Laser Technologies, Klienoostheim, Germany) every 30 s for acquisition of fluorescence spectra using a shutter system. In order to measure the fluence rate in the esophagus, and acquire fluorescence spectra from the esophageal wall during illumination, two 100 μm isotropic probes (Cardiofocus, Norton, MA, USA) were attached to the outer surface of the balloon, in direct contact with the esophageal wall. The probes were fixed with tape at the measured center of the linear diffuser before intra-esophageal placement. One isotropic probe was connected to a device that enabled the acquisition of real time fluence (rate) data (23). The other isotropic probe was connected to a fiber optic spectrograph (Avantes of Ocean Optics, Eerbeek, Netherlands) (figure 1). The isotropic detectors were calibrated in air at the start of each treatment day, using an integrating sphere. A correction factor of 1.07 was used to account for the index of refraction mismatch at the air-tissue interface between the inflated balloon and the esophageal wall. To test the inter-sample variation of the fluence rate measurements, the balloon catheter with the isotropic probe and cylindrical diffuser was moved in 1 cm increments first up and then back down in the esophagus. At each position the balloon was deflated and re-inflated before each measurement to 760 mm Hg and 380 mm Hg. The fluence rate was averaged at each point for a period of at least 20 s. Figure 2 shows that the mean fluence rates at three different places in the esophagus are comparable. The average measured fluence rate was 72.4 ± 5.0 mW cm^{-2} at 760 mm Hg and 67.7 ± 5.4 mW cm^{-2} at 380 mm Hg.
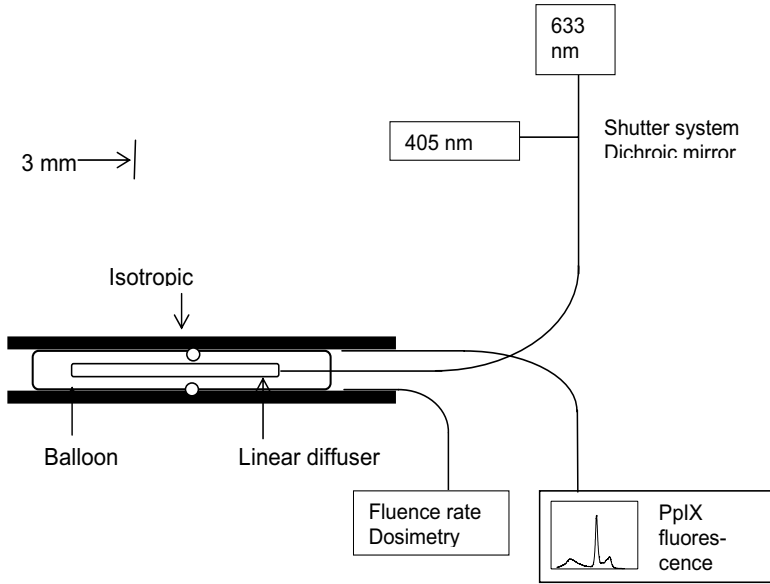
Figure 1 Experimental set up for PDT. Light emitted by the KTP/dye laser is transmitted through a connecting fiber to the treatment fiber. During 3 s dark intervals in the illumination, light emitted by the 405 nm laser is transmitted to the treatment fiber for fluorescence collection. Two isotropic probes are attached to the transparent balloon and connected to a dosimetry device and a spectrograph, respectively.
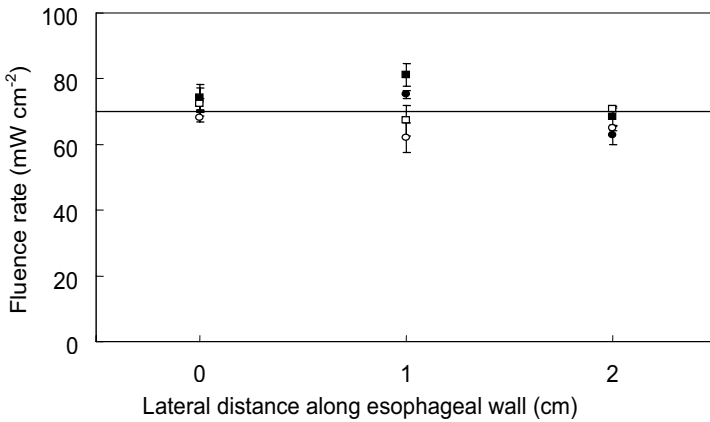
Figure 2 The variability in measured fluence rate at 3 positions within the esophagus of a single animal. The fiber probe was moved in 1 cm increments first up (closed symbols) and then back down (open symbols) the esophagus. At each position the balloon was inflated to 380 mm Hg (squares) 760 mm Hg (circles). The average measured fluence rate was 72.4 ± 5.0 mW cm^{-2} at 760 mm Hg and 67.7 ± 5.4 mW cm^{-2} at 380 mm Hg. The fluence rate was averaged for a period of at least 20 s for each measurement.

Light dosimetry. At the start of illumination, the output power of the laser was adjusted so that the measured fluence rate at the esophageal wall was 75 mW cm^{-2}. During ALA-PDT the fluence rate was monitored continuously using the isotropic probe. The illumination was stopped when a fluence of 54 J cm^{-2} was reached. After treatment the light output from the illumination fiber in the balloon catheter was determined using an integrating sphere. The build up factor β of the esophageal wall is defined by the ratio of the true fluence rate to the unscattered incident fluence rate.

Fluorescence measurements. Fluorescence emission spectra (550-750 nm) were acquired before ALA administration, pre and post illumination and at 30 s intervals during the therapeutic illumination. During the acquisition of fluorescence spectra the therapeutic illumination was interrupted for a period of 3 s. Integration times ranged between 1 and 1.5 s depending on the PpIX fluorescence intensity. Since the animals recovered between autofluorescence and sensitizer fluorescence measurements, care was taken to use the same area of the esophagus that was to subsequently undergo PDT by marking the balloon catheter. Fluorescence spectra were corrected for differences in power of the 405 nm laser. The spectra displayed the characteristic protoporphyrin signature and were analyzed in the same way as described previously (24), based on the method described by Foster and his co-workers, although reference spectra were not taken nor corrected for (25-27). Each spectrum was analyzed as a linear combination of basis fluorescence spectra using a singular value decomposition (SVD) algorithm. The 3 basis fluorescence spectra used in this analysis were averaged from 15 animals in 3 states (n=5 in each): the autofluorescence of normal rat esophagus, PpIX and the hydroxyaldehyde chlorine photoproducts of PpIX.

Handling of the specimens and quantification of PDT damage. Animals were weighed and sacrificed by exsanguination. The thoracic and abdominal cavities were inspected macroscopically and the esophagus was excised. The esophagus was opened longitudinally, examined for macroscopic abnormalities and the specimen was rolled up from distal to proximal as a Swiss roll and fixed in formalin. The specimens were embedded in paraffin wax, sectioned and stained with haematoxylin and eosin (H&E). Two investigators, blinded from the treatment, microscopically

evaluated the sections. Damage was scored semi-quantitatively on a scale from 0 to 3 for the separate esophageal layers. Ablation of the epithelium was scored as complete ablation when there were no epithelial cell layers left (0 = normal, 1 = >1 cell layer left, 2 = 1 cell layer left, 3 = complete ablation). Edema of the submucosa was scored based on the thickness of the submucosa (0 = normal 50-100 μm, 1 = 2 times thicker than normal, 2 = 3-5 times thicker, 3 = > 5 times thicker). Inflammation of the submucosa and muscularis propria was scored on the basis of the amount of inflammatory cells (mostly lymphocytes) using a grid with a 40x magnification (0 = none; 1 = <1 per grid; 2 = 1-2 per grid, 3 = > 2 grid). The severity of the necrosis of the muscularis propria was scored on the basis of the presence of vital muscle cells (0 = 100%; 1 = >75%; 2 = > 25%; 3 = < 25%).

Data analysis. The measured fluence rate at the start of ALA-PDT was used for calculation of means and standard deviations. A Student's t-test was used to compare the fluence and fluence rate between the treatment groups. A p-value < 0.05 was considered significant. PpIX fluorescence photobleaching data are normalized to the pre-illumination PpIX fluorescence intensity and plotted against the measured fluence. The reciprocal of the normalized PpIX fluorescence intensity was plotted in order to illustrate the kinetics of photobleaching (28).

RESULTS
ALA-PDT induced damage
All rats including the control group had lost 20-40 g of their initial weight after 2 days post PDT. However, this did not influence their well-being and after 3 weeks the animals had exceeded their pre-treatment weight. In group A the liver of the rats showed macroscopic damage to an area surrounding the esophagus of 0.4-1 cm^2. In the control group C and the treatment group B none of the rats showed any macroscopic or microscopic damage to the esophagus. In treatment group A, sacrificed at 48 h post PDT, a wide range of damage was observed, varying between no damage, edema of the esophageal wall and redness and erosion of the esophageal surface. Microscopically there was no damage to the epithelium in 3 rats and complete ablation of the epithelium in 6 animals. In table 1 the tissue damage scores for the esophageal layers are shown for each rat individually. The mean epithelial damage score was 2.0 ± 1.5.

Group A	Ep ablation	SM edema	SM inflamm	Musc inflamm	Musc necrosis
A 1■	3	3	2	3	3
A 2●	3	3	2	3	3
A 3△	0	0	0	0	0
A 4□	0	0	0	0	0
A5o	0	1	0	1	1
A6◆	3	2	2	3	2
A7+	3	1	2	2	2
A8▲	3	1	2	3	1
A9x	3	1	2	3	2
Total					
A	2.0 ± 1.5	1.3 ± 1.12	1.3 ± 1.0	2.0 ± 1.3	1.6 ± 1.1
B	0 ± 0	0 ± 0	0 ± 0	0 ± 0	0 ± 0
C	0 ± 0	0 ± 0	0 ± 0	0 ± 0	0 ± 0

Table 1 ALA-PDT induced damage scored for the esophageal layers of the individual rats (48h post PDT) (Ep=epithelium, SM=submucosa, Musc= muscularis propria, inflamm = inflammation). Damage was scored on a semi-quantitative base.
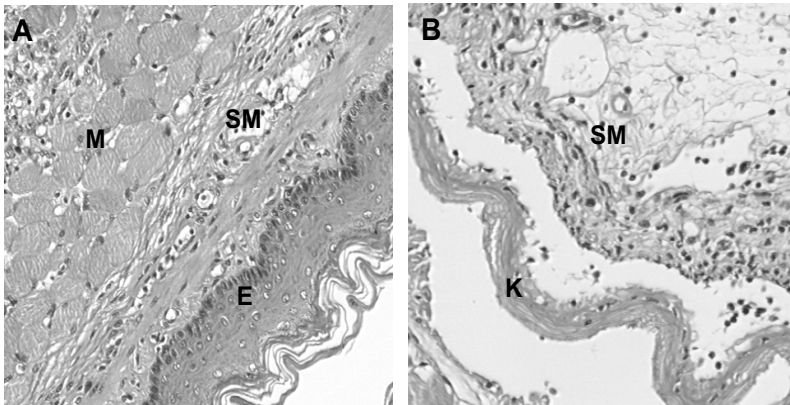
Figure 3A: H&E stained section through irradiated area, showing no response (rat A1); the epithelial layer (E) is intact, with its underlying submucosa (SM) and muscle (M). **B**: H&E stained section showing complete ablation of the epithelium (rat A3). Underlying the acellular keratin layer (K) submucosal edema (SM) is observed.

Figure 3 (A and B) illustrates the extremes of PDT-induced effects on the esophageal epithelium. Figure 3A shows an H&E stained section through an irradiated area, showing no response; the epithelial layer (E) is intact. Figure 3B shows an H&E stained section showing complete ablation of the epithelium.

Fluence Rate measurements

The mean fluence rates (with standard deviation) measured during illumination of the treatment groups A and B and control group C are shown in figure 4. The mean measured fluence rate of all animals at the start of the treatment was 76.5 ± 6.6 mW cm^{-2} and the mean fluence was 54.4 ± 0.3 J cm^{-2}. For the control group, the mean fluence rate was 80.4 ± 1.9 mW cm^{-2} with a total fluence of 54.3 ± 0.06 J cm^{-2}. The ALA-PDT groups received a mean fluence rate of 75.0 ± 7.2 mW cm^{-2} and a fluence of 54.4 ± 0.3 J cm^{-2}. The mean fluence rate and the delivered fluence were not significantly different between treatment and control groups. In 18 animals, the fluence rate decreased during the course of the illumination by 5.8 ± 4.7 mW cm^{-2}, whereas in 3 animals the fluence rate increased during illumination by 8.5 ± 2.2 mW cm^{-2}. The lowest and highest mean β during ALA-PDT were 1.4 and 3.0 respectively.
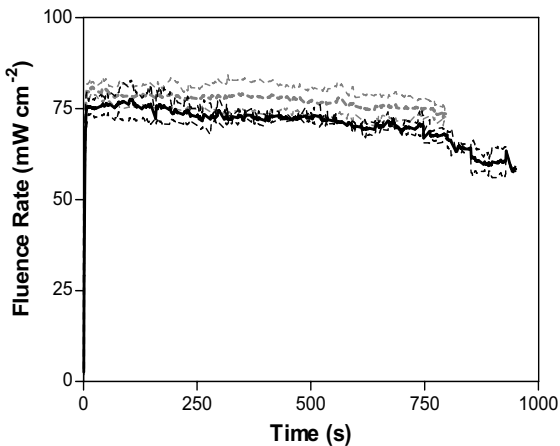
Figure 4 Mean measured fluence rates during illumination with standard deviation (thin dashed lines) of control (dashed gray line) (n=6) and ALA-PDT (black line) treated animals (n=15).

PpIX photobleaching

Figure 5 shows a raw fluorescence spectrum acquired under 405 nm excitation during a break in the therapeutic illumination approximately 90 s after the start of the illumination with the corresponding fitted tissue autofluorescence, PpIX fluorescence, and the photo-product fluorescence. Also shown is the residual between the fitted and raw spectra.
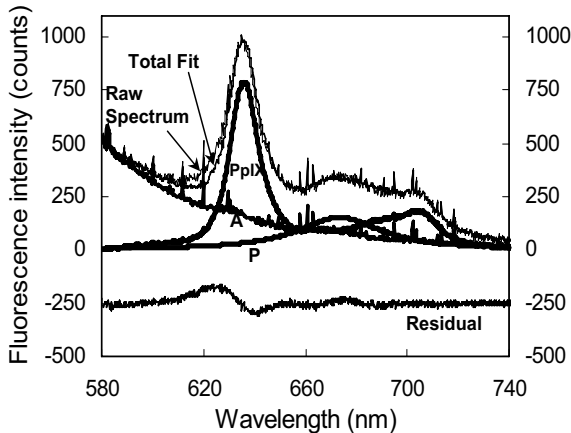
Figure 5 Raw fluorescence spectrum acquired approximately 90 s after the start of an illumination, 2 h after the administration of ALA using 405 nm excitation. SVD fitted component spectra; tissue autofluorescence (A, thick black line), PpIX fluorescence (PpIX, thick black line), photo-product fluorescence (P, thick black line), total fit and the residual between the fitted and raw spectra.

Figure 6 shows the kinetics of PpIX photobleaching and the response of the esophagus following illumination. The normalized PpIX fluorescence intensity is plotted against the measured fluence for each individual animal. Animals that did not respond are plotted with open symbols, animals that showed complete epithelial ablation are plotted with closed symbols. In each case the intensity of PpIX fluorescence decreased during illumination due to the photobleaching of PpIX. The initial rate and the overall extent of photobleaching are remarkably different between the different animals, despite the fact that the measured fluence rate was not significantly different for any of the animals. There was no correlation between the measured fluence rate for a particular animal and either the initial or the overall amount of photobleaching. The kinetics of photobleaching during illumination in the

esophagus are quite complex. There appears to be an initial rapid phase of photobleaching (within the first 1-2 J cm^{-2} or 25 seconds of the illumination) in some animals followed by a second slower phase that persists for the rest of the illumination.
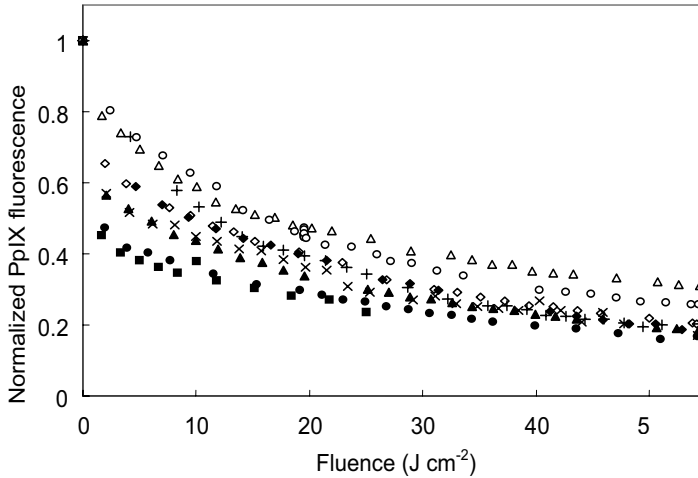
Figure 6: Mean normalized PpIX fluorescence during illumination (n=9). The corresponding rat ID is shown in Table 1.

Figure 7 shows the reciprocal of the normalized fluorescence intensity plotted against the measured fluence. The gradient of the curves plotted in this way is dependent on the local concentration of oxygen within the volume from which the fluorescence intensity is acquired (28). To allow the comparison of the kinetics between animals, we have defined for each decay an initial rapid phase to be the first measurement points. The second slower phase was then defined as the slope of a line fitted through the remaining measurement points. In animals that responded to ALA-PDT with complete epithelial ablation there is a significantly higher initial amount of photobleaching, compared to animals that showed no response, mean 1.9 ± 0.3 and 1.3 ± 0.2 respectively (p=0.036). Also the rate of photobleaching over the remaining second phase of the illumination was significantly greater in animals that responded with complete epithelial ablation (0.073 ± 0.005), compared to animals that showed no response (0.053 ± 0.01) (p=0.012).
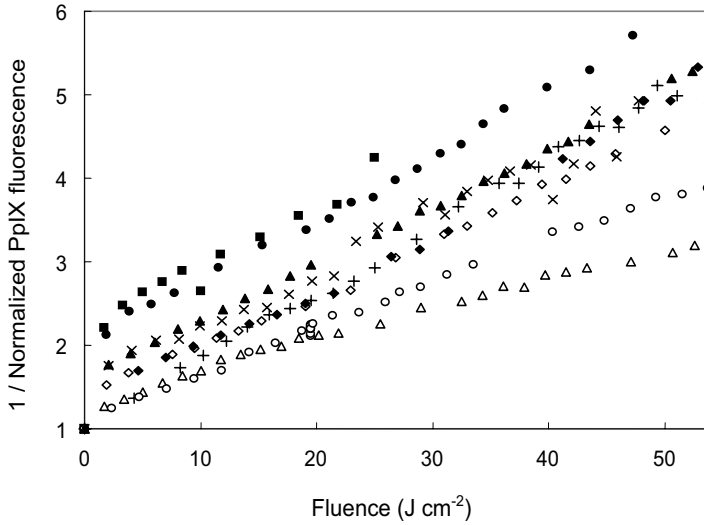
Figure 7: Reciprocal of the mean normalized PpIX fluorescence, during illumination (n=9). The corresponding rat ID is shown in Table 1.

DISCUSSION

Optical properties and equal fluence rates

The response of tissues to ALA-PDT has previously been shown to be dependent on the illumination parameters (22). Additionally, the maximum PDT induced damage at constant fluence rate is limited by the photobleaching of PpIX (19, 28). When illumination is performed with an equivalent total fluence, the PDT damage increases with decreasing fluence rate, due to depletion of molecular oxygen within the illuminated volume at high fluence rate (5, 7, 19, 25, 28, 29). Hypothetically, performing ALA-PDT with a measured standardized fluence and fluence rate should lead to an equivalent tissue response. The fluence rate measured in-situ at the esophageal wall consists of both non-scattered light directly emitted by the source fiber and tissue back-scattered light. The magnitude of the additional back-scattered light is determined by tissue optical properties, which are influenced by manipulations such as inserting and inflating a balloon catheter. Red tissues generally absorb more light and induce less scattering, white tissues are more likely to cause scattering and to increase the fluence rate. Also Barrett's esophagus is a histologically heterogeneous condition; it consists of columnar epithelium with villi and crypts, while any esophagitis involved causes vasodilatation. Consequently large differences in β

are expected between patients and within a treatment field. Since optical properties can vary significantly, the true fluence rate in-situ can also vary for the same source fiber output (16). Therefore, in order to obtain the same measured fluence rate at the esophageal wall, the administered laser power should be adjusted (30). In the present study, the mean fluence rate was 76.5 ± 6.6 mW cm^{-2} and the mean fluence 54.4 ± 0.3 J cm^{-2}. These variations represent a considerable improvement over using a fixed laser output power. Without this correction large variations in fluence rate within the esophagus (> factor 2) would have occurred. Although it is not possible to standardize the fluence rate at greater depths within the esophagus, it is sufficient for the treatment of superficial Barrett's esophagus. The use of isotropic probes to standardize the measured fluence rates and compensate for differences in β could also be useful during clinical ALA-PDT. Our group has recently reported the use of in-situ light dosimetry during clinical ALA-PDT of Barrett's esophagus (31). Two isotropic probes were placed within the esophagus and similar large differences in the measured fluence rate were observed. The non-uniformity of the tissue optical properties in Barrett's esophagus will make it challenging to monitor and compensate for the optical properties over the whole illuminated area.

PDT response

The PDT response following illumination, measured as damage to the esophageal epithelium, varied from no damage to complete ablation of the epithelium (table 1). This was unexpected, since each animal was treated using the same treatment parameters. Small differences in fluence rates between animals and changes in fluence rate during ALA-PDT could not be related to differences in PDT induced damage. The results presented here indicate clearly that other factors than differences in optical properties between animals influence the response of the esophagus following ALA-PDT.

PpIX fluorescence spectroscopy

It has previously been shown that PpIX fluorescence spectroscopy during illumination is useful for monitoring PDT dosimetry and determining the photodynamic response to therapy (32, 33). The kinetics of PpIX photobleaching during illumination have been shown to obey non-exponential, second order kinetics in the skin. The rate of

photobleaching at a particular time during illumination is dependent on the local concentration of oxygen, which is determined by the balance between photochemical or metabolic consumption and the supply of oxygen. In the present study we observed a wide variation in both the initial rate and the overall amount of PpIX photobleaching during illumination, although there was no significant difference between the measured fluence rates at the start of each illumination. Neither could a relation be found between PpIX fluorescence before illumination and the response, although absolute concentrations of PpIX were not determined. However, the initial rate and the overall amount of PpIX photobleaching correlated well with the response of the animals. Significant more initial photobleaching and a greater amount of total photobleaching were observed in animals that showed complete epithelial ablation of the esophagus, less initial and less overall photobleaching were observed in animals that showed no response. It is important to note that the fluorescence spectra acquired are not corrected for changes in tissue optical properties during illumination at either the excitation wavelength or in the fluorescence emission band of PpIX. While this would be a desirable addition to our measurement technique, similar quantitative rates of photobleaching have been observed with (25) and without (19) compensation for changing tissue optical properties during treatment. We have again used basis spectra to analyze the kinetics of PpIX photobleaching and the residual between the fitted spectra and the raw spectra. Figure 5 indicates that subtle changes in spectral shape and/or peak emission wavelength occur as the therapeutic illumination progresses. While these changes are significant and may provide (an) additional parameter(s) to monitor the process of photobleaching, their effects on the fitted intensity of fluorescence during illumination are much smaller than the differences in photobleaching kinetics that were observed in this study.

Fluence rate, PpIX fluorescence photobleaching and response
Many studies have shown that fluence rate and PDT induced damage are inversely related: lower fluence rates at equal fluence result in more damage. Other studies have shown that the kinetics of PpIX photobleaching during ALA-PDT in vivo are related to the fluence rate applied. For a superficial distribution of PpIX and appropriate excitation and detection wavelengths, the rate of photobleaching increases with decreasing fluence rate (25), although there have been some conflicting reports (34, 35). Furthermore, both the PDT induced damage and the

PpIX photobleaching rate are closely related to the local concentration and availability of oxygen during illumination (7, 19, 25, 28). Reducing the fluence rate reduces the photochemical demand for oxygen and allows more oxygen to diffuse into the illuminated volume during therapy, as was shown with direct O_2 measurements (29, 36). This principle has been used in studies on fractionated illumination in ALA-PDT. Short dark intervals (in the order of 60 seconds) lead to an increase in the rate of photobleaching immediately after the dark interval, in which re-oxygenation occurred within the treatment volume (37). The increase in rate of photobleaching that was observed is an indication of the increased availability of O_2. In the rat esophagus the kinetics of PpIX photobleaching indicate that there are two outcomes and the relationship between PDT effect and the photobleaching rate is explainable. Since oxygen radicals are responsible for both ALA-PDT induced tissue damage and PpIX photobleaching, the rate of PpIX photobleaching is likely to correlate to tissue damage. More intriguing is the fact why PpIX photobleaching occurs at a higher initial rate. It is important to distinguish between sensitizers when discussing sensitizer photobleaching. Other groups have previously observed a two-phased decay in sensitizer photobleaching that localize to lysozomes (38-40). These sensitizers redistribute to other cellular compartments during PDT. The redistribution has been correlated to a sudden increase in the oxygen consumption rate of spheroids (40). Also a two-phased decay has been shown for PDT with mTHPC in vivo by Finlay et al (26). For mTHPC, this phenomenon has not been shown in vitro with mTHPC-sensitized spheroids. Furthermore, there is no evidence for irradiation induced relocalization of mTHPC (41). Therefore, either the redistribution only occurs in an in vivo environment, or other processes are responsible for the two-phased decay. There is no evidence that PpIX undergoes significant re-distribution upon illumination in-vivo or that PpIX undergoes complex photobleaching kinetics. For Photofrin-PDT, it is known that through vascular shutdown, within minutes changes occur in the blood supply of the irradiated tissue, thus creating differences in local O_2 concentration. ALA-PDT however is not known to exert its effects through vascular shutdown, but through a mechanism of apoptosis, induced by production of singlet oxygen. However, if for any reason a change occurs in O_2 concentration, the photobleaching rate could change during ALA-PDT. To gain more insight in this mechanism, O_2 measurements in the esophagus would be useful. Low availability of O_2 could explain the lower initial rate of PpIX photobleaching and absence of a

response in some animals, compared to a high availability of O_2, higher rate of photobleaching and complete epithelial ablation in other animals. A number of factors could have affected the availability of O_2 during treatment, such as anesthesia. However, a small reduction in blood O_2 saturation is not expected to have a significant influence on the O_2 concentration within the esophageal epithelium, since hyperoxygenation of mice during ALA-PDT did not increase ALA-PDT induced tissue effects in other studies (32, 42). Probably, the amount of O_2 at the site of illumination is more important than the O_2 saturation in blood. It has been shown that the size of the balloon influences the outcome of Photofrin-PDT in canine esophagus, presumably through effects on local concentration of oxygen (43). Higher balloon pressures cause compression of the esophageal wall and decrease the blood and oxygen supply. This effect could be more pronounced in smaller species, such as rats. Although we measured balloon diameters, we did not measure balloon pressures. The significance of the effect of balloon pressures and O_2 concentration within the irradiated volume during ALA-PDT is obviously an area for future study.

In summary, we have demonstrated the feasibility of simultaneously monitoring light dosimetry and PpIX photobleaching during illumination in the rat esophagus. We have shown that it is possible to compensate for variations in tissue optical properties between animals and thus standardize the fluence rate and the fluence of the illumination at the esophageal wall. We also have shown that the response of the rat esophageal epithelium is highly variable and not simply determined by the fluence and fluence rate of the illumination. However, our results indicate that monitoring PpIX fluorescence kinetics may be a useful parameter for predicting the outcome of ALA-PDT.

REFERENCES

1. Blot, W. J. and J. K. McLaughlin (1999) The changing epidemiology of esophageal cancer. *Semin Oncol.* **26**, 2-8.

2. Greenlee, R. T., M. B. Hill-Harmon, T. Murray and M. Thun (2001) Cancer statistics, 2001. *CA Cancer J Clin.* **51**, 15-36.

3. Altorki, N. K., S. Oliveria and D. S. Schrump (1997) Epidemiology and molecular biology of Barrett's adenocarcinoma. *Semin Surg Oncol.* **13**, 270-80.

4. Kennedy, J. C., S. L. Marcus and R. H. Pottier (1996) Photodynamic therapy (PDT) and photodiagnosis (PD) using endogenous photosensitization induced by 5-aminolevulinic acid (ALA): mechanisms and clinical results. *J Clin Laser Med Surg.* **14**, 289-304.

5. Foster, T. H., R. S. Murant, R. G. Bryant, R. S. Knox, S. L. Gibson and R. Hilf (1991) Oxygen consumption and diffusion effects in photodynamic therapy. *Radiat Res.* **126**, 296-303.

6. Gibson, S. L. and R. Hilf (1985) Interdependence of fluence, drug dose and oxygen on hematoporphyrin derivative induced photosensitization of tumor mitochondria. *Photochem Photobiol.* **42**, 367-73.

7. Georgakoudi, I. and T. H. Foster (1998) Singlet oxygen- versus nonsinglet oxygen-mediated mechanisms of sensitizer photobleaching and their effects on photodynamic dosimetry. *Photochem Photobiol.* **67**, 612-625.

8. Niedre, M., M. S. Patterson and B. C. Wilson (2002) Direct near-infrared luminescence detection of singlet oxygen generated by photodynamic therapy in cells in vitro and tissues in vivo. *Photochem Photobiol.* **75**, 382-91.

9. Weishaupt, K. R., C. J. Gomer and T. J. Dougherty (1976) Identification of singlet oxygen as the cytotoxic agent in photoinactivation of a murine tumor. *Cancer Res.* **36**, 2326-9.

10. Barr, H., N. A. Shepherd, A. Dix, D. J. Roberts, W. C. Tan and N. Krasner (1996) Eradication of high-grade dysplasia in columnar-lined (Barrett's) oesophagus by photodynamic therapy with endogenously generated protoporphyrin IX. *Lancet.* **348**, 584-585.

11. Gossner, L., A. May, R. Sroka, M. Stolte, E. G. Hahn and C. Ell (1999) Photodynamic destruction of high grade dysplasia and early carcinoma of the esophagus after the oral administration of 5-aminolevulinic acid. *Cancer.* **86**, 1921-8.

12. Ackroyd, R., N. J. Brown, M. F. Davis, T. J. Stephenson, S. L. Marcus, C. J. Stoddard, A. G. Johnson and M. W. Reed (2000) Photodynamic therapy for dysplastic Barrett's oesophagus: a prospective, double blind, randomised, placebo controlled trial. *Gut.* **47**, 612-617.

13. Ackroyd, R., N. J. Brown, M. F. Davis, T. J. Stephenson, C. J. Stoddard and M. W. Reed (2000) Aminolevulinic acid-induced photodynamic therapy: safe and effective ablation of dysplasia in Barrett's esophagus. *Dis Esophagus.* **13**, 18-22.

14. Gossner, L., M. Stolte, R. Sroka, K. Rick, A. May, E. G. Hahn and C. Ell (1998) Photodynamic ablation of high-grade dysplasia and early cancer in Barrett's esophagus by means of 5-aminolevulinic acid. *Gastroenterology.* **114**, 448-55.

15. Orth, K., A. Stanescu, A. Ruck, D. Russ and H. G. Beger (1999) [Photodynamic ablation and argon-plasma coagulation of premalignant and early-stage malignant lesions of the oesophagus--an alternative to surgery?]. *Chirurg.* **70**, 431-8.

16. Staveren, H. J. v., M. Keijzer, T. Keesmaat, H. Jansen, W. J. Kirkels, J. F. Beek and W. M. Star (1996) Integrating sphere effect in whole-bladder wall photodynamic therapy: III. Fluence multiplication, optical penetration and light distribution with an eccentric source for human bladder optical properties. *Phys Med Biol.* **41**, 579-90.

17. Star, W. M. (1995) The relationship between integrating sphere and diffusion theory calculations of fluence rate at the wall of a spherical cavity. *Phys Med Biol.* **40**, 1-8.

18. Tan, I. B., H. Oppelaar, M. C. Ruevekamp, R. B. Veenhuizen, A. Timmers and F. A. Stewart (1999) The importance of in situ light dosimetry for photodynamic therapy of oral cavity tumors. *Head Neck.* **21**, 434-41.

19. Robinson, D. J., H. S. de Bruijn, N. van der Veen, M. R. Stringer, S. B. Brown and W. M. Star (1998) Fluorescence photobleaching of ALA-induced protoporphyrin IX during photodynamic therapy of normal hairless mouse skin: the effect of light dose and irradiance and the resulting biological effect. *Photochem Photobiol.* **67**, 140-9.

20. Weagle, G., P. E. Paterson, J. Kennedy and R. Pottier (1988) The nature of the chromophore responsible for naturally occurring fluorescence in mouse skin. *J Photochem Photobiol B.* **2**, 313-20.

21. Boogert, J. v. d., H. J. v. Staveren, R. W. d. Bruin, P. D. Siersema and R. v. Hillegersberg (2001) Fractionated illumination for oesophageal ALA-PDT: effect on blood flow and PpIX formation. *Lasers Med Sci.* **16**, 16-25.

22. Boogert, J. v. d., H. J. v. Staveren, R. W. d. Bruin, J. H. Eikelaar, P. D. Siersema and R. v. Hillegersberg (1999) Photodynamic therapy for esophageal lesions: selectivity depends on wavelength, power, and light dose. *Ann Thorac Surg.* **68**, 1763-1769.

23. Veen, P. v., J. H. Schouwink, W. M. Star, H. J. Sterenborg, J. R. van der Sijp, F. A. Stewart and P. Baas (2001) Wedge-shaped applicator for additional light delivery and dosimetry in the diaphragmal sinus during photodynamic therapy for malignant pleural mesothelioma. *Phys Med Biol.* **46**, 1873-83.

24. Robinson, D. J., H. S. de Bruijn, W. J. de Wolf, H. J. Sterenborg and W. M. Star (2000) Topical 5-aminolevulinic acid-photodynamic therapy of hairless mouse skin using two-fold illumination schemes: PpIX fluorescence kinetics, photobleaching and biological effect. *Photochem Photobiol.* **72**, 794-802.

25. Finlay, J. C., D. L. Conover, E. L. Hull and T. H. Foster (2001) Porphyrin bleaching and PDT-induced spectral changes are irradiance dependent in ALA-sensitized normal rat skin in vivo. *Photochem Photobiol.* **73**, 54-63.

26. Finlay, J. C., S. Mitra and T. H. Foster (2002) In vivo mTHPC photobleaching in normal rat skin exhibits unique irradiance-dependent features. *Photochem Photobiol.* **75**, 282-288.

27. Georgakoudi, I., B. C. Jacobson, J. Van Dam, V. Backman, M. B. Wallace, M. G. Muller, Q. Zhang, K. Badizadegan, D. Sun, G. A. Thomas, L. T. Perelman and M. S. Feld (2001) Fluorescence, reflectance, and light-scattering spectroscopy for evaluating dysplasia in patients with Barrett's esophagus. *Gastroenterology.* **120**, 1620-1629.

28. Robinson, D. J., H. S. de Bruijn, N. van der Veen, M. R. Stringer, S. B. Brown and W. M. Star (1999) Protoporphyrin IX fluorescence photobleaching during ALA-mediated photodynamic therapy of UVB-induced tumors in hairless mouse skin. *Photochem Photobiol.* **69**, 61-70.

29. Coutier, S., L. N. Bezdetnaya, T. H. Foster, R. M. Parache and F. Guillemin (2002) Effect of Irradiation Fluence Rate on the Efficacy of Photodynamic Therapy and Tumor Oxygenation in Meta-Tetra (Hydroxyphenyl) Chlorin (mTHPC)-Sensitized HT29 Xenografts in Nude Mice. *Radiat Res.* **158**, 339-345.

30. Vincent, G. M., J. Fox, G. Charlton, J. S. Hill, R. McClane and J. D. Spikes (1991) Presence of blood significantly decreases transmission of 630 nm laser light. *Lasers Surg Med.* **11**, 399-403.

31. Van Veen, R. L., M. C. Aalders, K. L. Pasma, P. D. Siersema, J. Haringsma, W. Van De Vrie, E. E. Gabeler, D. J. Robinson and H. J. Sterenborg (2002) In situ light dosimetry during photodynamic therapy of Barrett's esophagus with 5-aminolevulinic acid. *Lasers Surg Med.* **31**, 299-304.

32. Rhodes, L. E., M. M. Tsoukas, R. R. Anderson and N. Kollias (1997) Iontophoretic delivery of ALA provides a quantitative model for ALA pharmacokinetics and PpIX phototoxicity in human skin. *J Invest Dermatol.* **108**, 87-91.
33. Konig, K., H. Schneckenburger, A. Ruck and R. Steiner (1993) In vivo photoproduct formation during PDT with ALA-induced endogenous porphyrins. *J Photochem Photobiol B.* **18**, 287-90.
34. Iinuma, S., K. T. Schomacker, G. Wagnieres, M. Rajadhyaksha, M. Bamberg, T. Momma and T. Hasan (1999) In vivo fluence rate and fractionation effects on tumor response and photobleaching: photodynamic therapy with two photosensitizers in an orthotopic rat tumor model. *Cancer Res.* **59**, 6164-70.
35. Sorensen, R., V. Iani and J. Moan (1998) Kinetics of photobleaching of protoporphyrin IX in the skin of nude mice exposed to different fluence rates of red light. *Photochem Photobiol.* **68**, 835-40.
36. Sitnik, T. M., J. A. Hampton and B. W. Henderson (1998) Reduction of tumour oxygenation during and after photodynamic therapy in vivo: effects of fluence rate. *Br J Cancer.* **77**, 1386-94.
37. Curnow, A., J. C. Haller and S. G. Bown (2000) Oxygen monitoring during 5-aminolaevulinic acid induced photodynamic therapy in normal rat colon. Comparison of continuous and fractionated light regimes. *J Photochem Photobiol B.* **58**, 149-155.
38. Berg, K., K. Madslien, J. C. Bommer, R. Oftebro, J. W. Winkelman and J. Moan (1991) Light induced relocalization of sulfonated meso-tetraphenylporphines in NHIK 3025 cells and effects of dose fractionation. *Photochem Photobiol.* **53**, 203-10.
39. Peng, Q., G. W. Farrants, K. Madslien, J. C. Bommer, J. Moan, H. E. Danielsen and J. M. Nesland (1991) Subcellular localization, redistribution and photobleaching of sulfonated aluminum phthalocyanines in a human melanoma cell line. *Int J Cancer.* **49**, 290-5.
40. Georgakoudi, I. and T. H. Foster (1998) Effects of the subcellular redistribution of two nile blue derivatives on photodynamic oxygen consumption. *Photochem Photobiol.* **68**, 115-22.
41. Melnikova, V. O., L. N. Bezdetnaya, C. Bour, E. Festor, M. P. Gramain, J. L. Merlin, A. Potapenko and F. Guillemin (1999) Subcellular localization of meta-tetra (hydroxyphenyl) chlorin in human tumor cells subjected to photodynamic treatment. *J Photochem Photobiol B.* **49**, 96-103.
42. Pech, O., C. D. Nagy, L. Gossner, A. May and C. Ell (2002) Photodynamic therapy of human Barrett's cancer using 5-aminolaevulinic acid-induced protoporphyrin IX: an in-vivo dosimetry study in athymic nude mice. *Eur J Gastroenterol Hepatol.* **14**, 657-62.
43. Overholt, B. F., M. Panjehpour, R. C. DeNovo, M. G. Peterson and C. Jenkins (1996) Balloon photodynamic therapy of esophageal cancer: effect of increasing balloon size. *Lasers Surg Med.* **18**, 248-52.

Chapter 6

Protoporphyrin IX fluorescence photobleaching and the response of rat Barrett's esophagus following 5-aminolevulinic acid photodynamic therapy

I.A. Boere, D.J. Robinson, H.S. de Bruijn, J. Kluin, H.W. Tilanus, H.J.C.M. Sterenborg, R.W.F. de Bruin

Departments of Surgery and Radiation Oncology, Photodynamic Therapy & Optical Spectroscopy Research Program, Erasmus Medical Center Rotterdam, The Netherlands

ABSTRACT

Barrett's esophagus (BE) can experimentally be treated with 5-aminolevulinic acid based photodynamic therapy (ALA-PDT), in which ALA, the precursor of the endogenous photosensitizer PpIX and subsequent irradiation with laser light is applied to destroy the (pre)malignant tissue. Accurate dosimetry is critical for successful ALA-PDT. Here, in vivo dosimetry and kinetics of PpIX fluorescence photobleaching were studied in a rat model of BE. The fluence and fluence rate were standardized in vivo and PpIX fluorescence was measured simultaneously at the esophageal wall during ALA-PDT and plotted against the delivered fluence rather than time. Rats with BE were administered 200 mg kg^{-1} ALA (n=17) or served as control (n=4). Animals were irradiated with 633 nm laser light at a measured fluence rate of 75 mW cm^{-2} and a fluence of 54 Jcm^{-2}. Large differences were observed in the kinetics of PpIX fluorescence photobleaching in different animals. High PpIX fluorescence photobleaching rates corresponded with tissue ablation, whereas low rates corresponded with no damage to the epithelium. Attempts to influence tissue oxygenation by varying balloon pressure and ventilation were shown not to be directly responsible for the differences in effect. In conclusion, in vivo dosimetry is feasible in heterogeneous conditions such as BE and PpIX fluorescence photobleaching is useful to predict the tissue response to ALA-PDT.

INTRODUCTION

The incidence of esophageal adenocarcinoma is rapidly increasing in the western world. Many esophageal adenocarcinomas arise within Barrett's esophagus (BE) through a sequence of changes of the epithelium. In Barrett's esophagus the normal squamous epithelium is replaced by columnar epithelium with goblet cells, which resembles intestinal type epithelium and is therefore defined as intestinal metaplasia. Whereas esophageal adenocarcinoma should be treated surgically if possible, management of premalignant Barrett's esophagus is an issue of significant debate. In case of severe dysplasia, surgical esophagectomy is usually the therapy of choice. Others however favor a less aggressive approach that relies on monitoring the progression of dysplasia at endoscopy (1). There are also arguments to treat low grade dysplasia or Barrett's esophagus itself. Since most BE do not progress to esophageal adenocarcinoma, this should only be done with minimal invasive therapy. A potential candidate is photodynamic therapy. In 1996 Barr et al published their first study on 5-aminolevulinic acid based photodynamic therapy (ALA-PDT) for removal of dysplastic Barrett's esophagus. Although ALA-PDT was successful in removing dysplasia, it was not radical and Barrett's epithelium remained (2). Subsequent studies have focused at optimizing ALA-PDT and monitoring the results of ALA-PDT on BE, however residual Barrett's epithelium and dysplasia may remain in situ after treatment (3).

Briefly, ALA is administrated to induce accumulation of the endogenous photosensitizer PpIX. Subsequently, the esophagus is illuminated with 633 nm light at a defined fluence and fluence rate. Activated oxygen species, generated by ALA-PDT, notably singlet oxygen, act on critical cellular components resulting in epithelial ablation. Therefore, success of ALA-PDT depends on a number of drug and light related factors. Accurate irradiation with light of a proper wavelength, fluence and fluence rate has shown to be critical (4, 5). For equivalent total fluences, PDT is more effective at lower fluence rates. At high fluence rate molecular oxygen is rapidly depleted within the illuminated volume, which limits the effects of ALA-PDT (4, 6-10). Also, the ALA-PDT induced damage at constant fluence rate is limited by the photobleaching of the photosensitizer protoporphyrin IX (PpIX) (4, 6). Photobleaching is defined as the light induced loss of absorption or emission intensity. PpIX fluorescence spectroscopy to measure photobleaching during irradiation has shown

to be useful for monitoring PDT dosimetry and the response to therapy, since until very recently it was not possible to monitor the photochemically active substrates directly (11-13). The rate of photobleaching during illumination is dependent on the local concentration of oxygen, which is determined by the balance between photochemical consumption and the supply of oxygen. Thus, both the rate of photobleaching and PDT induced tissue damage are closely related to the tissue oxygen tension during illumination (4, 6, 7, 9). Therefore the rate of photobleaching increases with decreasing fluence rates (9). These correlations can be explained by the following principle: reducing the fluence rate reduces the photochemical demand for oxygen and permits more oxygen to diffuse within the irradiated volume during therapy. Furthermore, low fluence rates do not lead to oxygen depletion, in contrast to higher fluence rates (10, 14).

If ALA-PDT is performed on hollow organs such as the esophagus, there is a considerable contribution of tissue back-scattered light to the total fluence rate. The magnitude of the additional back-scattered light is determined by optical properties of the tissue and expressed by build up factor beta (β) (15, 16). Both biological factors and mechanical factors influence tissue optical properties. Barrett's esophagus consists of more heterogeneous tissue with crypts and villi and a variable degree of inflammation compared to the more homogeneous normal squamous epithelium. Therefore alterations of tissue optical properties, large differences in β and subsequently wide variations in true fluence rate and thus differences in effects of ALA-PDT between individuals can be expected when performing ALA-PDT on BE. This phenomenon has been illustrated by van Veen et al who found that during ALA-PDT for human BE, fluence rates at the site of illumination varied substantially between patients in a study on the use of in situ light dosimetry during clinical ALA-PDT of BE (17). This may add to the variation in results of clinical ALA-PDT. In a previous study in the normal rat esophagus we demonstrated the possibility to compensate for variations in β between animals by measuring the fluence rate at the esophageal wall in vivo and adjusting the intensity of the source fiber accordingly (18). However, this did not result in better outcomes. We also measured PpIX fluorescence during illumination with respect to the delivered fluence. We found that PpIX fluorescence photobleaching followed a two phased decay and that both the

initial amount and the total rate of PpIX photobleaching correlated with the degree of tissue response.

In the present study the same standardized in situ dosimetry is applied in the more clinically relevant animal model of BE. In this model, differences in outcome after ALA-PDT can also be expected. The effects of light dosimetry and kinetics of PpIX photobleaching during ALA-PDT on the ablation of BE were studied. To study the mechanism(s) responsible for differences in the rate of PpIX photobleaching rate and their relationship to tissue response we determined the effects of exogenous oxygen administration and balloon pressure in the treatment area during ALA-PDT.

We find that PpIX photobleaching correlates with tissue response to ALA-PDT, in all the experiments described, regardless the tissue-type treated, Barrett's or normal esophagus, or exogenously administered oxygen. We discuss the implications for the clinical application of this method of monitoring ALA-PDT.

MATERIALS AND METHODS

Tissue response of ALA-PDT and PpIX photobleaching rate in rats with Barrett's esophagus. Twenty-one Wistar rats with Barrett's epithelium (BE rats) were used in the present study. Barrett's epithelium in the lower esophagus was established by long term duodenal reflux as a result of an esophagojejunostomy. A gastrectomy was performed through a median laparotomy and the esophagus was attached end-to-site (continuous 7/0 silk sutures) to the jejunum (19, 20). The abdominal wall was closed in one layer using (continuous 2/0 silk sutures. Rats were administered buprenorphin (0.05 mg kg^{-1}) and drinking water directly after surgery. Chow (Hope farms type, The Netherlands) was provided ad libitum after 24 hours. This diet was free of chlorophyll in order to minimize the autofluorescence emission from the esophagus centered on 675 nm attributed to pheophorbide-α (4). Figure 1 shows the surgical procedure used in this animal model for BE. The experimental protocol was approved by the Animal Experiments Committee under the national Experiments on Animals Act and adhered to the rules laid down in this national law that serves the implementation of "Guidelines on the protection of experimental animals " by the Council of Europe (1986), Directive 86/609/EC. One year after esophagectomy, seventeen BE rats received ALA, 4 BE rats served as control (no

ALA) and were sacrificed after irradiation. ALA-PDT treated rats were sacrificed 48 h (n=11) or 3 weeks (n=6) after treatment to determine tissue damage and regeneration respectively. Ether anesthesia was used during measurement of the autofluorescence spectrum and ketamin and xylazin (25 and 2.5 mg kg^{-1} intramuscularly) during ALA-PDT. Buprenorphin (0.05 mg kg^{-1} intramuscularly) was administered in a single dose after ALA-PDT. ALA (Sigma Chemical Company, Zwijndrecht, The Netherlands) was dissolved in phosphate buffered saline and administered by oral gavage 2 h before PDT (200 mg kg^{-1}).
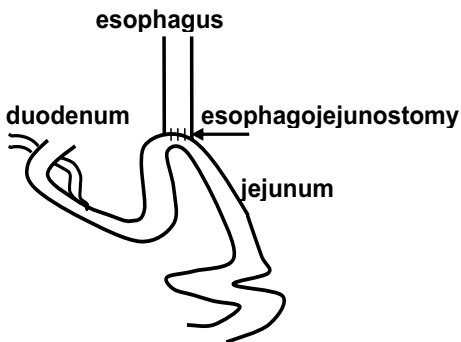
Figure 1 Surgical procedure to induce Barrett's esophagus.

Influence of balloon pressure on the rate of PpIX photobleaching. The influence of the balloon catheter pressure used for delivery of laser light during ALA-PDT on PpIX photobleaching was studied in fourteen male Wistar rats without BE (Harlan, The Netherlands). In previous experiments, we observed variability in tissue response to ALA-PDT, although the same measured fluence was applied. A possible explanation is that high balloon pressure may reduce blood flow and limit the availability of molecular oxygen in the esophageal mucosa. Depletion of molecular oxygen may inhibit the photochemical reaction and decrease the response to PDT. We hypothesized PpIX photobleaching to be reduced under these conditions. Low balloon pressure on the contrary may not limit blood flow and thus oxygen supply to the esophagus. Therefore, PpIX photobleaching is likely to occur at higher extent. Seven rats were allocated to the previously used high (760 mm Hg) balloon catheter pressures and seven rats to low (380 mm Hg) balloon catheter pressures. ALA-PDT was performed in all fourteen rats in the same manner as described above.

Influence of exogenous oxygen administration during ALA-PDT on the rate of PpIX photobleaching. Additionally fourteen normal rats were used to study the influence of exogenous oxygen supply on PpIX photobleaching. We hypothesized that ventilation with a reduced concentration of oxygen would deplete oxygen within the esophagus and at the site of treatment and thus inhibit the effects of ALA-PDT and decrease the amount of PpIX photobleaching. Rats were anesthetized with a gaseous mixture of 3% isoflurane, 64% N_2O and 33% O_2, thereafter they were intubated, and pressure control ventilated with 15 cm H_2O peak inspiratory pressure and 4 cm H_2O positive end expiratory pressure with a frequency of 30 breaths per minute (Siemens Servo, Solna, Sweden). The gaseous mixtures used were 64% N_2O with 33% O_2 in the high oxygen group and 84.5% N_2O and 12.5% O_2 in the low oxygen group with 3% isoflurane in each. Oxygen saturation was monitored with the Nellcor device (Tyco Healthcare, The Netherlands) in blood samples taken from the tail vein for blood gas analysis during therapy. Apart from the pressure control ventilation procedure, rats were treated in the same manner as described above.

Illumination setup. The same illumination set up as described previously was used (18). Briefly, a double lumen balloon catheter was used to homogeneously illuminate the esophagus (Cordis, The Netherlands, 40 mm long, 3 mm diameter, inflated with 0.6 ml air to a pressure of 760 mm Hg) with in its center a 200-micron fiber with a 10 mm length cylindrically diffusing tip (Cardiofocus, Norton MA, USA) to deliver both 633 nm and 405 nm light. The placement of the balloon catheter was measured to determine the area illuminated. Illumination was performed using 633 nm light (600 Series Dye Module and KTP/532 laser, Laserscope, San Jose CA, USA). Every 30 s the illumination was interrupted for 3 s 405 nm light (0.5 mW cm^{-2}) using a shutter system for acquisition of fluorescence spectra (LG Laser Technologies, Klienoostheim, Germany). Two 100 μm isotropic probes (Cardiofocus, Norton MA, USA) were attached to the outer surface of the balloon and placed directly at the esophageal wall. One isotropic probe was connected to a device to enable the acquisition of real time fluence (rate) data (21). The other was connected to a fiber optic spectrograph (Avantes of Ocean Optics, Eerbeek, Netherlands). The isotropic detectors were calibrated in air at the start of each treatment day, using an integrating sphere. A correction factor of 1.07 was used to account for the index of refraction mismatch at the air-tissue interface between the inflated balloon and the

esophageal wall (22). At the start of illumination, the output power of the laser was adjusted to a measured fluence rate at the esophageal wall of 75 mW cm^{-2}. During illumination the fluence rate was monitored continuously and the illumination was stopped when a fluence of 54 J cm^{-2} was reached. After treatment the light output from the illumination fiber in the balloon catheter was determined using an integrating sphere. The build up factor β of the esophageal wall is defined by the ratio of the true fluence rate to the unscattered incident fluence rate.

Fluorescence measurements. Fluorescence emission spectra (550-750 nm) were acquired before ALA administration, pre and post illumination and at 30s intervals during PDT. Integration times ranged between 1 and 1.5 s depending on the PpIX fluorescence intensity. It is important to note that the equal time intervals of fluorescence measurements (30 s) do not necessarily correspond to equal fluence intervals due to slight variations in the monitored fluence rate. This fact has special significance when analyzing sets of photobleaching curves from animals within the same treatment group (see below). Fluorescence spectra were corrected for differences in power of the 405 nm laser. The spectra were analyzed as described previously based on the method described by Finlay et al (9, 23-25). Each fluorescence spectrum was analyzed as a linear combination of basis fluorescence spectra (autofluorescence of the esophagus, PpIX and the hydroxyaldehyde chlorine photoproduct of PpIX) using a singular value decomposition (SVD) algorithm.

Handling of the specimens and quantification of PDT damage. Animals were sacrificed by exsanguination under isoflurane anesthesia. After excision, the esophagus was opened longitudinally, examined for macroscopic abnormalities, swiss rolled from distal to proximal and fixed in formalin after a suture had been placed to mark the illuminated area. The specimens were embedded in paraffin, sectioned and stained with haematoxylin and eosin (H&E) and Alcian blue. Two investigators evaluated the sections; damage to the esophageal layers was scored semi-quantitatively on a scale from 0 to 3. Ablation of the epithelium was scored as complete ablation when there were no epithelial cell layers left (0 = normal, 1 = >1 cell layer left, 2 = 1 cell layer left, 3 = complete ablation). A complete response was defined as epithelial ablation score 2-3, no response was defined when no epithelial ablation was observed. The epithelium adjacent to the PDT treated area was scored

as BE when intestinal metaplasia with goblet cells was present, squamous epithelium and squamous hyperplasia when the epithelial papillae were elongated and the epithelium was increased in thickness. Edema of the submucosa was scored based on the thickness of the submucosa (0 = normal 50-100 μm, 1 = 2 times thicker than normal, 2 = 3-5 times thicker, 3 = > 5 times thicker). Inflammation of the submucosa and muscularis propria was scored on the basis of the number of inflammatory cells (mostly lymphocytes) using a grid with a 40x magnification (0 = none; 1 = <1 per grid; 2 = 1-2 per grid, 3 = > 2 grid). The severity of the necrosis of the muscularis propria was scored on the basis of the presence of vital muscle cells (0 = 100%; 1 = >75%; 2 = > 25%; 3 = < 25%).

Data analysis. The measured fluence rate at the start of ALA-PDT was used for calculation of means and standard deviations. A Student's t-test was used to compare the fluence and fluence rate between groups of animals. A p-value < 0.05 was considered significant. PpIX fluorescence photobleaching data are plotted against the measured fluence and normalized to the pre-illumination PpIX fluorescence intensity. As stated above, each individual animal has slightly different measured fluence data-points on the x-axis. Thus, it is necessary to first fit the data from each animal as described below and then determine the mean and standard deviation of the fits from animals within the same treatment group. We have previously shown that the kinetics of PpIX photobleaching can be described by a second order function with respect to fluence (Equation 1) (4):

$$[S_0]_t = [S_0]_{t=0}\left[1 + \frac{[S_0]_{t=0}\,\alpha\phi_t\sigma\kappa_{os}}{\kappa_d + \kappa_{oa}[A]}\,\Phi t\right]^{-1} \qquad \text{(Eq 1)}$$

Here, $[S_0]$ is the concentration of PpIX in its ground state, α is the fraction of triplet state PpIX-ground state oxygen interactions that result in the formation of singlet oxygen, Φ_t is the triplet quantum yield of the PpIX, σ is the absorption cross section of ground state PpIX, κ_d is the monomolecular decay rate of singlet oxygen, Φ is the irradiance, κ_{os} is the bimolecular rate of chemical reaction between ground state PpIX and singlet oxygen and κ_{oa} is the bimolecular rate of chemical reaction rate between singlet oxygen and biological substrate [A]. If α, ϕ_t, σ, κ_d, κ_{os} and κ_{oa} remain constant during the period of irradiation, the rate of photobleaching (with respect to time) is

only dependent on the local fluence rate Φ and the initial concentration of sensitizer present, $[S_0]_{t=0}$.

An important consequence of this analysis is that the reciprocal of the PpIX fluorescence intensity is a linear function when plotted with respect to fluence. We have previously shown that the kinetics of photobleaching in the rat esophagus follows a bi-phasic decay (18). Therefore a separate decay curve was fitted through the first points in the initial phase of the PpIX photobleaching curve as shown in figure 4A. Subsequently second order fits were made. The means of the second order fits were plotted with the standard deviations. The reciprocal of the normalized PpIX fluorescence intensity was also plotted in order to illustrate the kinetics of photobleaching, the means and standard deviations of these fitted curves are plotted in the results section (6).

RESULTS

General observations and histology

Two BE rats died at 1 and 3 days after ALA-PDT due to impaired physical condition caused by long-term duodenal reflux in combination with ALA-PDT along with the handling of the animals, anesthesia, measurement of autospectra and medication. Four BE control rats, sacrificed directly after irradiation, and 11 BE animals treated with ALA-PDT sacrificed at 48h after ALA-PDT were examined for histology. Macroscopically, the esophagus was shortened and thickened due to chronic esophagitis and development of BE. In the lower esophagus, an area of smooth pinkish mucosa was present, separated by an area of erosion from hyperplastic-hyperkeratotic mucosa and normal appearing mucosa in the proximal esophagus. Microscopically, these areas could be identified as Barrett's epithelium, erosive and ulcerative inflammation, hyperplasia with hyperkeratosis and normal squamous epithelium respectively. At the illuminated area, identified by a suture, a broad range of damage was seen. An example of untreated BE is shown in figure 2a, an example of BE after ALA-PDT is shown in figure 2b. The histological results of the epithelium and the muscular layer, at 48 h after ALA-PDT, of individual rats (n=11) are shown in table 1.

Rat	Surrounding	Ep ablation	Musc necrosis
BE1	Sq	3	0
BE2	SqH	3	2
BE3	SqH	2	0
BE4	Sq	3	0
BE5	Sq	3	1
BE6	SqH	0	0
BE7	SqH	3	0
BE8	BE Sq	2	0
BE9	BE	0	1
BE10	SqH	0	0
BE11	BE Sq	3	2
mean		2.0	0.5
sd		1.3	0.8

Table 1 ALA-PDT induced damage scores shown for the epithelium and the muscularis propria of individual rats (48h post PDT) with the mean damage scores and standard deviations. (Sq = squamous epithelium, SqH = squamous hyperplasia, Ep = epithelium, Musc = muscularis propria; sd = standard deviation).
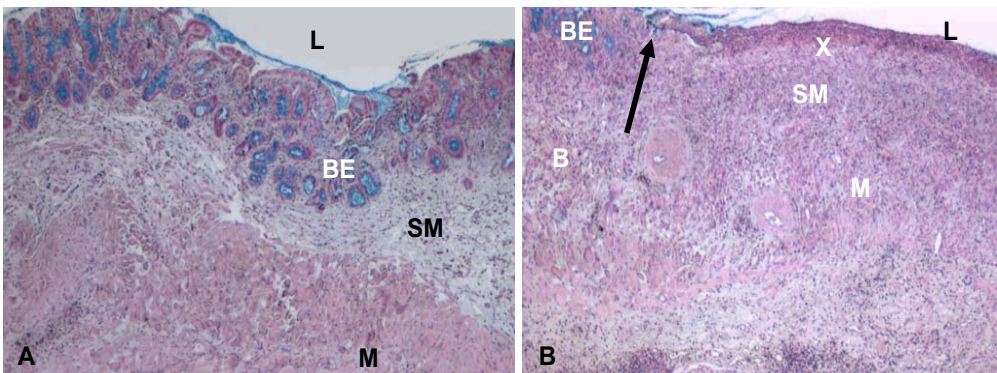
Figure 2 A: Alcian Blue stained section of rat BE (25x). **B**: Alcian Blue stained section of rat BE treated with ALA-PDT (t = 48h). Arrow indicates left border of PDT treated area. (L = esophageal lumen, X = PDT ablated epithelium, BE = Barrett's epithelium, SM = submucosa, M = muscularis propria).

Three BE rats showed normal appearing epithelium, 2 rats showed partial and 6 rats complete epithelial ablation, the mean damage score to the epithelium was 2.0 (± 1.3). The intact epithelium adjacent to the irradiated area was classified as squamous or hyperplastic squamous epithelium in eight rats, in three rats the adjacent epithelium was Barrett's mucosa. Partial necrosis of the muscularis propria was seen in 4 BE rats. The submucosa showed signs of inflammation in all, and the muscularis propria in 9 rats. Seven normal Wistar rats were treated with ALA-PDT with an intraesophageal balloon pressure of 760 mm Hg and seven with a balloon pressure of 380 mm Hg. Damage was scored according to the amount of epithelial ablation, edema of the submucosa and edema and necrosis of the muscle coat. As summarized in table 2, in the high pressure group, 4 rats showed complete epithelial ablation, whereas 3 rats did not show epithelial ablation and thus did not respond. In the low pressure group 5 rats showed complete epithelial ablation, whereas two rats did not respond. In the group that was ventilated with the normal amount of oxygen, one rat died during anesthesia, 4 of 6 rats showed complete epithelial ablation, whereas 2 of 7 rats in the group that were ventilated with less oxygen showed complete epithelial ablation and one rat showed partial epithelial ablation. These effects were not significantly different between the treatment groups.

Fluence rate measurements

The mean measured fluence rate, fluence and β of all animals in this study are shown in table 2. The measured fluence rate was standardized to remove the influence of tissue optical properties. The mean measured fluence rates at the start of the treatment were 73.77 ± 1.1 mW cm^{-2} and 80.45 ± 1.5 mW cm^{-2} for ALA-PDT treated BE rats and controls respectively. During irradiation, the fluence rate remained constant. Also, the mean fluences were comparable in all groups. The mean β of BE rats at the start of treatment was 2.48 ± 0.7, and ranged from 4.2 to 1.5. This was significantly higher than the mean β of normal rats (in the pressure and oxygen groups) (1.92 ± 0.09) (P = 0.004). The irradiation, real time fluence and fluence rate were comparable in all animals despite differences in β between individual animals.

	BE rat		Normal rat			
Treatment (n)	ALA-PDT (17)	Control (4)	High P (7)	Low P (7)	High O_2 (6)	Low O_2 (7)
Fluence rate	73.8 ± 1.1	80.4 ± 1.5	74.9 ± 0.6	73.5 ± 0.5	72.8 ± 2.7	71.1 ± 1.6
Fluence	54.1 ± 0.003	54.2 ± 0.02	54.1 ± 0.04	54.1 ± 0.04	54.0 ± 0.1	53.9 ± 0.2
β	2.3 ± 0.1	2.8 ± 0.6	2.0 ± 0.1	1.9 ± 0.2	1.9 ± 0.2	1.8 ± 0.2
Responder	8 (of 11)	0	4	5	4	2
Non responder	3 (of 11)	4	3	2	2	5

Table 2 Measured fluence rate (mW cm^{-2}), fluence (J cm^{-2}) and β during ALA-PDT and control irradiation of BE rats and rats in pressure and oxygen experiments. Also shown are the numbers of responders and non responders to treatment.

PpIX photobleaching

The auto- and pre-PDT fluorescence were 4.6 times larger in BE than in normal rats. Figure 3 shows a raw fluorescence spectrum acquired under 405 nm excitation during a break in the therapeutic illumination approximately 90 s after the start of the illumination with the corresponding fitted tissue autofluorescence, PpIX fluorescence, and the photo-product fluorescence. Also shown is the residual between the fitted and raw spectra.
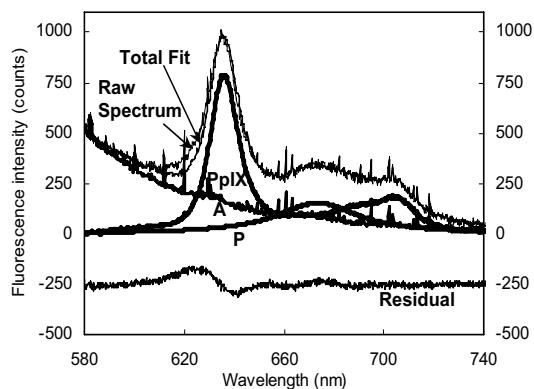
Figure 3 Raw fluorescence spectrum acquired approximately 90 s after the start of an illumination, 2 h after the administration of ALA using 405 nm excitation. SVD fitted component spectra; tissue autofluorescence (A, thick black line), PpIX fluorescence (PpIX, thick black line), photo-product fluorescence (P, thick black line), total fit and the residual between the fitted and raw spectra.

In figure 4, subplots B, D and F, the mean calculated 2nd order kinetic fitted curves of PpIX photobleaching are plotted against the measured fluence with standard deviations. Subplots C, E and G show the reciprocal of the normalized fluorescence intensity plotted against the measured fluence. The gradient of the curves plotted in this way is proportional to the local concentration of oxygen within the volume from which the fluorescence intensity is acquired (6). Figure 4A shows the measured data and the fitted 2nd order kinetic curves with the rapid decay in the first points of an individual BE rat as an example. In all subplots, animals that responded with epithelial ablation are plotted against rats that did not show epithelial ablation. In figure 4B and 4C, the mean normalized PpIX fluorescence during illumination is shown of BE rats (n=11, responders n=8, non-responders n=3). Normal rats in the experiments with different balloon pressure (n=14, responders n=9, non responders n=5) and oxygen supply (n=13, responders n=6, non responders n=7) are shown in figure 4 D & E, and 4 F & G respectively.
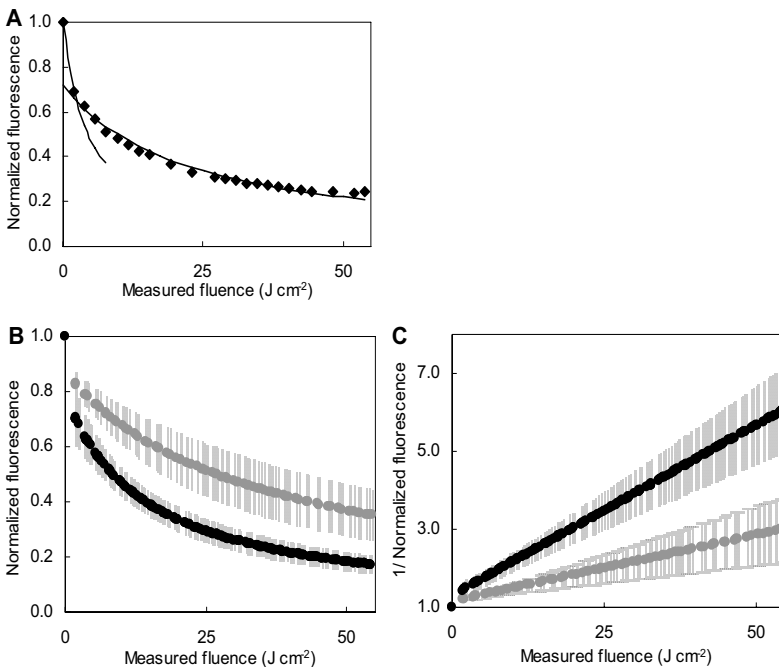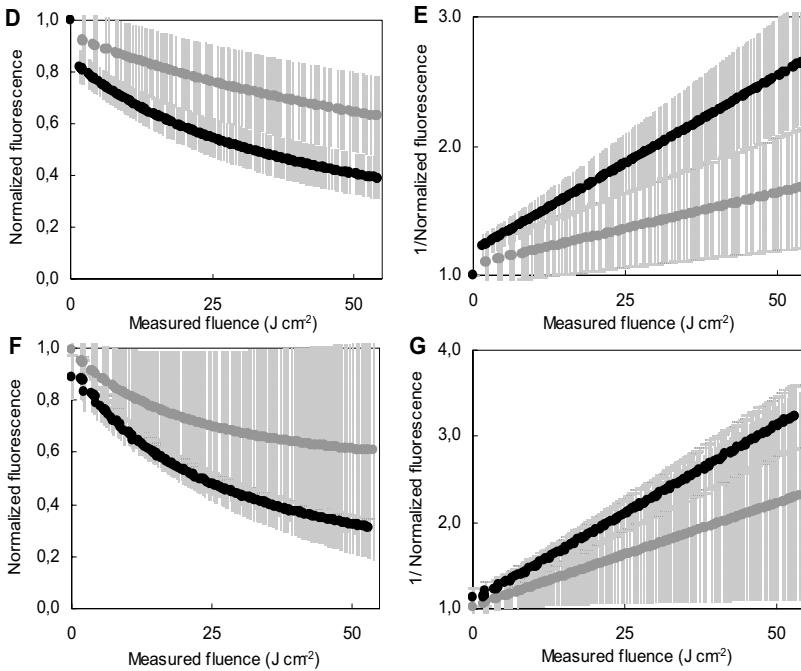
Figure 4 The mean normalized PpIX fluorescence with the standard deviation during illumination is shown of BE (n=11) and normal rats in the experiments with different balloon pressure (n=14) and oxygen supply (n=13). In subplot **A**, the normalized measured PpIX fluorescence and the fitted 2nd order kinetic curve with the rapid decay in the first points of an individual BE rat is shown as a representative example. In subplots B, D and F the mean second order fits of the fluorescence data, using the SVD routine, from animals that responded with epithelial ablation are plotted along with the mean second order fits of the fluorescence data from animals that did not show epithelial ablation. In subplots C, E and G, the reciprocal of the mean normalized PpIX fluorescence is shown for responders and non-responders. In each plot, the responders are plotted in black and the non-responders are plotted in grey. **B&C**: BE rats (black n=8; grey, n=3). **D&E:** Normal rats with normal or decreased balloon pressure (black n=9; grey n=5). **F&G:** Mean normalized PpIX fluorescence during illumination in the oxygen experiment (black n=6, grey n=7).

Similar to the normal rat esophagus (18), a two phased decay in PpIX photobleaching is observed in animals that responded to PDT with epithelial damage. Both the initial gradient and the gradient over the total PpIX fluorescence decay correlated to the tissue effects. Importantly, in BE and normal rats, in each of the three separate experiments described, the rate of photobleaching correlated with the outcome of the treatment. Figure 5 shows a box plot of the initial gradient of PpIX

fluorescence decay for all rats. The gradients during illumination of the normal rats are shown on the left, responders with complete epithelial ablation are represented by closed symbols and non-responders are represented by open symbols. On the right, the gradient during illumination of rats with BE are shown, responders are represented by closed symbols and non-responders by open symbols. BE rats with complete epithelial ablation showed a more rapid initial and second phase decay, P = 0.04 and P = 0.003 respectively. Also in the normal rat esophagus in the high and low pressure groups, a two phased decay in PpIX fluorescence was observed. The initial gradient and the gradient over the total PpIX fluorescence decay correlated to the response: rats that showed complete epithelial ablation showed a more rapid initial and total fluorescence decay, P= 0.03 and P = 0.003 respectively. In the oxygen treated rats, rats that showed a complete response showed a larger PpIX fluorescence decay, but the difference in gradient was below significance, P > 0.05. However, the difference in gradient of all normal rats was significant between responders and non responders, P = 0.004 and P = 0.02 respectively for the initial and total gradient.
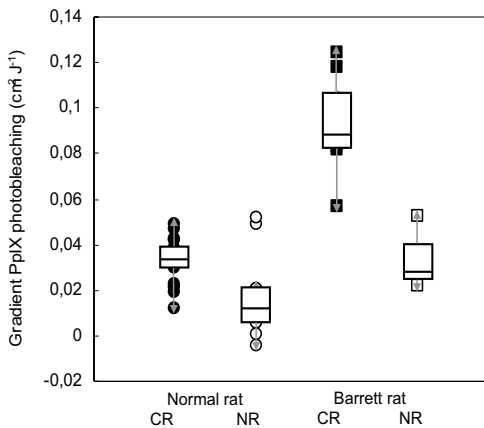
Figure 5: Box plot of the gradient (cm^2 J^{-1}) of PpIX fluorescence decay, shown for all rats. The gradients during illumination of the normal rats are shown on the left (responders n = 15, non-responders n = 12). On the right, the gradient during illumination of rats with BE are shown (responders n = 8, non-responders n = 3). Responders with complete epithelial ablation (CR) are represented by closed symbols and non-responders are represented by open symbols (NR). The median, 25th and 75th percentile are shown by the box. There are 2 mild outliers in the non-responding normal rats.

DISCUSSION

In this experimental animal model for BE, the kinetics of PpIX photobleaching during ALA-PDT were investigated. In a previous study we used the normal rat esophagus to determine the possibility of measuring and adjusting the real time fluence rate and monitoring PpIX fluorescence in vivo during ALA-PDT (18). Although the same measured fluence rate was applied, differences in effects were observed. We also found that the kinetics of PpIX fluorescence photobleaching during ALA-PDT followed a two-phased decay and that the gradient of the decay and thus the amount of PpIX photobleaching corresponded to the response of the tissue to ALA-PDT. It has been found previously that the fluence rate shows a correlation with the amount of PpIX photobleaching, lower fluence rates result in a higher rate of PpIX photobleaching for the same total fluence (4). It is also known that for the same total fluence applied, low fluence rates correspond to more tissue damage and to more PpIX fluorescence photobleaching, whereas higher fluence rates correspond to less tissue ablation and less PpIX fluorescence photobleaching (4). However, these phenomena have not been studied in BE. In clinical ALA-PDT for Barrett's esophagus, large differences are observed in the measured fluence rate and thus total measured fluence, due to differences in clinical optical properties (17). Furthermore, results of clinical ALA-PDT are suboptimal. Based on histologic evaluation of biopsies taken directly after PDT, in some cases combined with argon plasma coagulation, complete ablation of Barrett's esophagus is achieved in the vast majority of patients. However, islets of Barrett's epithelium are discovered on follow-up in a substantial number of patients. This aberrant epithelium may still harbor molecular aberrations and thus be at risk of progression to adenocarcinoma (3, 26). These findings underscore the importance of accurate dosimetry and monitoring of PpIX fluorescence. The present study aimed to determine if the correlations between PpIX photobleaching and results of ALA-PDT could also be observed in the more clinically relevant animal model of BE.

After treatment, the BE and normal rat esophagus showed wide variations in response ranging between total epithelial ablation and no response, while the same measured fluence rate was applied. Furthermore, there was a wide variation in the amount and rate of PpIX fluorescence photobleaching. In responders, a two-phased

decay in PpIX fluorescence could be observed, with a rapid initial phase at the start of the illumination. Both the initial and second phase gradient of the PpIX photobleaching related to the tissue effects of ALA-PDT. Rapid PpIX photobleaching corresponded to complete epithelial ablation, whereas in non-responders PpIX photobleaching occurred with less initial and total PpIX photobleaching ($P < 0.05$).

Additional experiments were done in an attempt to explain this observation. Both the tissue response and PpIX photobleaching depend on the supply and consumption of molecular oxygen. It is thought that with higher fluence rates, molecular oxygen is consumed more rapidly, whereas with lower fluence rates there is a balance between supply and consumption of molecular oxygen (9). It is also thought that vascular shutdown and limitation of supply of oxygen has an impact on the outcome of ALA-PDT (14). When the fluence rate is kept constant, other factors must be responsible for the hypothesized difference in availability in oxygen. The blood supply of the esophagus consists of longitudinal vessels from which penetrating capillaries feed the submucosa and oxygen diffuses into the mucosa. Higher balloon pressures within the esophagus may compromise the blood flow and thus the supply of oxygen and therefore limit the effects of ALA-PDT. In the present study, this hypothesis could not be proven. The results of this study indicate that oxygen tension under these conditions is sufficient to allow a photochemical reaction, since hypothesized depletion of oxygen through higher balloon pressures did not result in a significantly worse outcome. In addition, lower balloon pressures did not result in a significantly better outcome. However, since it is not possible to measure oxygen tension at the treatment site during PDT, this experiment is not conclusive. The results of the higher balloon pressure experiment indicate that the balloon pressure used, does not compromise blood and oxygen supply in the esophageal mucosa. Pech et al (27) have shown previously that external supply of additional oxygen did not increase the effects of ALA-PDT. In the present study rats were mechanically ventilated with a gaseous mixture of air partially depleted of oxygen. However, the outcome was not significantly different in normally ventilated rats or low oxygen ventilated rats. In the normally ventilated rats, 4 out of 6 rats showed complete response, whereas only 2 out of 7 rats in the depleted oxygen group showed complete epithelial ablation. Limitation of external oxygen supply had no significant effect at the treatment site. The absolute rate of photobleaching was greater in the responders in the oxygenated

group, although this was not significant. However, when the initial gradient of PpIX photobleaching are compared in all normal rats between responders and non-responders, the difference is highly significant.

More interesting are the observed relationships between response and amount and rate of PpIX photobleaching. In all experiments described, more PpIX photobleaching corresponded to complete epithelial ablation. PpIX fluorescence measurement therefore is a feasible parameter to predict the outcome of ALA-PDT in vivo. A more direct parameter to measure the effectiveness of the photochemical reaction would be direct monitoring of reactive oxygen species at the treatment site. At present, this is a very complicated technique, although imaging of PDT generated reactive oxygen species has recently been described (28). Another observed phenomenon is that the rate of PpIX fluorescence decay in BE rats was higher than in the normal esophagus. For other tumor models, such as skin tumors, the PpIX fluorescence decay is the same or less than in normal tissue during ALA-PDT, because of reduced vascular and oxygen supply in such tumors (6).The thickness of the mucosa in BE is significantly increased, with more cellular layers, compared to normal esophageal epithelium. Also, the photosensitizer PpIX is preferentially located in the mucosa (29). Therefore, both PpIX fluorescence before PDT and the PpIX fluorescence decay may well be increased in BE, which further supports the potential of ALA-PDT as treatment of premalignant BE.

REFERENCES

1. Schnell, T. G., S. J. Sontag, G. Chejfec, G. Aranha, A. Metz, S. O'Connell, U. J. Seidel and A. Sonnenberg (2001) Long-term nonsurgical management of Barrett's esophagus with high-grade dysplasia. *Gastroenterology.* **120**, 1607-19.

2. Barr, H., N. A. Shepherd, A. Dix, D. J. Roberts, W. C. Tan and N. Krasner (1996) Eradication of high-grade dysplasia in columnar-lined (Barrett's) oesophagus by photodynamic therapy with endogenously generated protoporphyrin IX. *Lancet.* **348**, 584-585.

3. Siersema, P. D. (2005) Photodynamic therapy for Barrett's esophagus: not yet ready for the premier league of endoscopic interventions. *Gastrointest Endosc.* **62**, 503-7.

4. Robinson, D. J., H. S. de Bruijn, N. van der Veen, M. R. Stringer, S. B. Brown and W. M. Star (1998) Fluorescence photobleaching of ALA-induced protoporphyrin IX during photodynamic therapy of normal hairless mouse skin: the effect of light dose and irradiance and the resulting biological effect. *Photochem Photobiol.* **67**, 140-9.

5. Boogert, J. v. d., H. J. v. Staveren, R. W. d. Bruin, J. H. Eikelaar, P. D. Siersema and R. v. Hillegersberg (1999) Photodynamic therapy for esophageal lesions: selectivity depends on wavelength, power, and light dose. *Ann Thorac Surg.* **68**, 1763-1769.

6. Robinson, D. J., H. S. de Bruijn, N. van der Veen, M. R. Stringer, S. B. Brown and W. M. Star (1999) Protoporphyrin IX fluorescence photobleaching during ALA-mediated photodynamic therapy of UVB-induced tumors in hairless mouse skin. *Photochem Photobiol.* **69**, 61-70.

7. Georgakoudi, I. and T. H. Foster (1998) Singlet oxygen- versus nonsinglet oxygen-mediated mechanisms of sensitizer photobleaching and their effects on photodynamic dosimetry. *Photochem Photobiol.* **67**, 612-625.

8. Foster, T. H., R. S. Murant, R. G. Bryant, R. S. Knox, S. L. Gibson and R. Hilf (1991) Oxygen consumption and diffusion effects in photodynamic therapy. *Radiat Res.* **126**, 296-303.

9. Finlay, J. C., D. L. Conover, E. L. Hull and T. H. Foster (2001) Porphyrin bleaching and PDT-induced spectral changes are irradiance dependent in ALA-sensitized normal rat skin in vivo. *Photochem Photobiol.* **73**, 54-63.

10. Coutier, S., L. N. Bezdetnaya, T. H. Foster, R. M. Parache and F. Guillemin (2002) Effect of Irradiation Fluence Rate on the Efficacy of Photodynamic Therapy and Tumor Oxygenation in Meta-Tetra (Hydroxyphenyl) Chlorin (mTHPC)-Sensitized HT29 Xenografts in Nude Mice. *Radiat Res.* **158**, 339-345.

11. Rhodes, L. E., M. M. Tsoukas, R. R. Anderson and N. Kollias (1997) Iontophoretic delivery of ALA provides a quantitative model for ALA pharmacokinetics and PpIX phototoxicity in human skin. *J Invest Dermatol.* **108**, 87-91.

12. Konig, K., H. Schneckenburger, A. Ruck and R. Steiner (1993) In vivo photoproduct formation during PDT with ALA-induced endogenous porphyrins. *J Photochem Photobiol B.* **18**, 287-90.

13. Niedre, M. J., C. S. Yu, M. S. Patterson and B. C. Wilson (2005) Singlet oxygen luminescence as an in vivo photodynamic therapy dose metric: validation in normal mouse skin with topical amino-levulinic acid. *Br J Cancer.* **92**, 298-304.

14. Sitnik, T. M., J. A. Hampton and B. W. Henderson (1998) Reduction of tumour oxygenation during and after photodynamic therapy in vivo: effects of fluence rate. *Br J Cancer.* **77**, 1386-94.

15. Staveren, H. J. v., M. Keijzer, T. Keesmaat, H. Jansen, W. J. Kirkels, J. F. Beek and W. M. Star (1996) Integrating sphere effect in whole-bladder wall photodynamic therapy: III.

Fluence multiplication, optical penetration and light distribution with an eccentric source for human bladder optical properties. *Phys Med Biol.* **41**, 579-90.

16. Star, W. M. (1995) The relationship between integrating sphere and diffusion theory calculations of fluence rate at the wall of a spherical cavity. *Phys Med Biol.* **40**, 1-8.

17. Van Veen, R. L., M. C. Aalders, K. L. Pasma, P. D. Siersema, J. Haringsma, W. Van De Vrie, E. E. Gabeler, D. J. Robinson and H. J. Sterenborg (2002) In situ light dosimetry during photodynamic therapy of Barrett's esophagus with 5-aminolevulinic acid. *Lasers Surg Med.* **31**, 299-304.

18. Boere, I. A., D. J. Robinson, H. S. de Bruijn, J. van den Boogert, H. W. Tilanus, H. J. Sterenborg and R. W. de Bruin (2003) Monitoring in situ dosimetry and protoporphyrin IX fluorescence photobleaching in the normal rat esophagus during 5-aminolevulinic acid photodynamic therapy. *Photochem Photobiol.* **78**, 271-7.

19. Levrat, M., R. Lambert and G. Kirschbaum (1962) Esophagitis produced by reflux of duodenal contents in rats. *Am J Dig Dis.* **7**, 564-573.

20. Santini, A. M. E. and M. Baccarini (1984) Jejunal transposition after total or partial gastrectomy - an experimental model in the rat. In Handbook of microsurgery Vol. (Edited by W. Olszewski), pp. CRC press, Boca Raton, Florida.

21. Veen, P. v., J. H. Schouwink, W. M. Star, H. J. Sterenborg, J. R. van der Sijp, F. A. Stewart and P. Baas (2001) Wedge-shaped applicator for additional light delivery and dosimetry in the diaphragmal sinus during photodynamic therapy for malignant pleural mesothelioma. *Phys Med Biol.* **46**, 1873-83.

22. Marijnissen, J. P. and W. M. Star (1996) Calibration of isotropic light dosimetry probes based on scattering bulbs in clear media. *Phys Med Biol.* **41**, 1191-1208.

23. Robinson, D. J., H. S. de Bruijn, W. J. de Wolf, H. J. Sterenborg and W. M. Star (2000) Topical 5-aminolevulinic acid-photodynamic therapy of hairless mouse skin using two-fold illumination schemes: PpIX fluorescence kinetics, photobleaching and biological effect. *Photochem Photobiol.* **72**, 794-802.

24. Finlay, J. C., S. Mitra and T. H. Foster (2002) In vivo mTHPC photobleaching in normal rat skin exhibits unique irradiance-dependent features. *Photochem Photobiol.* **75**, 282-288.

25. Georgakoudi, I., B. C. Jacobson, J. Van Dam, V. Backman, M. B. Wallace, M. G. Muller, Q. Zhang, K. Badizadegan, D. Sun, G. A. Thomas, L. T. Perelman and M. S. Feld (2001) Fluorescence, reflectance, and light-scattering spectroscopy for evaluating dysplasia in patients with Barrett's esophagus. *Gastroenterology.* **120**, 1620-1629.

26. Hage, M., P. D. Siersema, K. J. Vissers, E. W. Steyerberg, J. Haringsma, E. J. Kuipers and H. van Dekken (2005) Molecular evaluation of ablative therapy of Barrett's oesophagus. *J Pathol.* **205**, 57-64.

27. Pech, O., C. D. Nagy, L. Gossner, A. May and C. Ell (2002) Photodynamic therapy of human Barrett's cancer using 5-aminolaevulinic acid-induced protoporphyrin IX: an in-vivo dosimetry study in athymic nude mice. *Eur J Gastroenterol Hepatol.* **14**, 657-62.

28. Niedre, M. J., M. S. Patterson, A. Giles and B. C. Wilson (2005) Imaging of Photodynamically Generated Singlet Oxygen Luminescence In Vivo. *Photochem Photobiol.*

29. Boogert, J. v. d., R. v. Hillegersberg, F. W. d. Rooij, R. W. d. Bruin, A. Edixhoven-Bosdijk, A. B. Houtsmuller, P. D. Siersema, J. H. Wilson and H. W. Tilanus (1998) 5-Aminolaevulinic acid-induced protoporphyrin IX accumulation in tissues: pharmacokinetics after oral or intravenous administration. *J Photochem Photobiol B.* **44**, 29-38.

Chapter 7

Use of fiber optic probes for detection of Barrett's epithelium in the rat esophagus by Raman spectroscopy

I.A. Boere, T.C. Bakker Schut, J. van den Boogert, R.W.F. de Bruin, G.J. Puppels

Departments of Surgery and Radiation Oncology, Photodynamic Therapy & Optical Spectroscopy Research Program, Erasmus MC Rotterdam, Netherlands

ABSTRACT

In the last decades, there has been a dramatic increase in the incidence of Barrett's esophagus and the associated esophageal adenocarcinoma. Therefore, patients with a Barrett's esophagus undergo regular endoscopic surveillance with randomly taken biopsies to detect the presence of high-grade dysplasia or carcinoma. Sampling errors and observer variation, inherent to such a surveillance protocol warrant other detection methods. Raman spectroscopy is a non-invasive optical spectroscopic technique that provides detailed information about the molecular composition and structure of tissues. Changes in molecular composition in tissues as a consequence of pathologic processes, can thus be recognized. For clinical application of Raman spectroscopy, thin and flexible fiber optic probes can be used that fit in the auxiliary channel of an endoscope. In this study, a multivariate classification model was developed for detection of Barrett's epithelium, based on ex vivo Raman spectra of the rat esophagus. The spectra were collected with three different fiber optic probes and on 11 different days. This mimics the way a database is collected in a clinical situation, including all instrument calibration, probe-to-probe and day-to-day variation. After elimination of interfering background signal contributions from the different probes using a vector-correction procedure, we could discriminate between Barrett's and normal epithelium with accuracy higher than 93 percent. The model yields a spectral discriminant that best separates the two groups. To facilitate interpretation of this discriminant, we obtained Raman spectra from tissue sections of normal esophageal epithelium, keratin and muscle layer using a confocal Raman microscope.

INTRODUCTION

Barrett's esophagus is a condition in which the cells that normally line the inner surface of the esophagus (epithelium) more resemble the epithelium of the gut. Microscopically, the normal squamous epithelium has been replaced by a more glandular type of epithelium, a process called intestinal metaplasia (1). It is believed that Barrett's esophagus develops through longstanding gastro-esophageal reflux of acid and bile, occasionally accompanied by symptoms like heartburn. Barrett's esophagus carries a 30-125 fold increased risk of becoming malignant, through a process of further changes of the epithelium. Within this sequence of metaplasia, dysplasia and carcinoma, the epithelial cells show morphologic changes as well as some functional changes, such as a higher proliferation rate (2). In the past decennia, the incidence of Barrett's esophagus and the associated esophageal adenocarcinoma have increased dramatically (3, 4), whereas the prognosis of esophageal cancer has remained poor (mean 5-year-survival 8-20% (5)). Therefore, patients with a Barrett's esophagus undergo regular endoscopic follow up with biopsies taken in 4 quadrants at 2 cm intervals and from apparent lesions to detect malignancies at earlier stages. Whereas its salmon-like aspect within the paler normal surface can usually identify larger areas of Barrett's esophagus during endoscopy, dysplasia and small carcinomas cannot be distinguished from the surrounding area. If biopsy tissue contains high-grade dysplasia or carcinoma, esophageal resection is the treatment of choice. The efficacy of surveillance is negatively influenced by biopsy sampling error and inter-observer variation in pathological assessment of the biopsies. Several techniques have been used to decrease sampling errors. These techniques include chromoendoscopy, endosonography, optical coherence tomography, light scattering spectroscopy (6) and fluorescence detection techniques, but until now with limited success (7). For example, fluorescence detection with administration of the 5-aminolevulinic acid induced photosensitizer protoporphyrin IX, can achieve high sensitivity in detecting dysplasia, but lacks appropriate selectivity due to the presence of inflammatory cells which induce high fluorescence as well (8). Therefore, other techniques to increase the efficacy of biopsies are warranted.

Raman spectroscopy is a technique that is able to detect molecular differences between tissues, based on their Raman signature. Tissue components, such as

collagen, show clearly recognizable Raman peaks. Different types of tissue can be discriminated using Raman spectroscopy, as well as molecular changes in a tissue that accompany pathological processes. In this way, Raman spectroscopy can be used as a diagnostic tool to detect (pre-) malignant lesions (9-12). Previously, using in vitro microscopic Raman spectroscopic techniques and a multivariate statistical model, Barrett's epithelium could be discriminated from normal esophagus (13). To be clinically applicable for Barrett's surveillance, Raman spectroscopy has to be able to detect dysplasia within Barrett's esophagus in vivo. This means that a fiber optic probe, limited to the size of the biopsy canal in an endoscope, must be used for excitation and detection of the Raman signal (14, 15). Fast and accurate signal analysis should then identify suspect lesions within the esophagus. In this way, surveillance of Barrett's esophagus could become more efficient.

In the present study, we have investigated the use of such fiber optic probes for collecting a spectral database, which is then used to build a multivariate classification model. Primarily, the aim was to evaluate whether we could build an accurate Raman spectroscopic classification model, using a database collected on different days and with different probes. This is comparable to the circumstances in which a clinically relevant database would be collected. Secondly, it was determined if Raman spectroscopy could detect intestinal metaplasia in a rat model for Barrett's esophagus (16, 17). A database of ex vivo Raman spectra from both normal and Barrett's esophagus was collected. Subsequent tissue histology was used as the gold standard. A multivariate statistical model was designed, based on the differences in Raman spectra of the different tissues. Raman microspectroscopic measurements of pure rat esophageal keratin, normal epithelium and esophageal muscle were used as references for interpretation of the data collected with fiber optic probes.

MATERIALS AND METHODS

Experimental design A rat model of Barrett's esophagus was used in which intestinal metaplasia is induced by reflux of duodenal contents. This model is used to study the etiology of the disease as well as treatment modalities. Reflux was caused through a surgical procedure, an esophagojejunostomy (figure 1). The esophagus was attached to the jejunum after a total gastrectomy according to the method

described by Levrat (16, 18, 19). Ether inhalation was used as anesthesia and buprenorphin (0.05 mg kg^{-1} im, single dose) was used as analgesic during and directly after surgery respectively. The "Committee on Animal Research" of the Erasmus MC Rotterdam approved the experimental design. The area of intestinal metaplasia expanded in time from the site of the anastomosis to more proximally in the esophagus. The animals used in this study were sacrificed 9-12 months after surgery by exsanguination. In total, 66 rat esophagi were used. In addition, the esophagi of 3 healthy rats were used in Raman microspectroscopic measurements. After excision, the esophagus was opened longitudinally and examined for macroscopic abnormalities. On each esophagus, multiple spots were measured by Raman spectroscopy. A suture marked the area from which the Raman spectrum was obtained. Samples were obtained from both the Barrett's epithelium, if present, and from the normal segment more proximally. After Raman measurement, samples were fixed in formalin and embedded in paraffin, 5 μm sections were cut, stained with both haematoxylin and eosin (H&E) and alcian blue, and then used for histological examination. During examination, the sutures were identified in all samples and the sections were scored either as normal or as Barrett's epithelium.
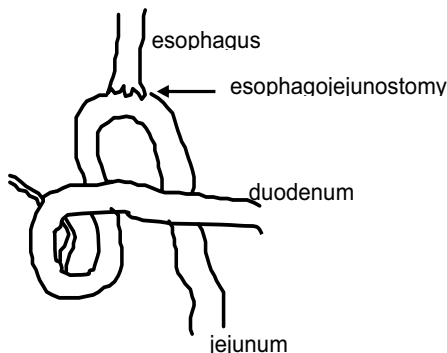
Figure 1 Scheme of the surgical procedure to induce Barrett's esophagus. After resection of the stomach, the esophagus is attached to the jejunum and the duodenum is closed with sutures.

Raman spectroscopy: Ex vivo probe measurements. For the ex vivo measurements a Raman spectroscopic system equipped with a fiber-optic probe was used. The system was built in-house (15). In this study, Enviva gaser-level 10 fiber optic Raman probes (Visionex Inc, Atlanta, GA) were used to guide the laser light to

the tissue and collect the Raman light. The principles and performance of the probe have been described in detail earlier (20, 21). The probe consists of one excitation fiber (400 micron in diameter) surrounded by seven collection fibers (each 300 micron in diameter). The collection fibers are beveled to limit the actual measurement volume (defined by the overlap between the fields of view of the excitation fiber and the collection fibers) to the first 100-600 microns of tissue. The probes were further optimized to collect Raman signal from the first 400 micron of tissue by placing a quartz or CaF_2 window with a thickness of 200 micron at the end of the probe tip. This significantly reduces the sampling depth of the probes to the biologically more interesting epithelial layers where the first biochemical changes of (pre-) malignancy take place. There are however two disadvantages of placing a window at the end of probe tip. First the background Raman signal generated in the probe itself increases (whereas the amount of tissue Raman signal that is collected decreases). Therefore placing a window significantly decreases the signal to background ratio of the collected spectra. Secondly, adding an optical element to the probe introduces an extra source of variation and therefore reduces the reproducibility of the probes with respect to its background signal, making it more difficult to compare tissue spectra measured with different probes. During this study three different but similar gaser-level 10 probes were used, two with a CaF_2 window, and one with a quartz window. For illumination the output from a diode laser, operating at 830 nm (PI-ECL-830-500 diode laser, Process Instruments, Salt Lake City, UT), is coupled into the excitation fiber of the probe, with an output power at the tissue of 150 mW. The collection fibers of the probe are coupled to a modified dispersive imaging spectrometer (RA 100, Renishaw Inc, Wotton under Edge, UK). A spectral interval from 400 to 1800 cm^{-1}, with a spectral resolution of 8 cm^{-1}, is imaged on the CCD-camera of the spectrometer. The spectra were acquired with 60 s signal integration time with Grams-software (Galactic Industries Corp., Salem, NH, USA) running on a desktop computer. The excised esophagi, which are very thin and therefore partly transparent to the illuminating light, were mounted on a black absorbing surface to prevent collection of backscattered laser light from the surface, with the epithelial side facing the probe.

Microscopic measurements. Raman spectra of the tissue sections were obtained by a Raman microscope built in-house, which has recently been described

in more detail (22). Briefly, the set up consists of an automated microscope (DM-RXE, Leica, Cambridge, UK) coupled to a Raman spectrometer (System 100, Renishaw, Wotton under Edge, UK). An 80x NIR optimized objective (Olympus, Japan) was used to focus laser light of 847 nm on the sample and to collect the light that was scattered by the sample. The collected light was filtered to reject Rayleigh scatter and analyzed by the spectrometer. A spectral interval from 400 to 1800 cm^{-1}, with a spectral resolution of 8 cm^{-1} was imaged on the CCD-camera of the spectrometer. Acquisition of Raman spectra was controlled by the WiRE 1.2 software (Renishaw) running under Grams/32 Spectral Notebase Software (Galactic Industries Corp., Salem, NH, USA). For the Raman microscopic measurements unstained cryo-sections with a thickness of 12 μm, mounted on CaF_2 slides, were placed on a xyz-motorized, computer controlled sample stage (Leica DM STC, Cambridge, UK). Raman mapping software to enable automatic scanning of the sample was implemented in Array Basic (the internal software platform of Grams), which controlled the microscope unit, the microscope stage and the spectrometer during spectral acquisition. The scanning area and the scanning step size were manually adjusted, which divided the area of interest into small square areas, called Raman pixels. Spectra were obtained consecutively from each of these Raman pixels, the size of which varied between 10-50 μm^2 for the different measurements. The 80x microscope objective focused the laser light to a spot of less than 1 μm^2. Therefore, in order to obtain a spectrum that is representative for all the tissue in a Raman pixel, the whole area of the Raman pixel was scanned during each acquisition. The laser light was focused 2 micron below the surface of the tissue section to maximize Raman signal intensity. The samples were illuminated with 100 mW of laser power. The signal collection time per Raman-pixel was 5 seconds.

Spectral analysis All spectral analysis software was developed in a Matlab environment (Matlab 6.1: The MathWorks, Inc., Natick MA, USA) using the multivariate statistical analysis toolbox PLS-toolbox 2.0.0c (Eigenvector Research, Inc., Manson, WA, USA). All spectra were calibrated (400 to 1800 cm^{-1}) and corrected for the spectral sensitivity of the set-up as described in a previous study (15).

Ex vivo measurements. In order to enhance the Raman features and reduce the influence of slowly varying backgrounds, all spectra were Savitzky-Golay differentiated with a smoothing window of 15 wavenumbers prior to modeling. The interfering background signal, generated in the probe itself by backscattered light from the window surface and the tissue, varied from probe to probe and could not easily be subtracted to yield the pure tissue spectrum. To prevent the presence of residual probe signal from influencing the model, all spectral variation that could be attributed to probe signal was eliminated by a vector-correction procedure described earlier (23). Briefly, this procedure is as follows, the Raman signal that is generated in the probe by backscattered light was measured separately by collecting the scattered light from a highly reflective aluminum surface, which does not give rise to any measurable Raman signal itself. Since the backscatter signal was slightly dependent on the angular distribution of the scattered light, multiple measurements were done with different orientations with regard to the scattering surface. This procedure was repeated for each probe and for each day, resulting in a dataset, which contains the spectral variance that can be attributed to all probes used in this study. Principal Component Analysis (PCA) was applied on this data set to derive a new and smaller set of orthogonal spectral parameters that describe the variance present. The tissue spectra (with the interfering probe contributions) are then projected on these Principal Components (PCs). All variance that can be explained by these PCs, and therefore might be caused by the probe itself, is thus removed from the tissue spectra and the residuals are kept as the new (pure tissue) spectra. Subsequently the spectra were autoscaled, i.e. scaled to have zero mean and unit variance. With these pure tissue spectra, a multivariate statistical classification model was built. Clear outliers, defined as spectra outside five times the standard deviation from the mean, were removed from the data set. PCA was used on the corrected data set to orthogonalize and reduce the number of parameters needed to represent the variance in the spectral data set. Only PCs that accounted for more than 0.5 pct of the variance in the data set were retained. A two-sided t-test was used to individually select those PC that showed significance higher than 0.9 in discriminating the different tissue classes. These PCs were used as variables in a Linear Discriminant Analysis (LDA) model. An LDA-model yields N-1 linear discriminants (LDs) that best separate N given groups by finding the directions in spectral space that yield the highest ratios between inter- and intragroup distances (24). The number

of PCs that were included in the LDA model was much lower than the number of spectra in the smallest model group, thus minimizing the chance of overfitting. Histopathology was used as gold standard for classifying the spectra as originating from Barrett's or from normal epithelium. The LDA model was tested by cross validation.

Microscopic measurements. After calibration, the spectra were corrected for interfering background Raman signal originating from the optical elements in the laser light delivery pathway and the CaF_2 slide. The measured areas were averaged over all Raman pixels, after removal of clear outliers defined as spectra outside 5 times the standard deviation from the mean spectrum of the map.

RESULTS AND DISCUSSION

In total 131 epithelial spectra of 66 excised rat esophagi were acquired on 11 different days during a period of 4 months, using the fiber-optic Raman set-up. 16 spectra were identified as clear outliers, due to low signal to noise ratio, very high fluorescence backgrounds or interfering high contributions of blood or of the suture. The remaining 115 spectra of 60 different rats were included to build a spectral classification model, 68 spectra from normal epithelium and 47 from Barrett's epithelium.

Figure 2, row A, shows the calibrated and autoscaled esophageal spectra that were measured on two different days with two different probes. The probes were similar but had a different window material, calcium-fluoride (day 5) or fused silica (day 12). The spectra of normal rat esophagus are plotted in black, those of Barrett's epithelium in grey. The spectra of the background signal, generated in the probe itself by backscattered light from the window surface and the tissue, are shown in row B of figure 2. Variation in the spectra of one probe is due to different angular intensity distributions of the scattered light. These interfering background signals could not easily be subtracted to yield the pure tissue spectrum, as can be seen from the spectra shown in row C. Here, the relative contributions of the probe signal, shown in row B were estimated by a fitting procedure and subtracted from the spectra shown in row A.
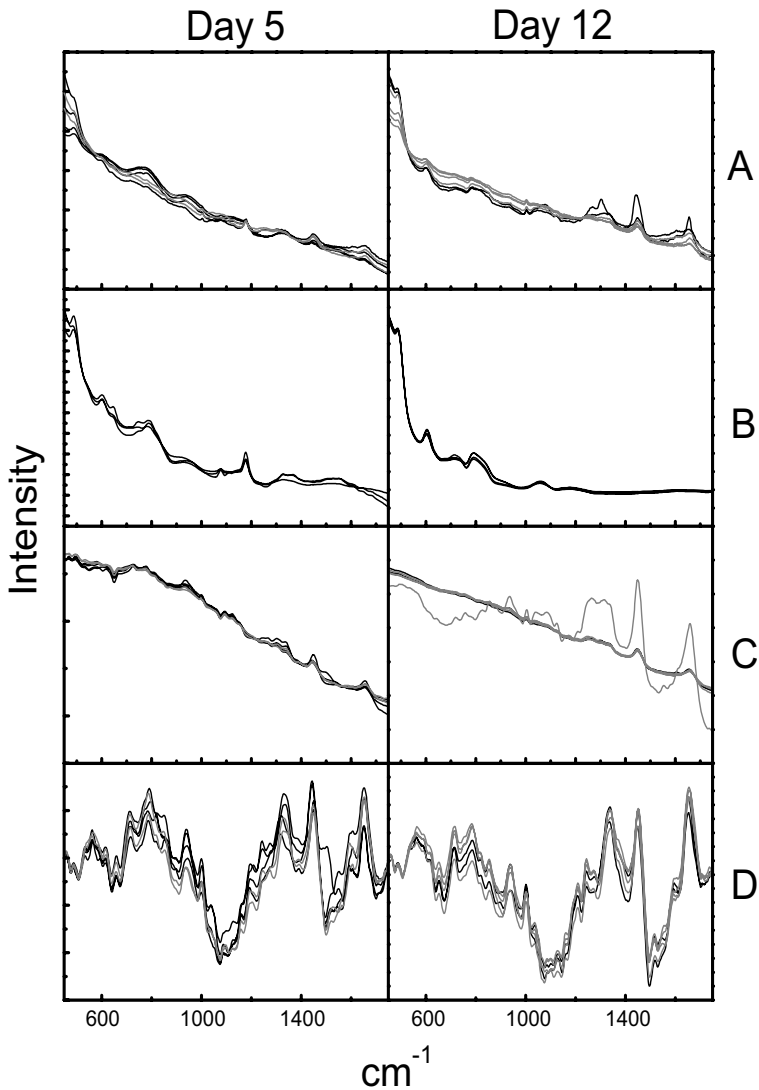
Figure 2 Influence of different signal processing procedures on rat esophagus spectra measured with two different probes. On day 5, a fiber optic probe with a calcium-fluoride window was used, on day 12 a probe with a fused silica window. The spectra of normal rat esophagus are plotted in black, those of Barrett's epithelium in grey.

row **A**: Calibrated spectra of normal rat esophagus epithelium and Barrett's epithelium with interfering probe contributions.

row **B**: Calibrated spectra of the signal that is generated in the probe by backscattered light.

row **C**: Spectra of row A, corrected for the probe spectra of row B by scaled subtraction.

row **D**: Spectra of row A, corrected for the signal of all probes, used in this study, by a vector-correction procedure

The spectra are corrected only for the specific probe contributions measured on that specific day. Although most probe signal is eliminated, the spectra still show residual probe characteristics, which is most clear for the probe with a calcium-fluoride window (day 5). Elimination of all spectral variation that can be attributed to probe signal using the vector-correction procedure described above, yield the spectra shown in row D of figure 2. The spectra were integrated to facilitate comparison. This procedure, which removes the variance that can be attributed to any of the probes used in this study, yields residual spectra that are clearly better comparable, although still some residual probe effects seem to be present.

PCA was used to transform this vector-corrected data set to 25 new orthogonal variables, PCs. From this set the 6 most significant PCs were selected as input variables to the LDA model. This number of input variables to the model was much lower than the number of spectra in the smallest (25) group and thus overfitting was prevented. An LDA model yields one discriminant, which is the direction in spectral space that best separates the two groups. The representation of this discriminant in the original spectral space (after back-transformation from PC-space and integration) is shown in figure 3A. A spectrum can be classified by projecting it on the discriminant. When this projection gives a positive result the spectrum is classified as normal, when negative the spectrum is classified as Barrett's. The validity of the LDA model was tested by "leave one esophagus out" cross validation. In this validation method all spectra belonging to one rat esophagus (ranging from 1 to 4 spectra) were left out of the model data, a new LDA-model was build and the left out spectra were predicted by this new model. This validation method, which tests the prediction accuracy for 'new' spectra, yields a 93.9% correct prediction.

The validity of the model was further tested by "leave one day out" cross validation. In this validation all spectra measured on a single day (ranging from 3 to 20 spectra) were left out and a model was built on the spectra of the remaining days. This validation method, which tests the prediction accuracy for 'new' spectra while including the effects of day-to-day variation due to calibration variations and the use of different fiber-optic probes, yields a 93.0% correct prediction.
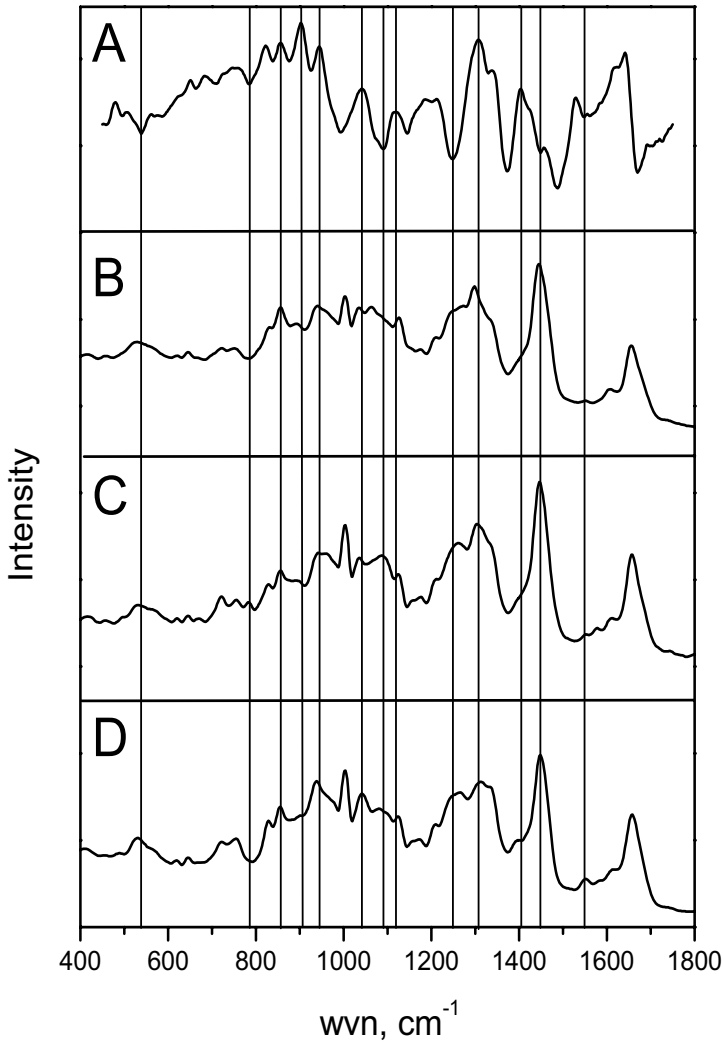
Figure 3 Comparison of the model discriminant to spectra of different epithelial structures.

A: Discriminant of the Linear Discriminant Analysis model to classify normal and Barrett's epithelium in rat-esophagus by fiber optic probe measurements.

B: Average spectrum of a small area of the keratin layer from a frozen section of a normal rat esophagus, measured with a confocal Raman microscope

C: Average spectrum of a small area of the epithelium below the keratin layer from a frozen section of a normal rat esophagus, measured with a confocal Raman microscope

D: Average spectrum of a small area of muscle below the epithelium from a frozen section of a normal rat esophagus, measured with a confocal Raman microscope

The best way to evaluate an LDA-model would be to test the model accuracy with a completely independent data set, preferably measured with a probe that is not used for collecting the data in the model set. The limited amount of data and the heterogeneity of the data set, due to the use of different probes, prevented us to do a leave-one-probe-out validation procedure. However, the cross validation results show that the accuracy of the model is practically independent of the spectra of a single rat and even of the spectra of a single day.

The spectral features in the discriminant yielded by the LDA-model (figure 3A) must be related to differences in composition and / or tissue architecture between the normal and Barrett's epithelium. Figure 4 shows haematoxylin and eosin (H&E) stained sections of normal rat and of Barrett's esophagus. The differences between the 2 sections are the type of epithelium (E), the presence of a keratin layer in the normal rat esophagus (K) and the elongation of the epithelial papillae and villi in Barrett's esophagus. Furthermore, an inflammatory infiltrate is present mainly in the submucosa of Barrett's esophagus. These factors increase the total thickness of the esophageal wall and in particular the distance between the esophageal surface and the muscle layer. The probes obtain spectra from the first 400 microns of tissue. Therefore, all esophageal layers, epithelium with the keratin layer, submucosa and muscularis, contribute to the Raman signal. Considering the differences in thickness of these layers for normal and Barrett's epithelium, the layers will have different contributions to the spectra of normal and Barrett's epithelium. Therefore, the discriminant is likely to have features at positions that mark the spectral differences between the three layers (differences in relative peak height and / or peak position). To compare the discriminant with the spectral differences of these esophageal structures, Raman microscope spectra of small areas of keratin, epithelium and muscle were obtained from frozen sections of a normal rat esophagus. The average spectra of these three histologically distinct esophageal layers are shown in figure 3B to 3D. The vertical lines indicate the positive and negative features in the discriminant that can be related to prominent spectral differences in these three spectra. The discriminant acts as a weighing function and its features need not have the same shape as the spectral features. Figure 3 shows that many, but not all, of the strong features in the discriminant can be attributed to different contributions of these three histological structures in normal and Barrett's epithelium. Normal esophageal

spectra, which have higher contributions of keratin (row B) and muscle (row D), yield a positive result when projected on the discriminant. Therefore many of the positive features in the discriminant are associated with relative higher features in the spectra of muscle and / or keratin. Barrett's spectra, which have a relative higher contribution of the epithelial layer, yield a negative result and many of the negative features in the discriminant are associated with relative higher features in the spectra of epithelium (row C). The features that cannot be explained by differences in the spectra of these structures may be explained by differences between Barrett's and normal epithelium, since muscle layers are not likely to differ between Barrett's and normal rat esophagus.
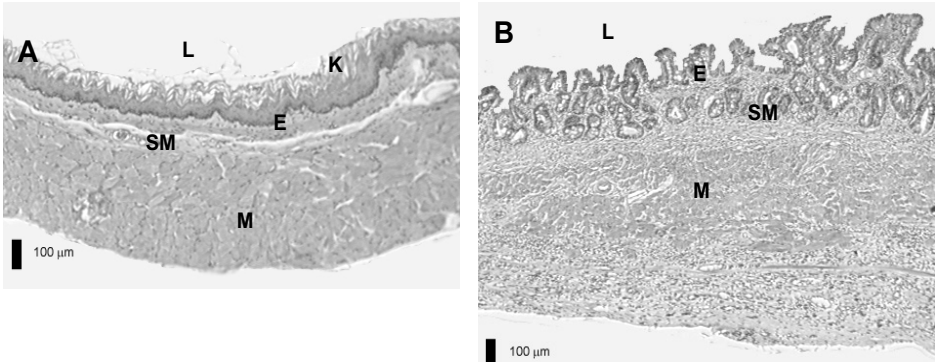
Figure 4A: H&E stained transmural section of the normal rat esophagus (obj 5x). (L = esophageal lumen, K = keratin, E = epithelium, SM = submucosa, M = muscle layer). **B**: H&E stained transmural section of a rat Barrett's esophagus (L = esophageal lumen, E = epithelium, SM = submucosa, M = muscle layer)

The aims of this ex vivo study were to investigate if an accurate Raman spectroscopic classification model could be build with a database collected on different days and with different probes and secondly if Raman spectroscopy could differentiate between Barrett's epithelium and normal esophageal epithelium. This study was performed in rats, since this particular animal model for Barrett's esophagus is frequently used for studies on Barrett's esophagus. The progression of Barrett's esophagus in animal models could thus potentially be observed non-invasively with fiber optic probes in vivo, using side-viewing probes with a diameter of 1-2 mm maximum.

In this study, a Raman database of the rat esophagus and a statistical model were developed based on esophagus samples of Barrett's and normal epithelium. The database was collected with different fiber optic probes and measured on many different days over a prolonged period of time. Any problems that may arise from day-to-day variations in instrumentation, as the probes used were clearly different in performance and calibration, were thus incorporated. Therefore the data were filtered rigorously to obtain pure tissue spectra, although some variance of the tissue spectra was also removed in this way. Nevertheless, this resulted in a classification model that was correct in > 93%. The misclassifications generated in the leave-one-esophagus-out validation and leave-one-day-out validation concerned the same samples, although 1-2 extra misclassifications occurred in the leave-one-day-out validation, probably due to a decrease of the data set. There is a considerable difference between Barrett's epithelium and normal epithelium, but for recognition of more subtle differences within a Barrett's esophagus, the probes need to be optimized further to collect only the Raman signal from the first 100 to 200 micron, which includes the normal epithelium. The probes used in this study lacked appropriate reproducibility in performance, therefore generating the need of extensive software filtering. Even after filtering there is some residual probe influence left, as can be seen from comparing the spectra from day 5 and 12 in figure 2, row D. Since this way of filtering can also cause loss of relevant biological information, the use of probes with more reproducible performance would permit less filtering and consequently would provide more detailed information.

Another disadvantage of this type of fiber optic probes is the limited collection efficiency. Higher collection efficiency would permit shorter integration times. In a previous study, integration times as short as ten seconds were sufficient to classify spectra of normal and dysplastic rat palate after a discriminating model was achieved, with the same type of probes (9). However for surveillance of human Barrett's esophagus, a further reduction in signal collection time to 1-2 s is essential, since larger areas of the esophagus have to be examined (14). Improvements in the probe design and efficiency of the in vivo Raman set up should permit clinical Raman application, integrated in the routine endoscope of the gastroscopist.

REFERENCES

1. Spechler, S. J. and R. K. Goyal (1996) The columnar-lined esophagus, intestinal metaplasia, and Norman Barrett. *Gastroenterology.* **110**, 614-621.

2. Hameeteman, W., G. N. Tytgat, H. J. Houthoff and J. G. van den Tweel (1989) Barrett's esophagus: development of dysplasia and adenocarcinoma. *Gastroenterology.* **96**, 1249-56.

3. Blot, W. J., S. S. Devesa, R. W. Kneller and J. F. Fraumeni, Jr. (1991) Rising incidence of adenocarcinoma of the esophagus and gastric cardia. *JAMA.* **265**, 1287-9.

4. Macfarlane, G. J. and P. Boyle (1994) The epidemiology of oesophageal cancer in the UK and other European countries. *J R Soc Med.* **87**, 334-7.

5. Lightdale, C. J. (1999) Esophageal cancer. American College of Gastroenterology. *Am J Gastroenterol.* **94**, 20-9.

6. Georgakoudi, I., B. C. Jacobson, J. Van Dam, V. Backman, M. B. Wallace, M. G. Muller, Q. Zhang, K. Badizadegan, D. Sun, G. A. Thomas, L. T. Perelman and M. S. Feld (2001) Fluorescence, reflectance, and light-scattering spectroscopy for evaluating dysplasia in patients with Barrett's esophagus. *Gastroenterology.* **120**, 1620-1629.

7. Dacosta, R. S., B. C. Wilson and N. E. Marcon (2002) New optical technologies for earlier endoscopic diagnosis of premalignant gastrointestinal lesions. *J Gastroenterol Hepatol.* **17 Suppl**, S85-104.

8. Endlicher, E., R. Knuechel, T. Hauser, R. M. Szeimies, J. Scholmerich and H. Messmann (2001) Endoscopic fluorescence detection of low and high grade dysplasia in Barrett's oesophagus using systemic or local 5-aminolaevulinic acid sensitisation. *Gut.* **48**, 314-319.

9. Nijssen, A., T. C. Bakker Schut, F. Heule, P. J. Caspers, D. P. Hayes, M. H. Neumann and G. J. Puppels (2002) Discriminating basal cell carcinoma from its surrounding tissue by Raman spectroscopy. *J Invest Dermatol.* **119**, 64-9.

10. Bakker Schut, T. C., M. J. Witjes, H. J. Sterenborg, O. C. Speelman, J. L. Roodenburg, E. T. Marple, H. A. Bruining and G. J. Puppels (2000) In vivo detection of dysplastic tissue by Raman spectroscopy. *Anal Chem.* **72**, 6010-8.

11. Mahadevan-Jansen, A., M. F. Mitchell, N. Ramanujam, A. Malpica, S. Thomsen, U. Utzinger and R. Richards-Kortum (1998) Near-infrared Raman spectroscopy for in vitro detection of cervical precancers. *Photochem Photobiol.* **68**, 123-32.

12. Stone, N., C. Kendall, N. Shephard, P. Crow and H. Barr (2002) Near infrared Raman spectroscopy for the classification of epithelial precancers and cancers. *J of Raman spectroscopy.* **33**, 564-573.

13. Bakker Schut, T. C., N. Stone, C. Fulljames, H. Barr, H. A. Bruining and G. J. Puppels (2000) Progress in the detection of neoplastic progress and cancer by Raman spectroscopy. In Biomedical Spectroscopy:Vibrational Spectroscopy and Other Novel Techniques Vol. 3918. (Edited by A. Mahadevan-Jansen and G. J. Puppels), pp. 106-113. SPIE.

14. Shim, M. G., L. M. Song, N. E. Marcon and B. C. Wilson (2000) In vivo near-infrared Raman spectroscopy: demonstration of feasibility during clinical gastrointestinal endoscopy. *Photochem Photobiol.* **72**, 146-50.

15. Wolthuis, R., T. C. Bakker Schut, P. J. Caspers, H. P. J. Buschman, T. J. Romer, H. A. Bruining and G. J. Puppels (1999) Raman Spectroscopic Methods for In Vitro and In Vivo Tissue Characterization. In Fluorescent and luminescent probes for biological activity Vol. (Edited by W. T. Mason), pp. 433-455. San Diego: Academic Press.

16. Pera, M., M. J. Brito, R. Poulsom, E. Riera, L. Grande, A. Hanby and N. A. Wright (2000) Duodenal-content reflux esophagitis induces the development of glandular metaplasia and adenosquamous carcinoma in rats. *Carcinogenesis.* **21**, 1587-91.

17. Boogert, J. v. d., A. B. Houtsmuller, F. W. d. Rooij, R. W. d. Bruin, P. D. Siersema and R. v. van Hillegersberg (1999) Kinetics, localization, and mechanism of 5-aminolevulinic acid-

induced porphyrin accumulation in normal and Barrett's-like rat esophagus. *Lasers Surg Med.* **24**, 3-13.

18. Levrat, M., R.Lambert, G.Kirschbaum (1962) Esophagitis produced by reflux of duodenal contents in rats. *Am J Dig Dis.* **7**, 564-573.

19. Miwa, K., H. Sahara, M. Segawa, S. Kinami, T. Sato, I. Miyazaki and T. Hattori (1996) Reflux of duodenal or gastro-duodenal contents induces esophageal carcinoma in rats. *Int J Cancer.* **67**, 269-74.

20. Shim, M. G., B. C. Wilson, E. T. Marple and M. Wach (1999) Study of Fiber-Optic Probes for in Vivo Medical Raman Spectroscopy. *Appl. Spectrosc.* **53**, 619-627.

21. Shim, M. G. and B. C. Wilson (1996) The effects of ex vivo handling procedures on the near-infrared Raman spectra of normal mammalian tissues. *Photochem Photobiol.* **63**, 662-71.

22. Poll, S. W. v. d., D. J. Delsing, J. W. Jukema, H. M. Princen, L. M. Havekes, G. J. Puppels and A. van der Laarse (2002) Raman spectroscopic investigation of atorvastatin, amlodipine, and both on atherosclerotic plaque development in APOE*3 Leiden transgenic mice. *Atherosclerosis.* **164**, 65-71.

23. Maquelin, K., L. P. Choo-Smith, T. van Vreeswijk, H. P. Endtz, B. Smith, R. Bennett, H. A. Bruining and G. J. Puppels (2000) Raman spectroscopic method for identification of clinically relevant microorganisms growing on solid culture medium. *Anal Chem.* **72**, 12-9.

24. Tabachnick, B. and L. Fidell (1989) Using Multivariate Statistics. In Vol. (Edited by pp. 507. HarperCollins Publishers, New York.

25. Barrett, N. (1950) Chronic peptic ulcer of the oesophagus and "oesophagitis". *Br J Surg.* **38**, 175-182.

Chapter 8

Summary and general conclusions

I.A. Boere, J. Kluin, H.W. Tilanus, R.W.F. de Bruin

Department of Surgery

SUMMARY

The incidence of esophageal carcinoma has been steadily increasing in many western countries in the last 30 years (1). Despite new developments in diagnosis and treatment, 5 year survival rates are still poor. A current hypothesis is that the majority of the adenocarcinomas arise in Barrett's esophagus (BE), following a sequence of metaplasia through dysplasia to carcinoma (2). The presence of BE increases the risk of esophageal adenocarcinoma 30-125 fold, with an estimated incidence of 0.5% per patient per year (3). BE is characterized by the presence of columnar epithelium with intestinal metaplasia in the distal esophagus (4). Whereas BE is a histological diagnosis, endoscopic techniques are used for detection and surveillance. When BE progresses to high grade dysplasia or adenocarcinoma, esophageal resection is the treatment of choice in patients fit for surgery. This is complicated by the fact that high grade dysplasia usually occurs at higher age (5). However, most patients with esophageal adenocarcinoma have not been recognized with BE previously, and the majority of patients with BE will not develop esophageal adenocarcinoma (6). Therefore less invasive endoscopic therapy has been used for treatment of BE with dysplasia for patients unfit for surgery. Also, endoscopic therapy has been used as preventive strategy for development of esophageal cancer by ablation of the premalignant Barrett's epithelium.

Photodynamic therapy (PDT) with use of 5-aminolevulinic acid (ALA) is a relatively new treatment option ideally leading to endoscopic ablation of the Barrett's mucosa. PDT involves systemic administration of a photosensitizer to accumulate in the target tissue. Subsequent irradiation with light of a specific wavelength, absorbed by the photosensitizer, results in a photochemical reaction that destroys the sensitized tissue. ALA is not a photosensitizer by itself, but an endogenously occurring intermediary in the haem biosynthetic pathway. It is metabolized at tissue level to the photoactive agent protoporphyrin IX (PpIX). ALA induced PpIX accumulates in tumour tissue, glands and cells that line surfaces, such as gastrointestinal mucosa (7, 8). At present, results of clinical ALA-PDT are suboptimal (9-12). Removal of dysplasia has been successful, but residual BE remains. Complete ablation of all BE can be achieved in 19% after one ALA-PDT treatment, and in 82-90% in combination with argon plasma coagulation (9). During follow up, buried residual Barrett's epithelium is found under normal appearing mucosa in 4-6% of patients after ALA-

PDT (13, 14). In order to optimize ALA-PDT for treatment of BE, more accurate light dosimetry and monitoring of PpIX fluorescence decay may be valuable tools. Light dosimetry, standardized for all patients in vivo and adjusted to tissue optical properties, may improve outcome of ALA-PDT. With PpIX fluorescence monitoring, ALA-PDT can be monitored during treatment. In this thesis, these parameters have been studied using the rat as experimental model.

In **chapter 1** an overview is given on the use of ALA-PDT for Barrett's esophagus. It has been found that PpIX concentration was highest in esophageal mucosa. In BE, PpIX also preferentially accumulates in the epithelium, without discriminating between normal and BE epithelium (7). This makes ALA an ideal photosensitizer to use for treatment of BE. The position of the laser fibre determines the area of treatment. It has been shown that the irradiation parameters and dosage interval determine to a great extent the success or failure of ALA-PDT (15).

In **chapter 3** we studied two different animal models for BE. The effects of duodenal reflux were examined both in rat and opossum (Monodelphis domestica) esophagus. Opossums have a gastrointestinal tract that more resembles the human situation with non-keratinitized squamous epithelium in the esophagus, esophageal glands and a gall bladder. Twelve months after the esophagojejunostomy all rats showed microscopic and macroscopic specialised intestinal metaplasia, whereas opossums (with or without cholecystectomy) did not develop Barrett's esophagus, and showed only marginal changes. In rats, the duration of the reflux correlated with the length of specialised intestinal metaplasia, and the microscopic appearance well resembled human Barrett's esophagus. Although the rat model is suitable for investigating experimental treatment modalities for BE, extrapolating observations concerning the pathogenesis of Barrett's esophagus from rat studies to the human situation is in our view controversial due to differences in anatomy and histology of the upper gastrointestinal tract. The absence of Barrett's esophagus in opossums following longstanding reflux precludes its use in pathogenetic, etiologic or therapeutic studies on Barrett's esophagus**.**

Data from human and animal studies have identified bile reflux as a factor that contributes to the development of BE (16, 17). However the role of the primary and

secondary bile acids in the pathogenesis of BE has not yet been elucidated. Increased secondary bile acids have been observed in patients with BE (18) Therefore in **chapter 4**, it was determined whether the development of BE in a rat model is associated with altered bile acid composition and bacterial overgrowth in the small intestine. Rats underwent esophagojejunostomy and gastrectomy, and length of BE, bile acid composition in the common bile duct, and bacterial colonisation of jejunum, ileum, cecum and colon were determined after 6 months. BE developed in 23/24 rats. The presence of BE was associated with a fivefold increased concentration of the secondary bile acid deoxycholic acid (DCA) in the EJ-group compared to the sham operated control group. The length of BE correlated with the increase in DCA concentration. The jejunum and ileum of rats with esophagojejunostomy was colonised by *Clostridium perfringens* and *Bacteroides* spp. From this study we conclude that the development of BE is associated with a changed bile acid composition and overgrowth of the small intestine with bacteria capable of metabolising bile acids.

ALA-PDT FOR BARRETT'S ESOPHAGUS

Chapter 5 investigates the possibility of monitoring in situ dosimetry and PpIX fluorescence photobleaching in the normal rat esophagus during 5-aminolevulinic acid photodynamic therapy. Experimental therapies for Barrett's esophagus like ALA-PDT aim to ablate the premalignant Barrett's epithelium. However, the reproducibility of the effects should be improved to optimize treatment outcome (19). Also in clinical ALA-PDT, large differences in total measured fluence and fluence rate in situ have been found between and within patients (20). Accurate irradiation with light of a proper wavelength (633 nm), fluence and fluence rate, has shown to be critical for successful ALA-PDT. In the present study, in situ light dosimetry was used to adjust the fluence rate measured within the esophagus for individual animals and monitored PpIX fluorescence photobleaching simultaneously. Animals were irradiated with an in-situ measured fluence rate of 75 mW cm^{-2} and a fluence of 54 J cm^{-2}. This more accurate method of light dosimetry did not decrease the variation in tissue response. Large differences were also observed in the dynamics of PpIX fluorescence photobleaching in animals that received the same measured illumination parameters. We found that higher PpIX fluorescence photobleaching rates corresponded with more epithelial damage, whereas lower rates corresponded with no response. A two-

phased decay in PpIX fluorescence could be identified in the response group, with a rapid initial phase followed by a slower rate of photobleaching. Non-responders did not show the rapid initial decay and had a significantly lower rate of photobleaching during the second phase of the decay. Therefore, the amount and rate of PpIX fluorescence photobleaching may well be indicative of the tissue response to ALA-PDT.

In **chapter 6**, the same in situ light dosimetry technique and PpIX fluorescence measurements were used for ALA-PDT in rats with BE. The fluence and fluence rate were standardized in vivo and the PpIX fluorescence was measured simultaneously at the esophageal wall during ALA-PDT. In concordance with the findings in chapter 4, large differences were observed in the dynamics of PpIX fluorescence photobleaching in different animals. A high PpIX fluorescence photobleaching rate corresponded with tissue ablation, whereas a low rate corresponded with no damage to the epithelium. Differences in tissue oxygenation or vascular flow at the site of treatment have previously been identified as factors that determine the treatment outcome (21). In the present study this could not be confirmed by additional experiments. In conclusion, in vivo dosimetry is feasible in heterogeneous tissue such as Barrett's esophagus and the kinetics of PpIX fluorescence photobleaching is a useful measure to predict the tissue response to ALA-PDT.

IN SEARCH OF A NEW DIAGNOSTIC TOOL FOR BE

Patients with BE undergo regular endoscopic surveillance with randomly taken biopsies to detect the presence of high-grade dysplasia or carcinoma. Sampling errors and observer variation, inherent to such a surveillance protocol, warrant the search for other detection methods (22, 23). Raman spectroscopy is a non-invasive optical spectroscopic technique that provides detailed information about the molecular composition and structure of tissues. Changes in molecular composition in tissues as a consequence of pathologic processes, can thus be recognized. For clinical application of Raman spectroscopy, thin and flexible fibre optic probes can be used that fit in the auxiliary channel of an endoscope. In the study described in **chapter 7**, a multivariate classification model was developed for detection of Barrett's epithelium, based on ex vivo Raman spectra of the rat esophagus. The model yields a spectral discriminant that best separates the two groups. To facilitate interpretation

of this discriminant, we obtained Raman spectra from tissue sections of normal esophageal epithelium, keratin and muscle layer using a confocal Raman microscope. After elimination of interfering background signal contributions from the different probes using a vector-correction procedure, we could discriminate between Barrett's and normal epithelium with accuracy higher than 93 percent. In future, Raman spectroscopy using a flexible fiberoptic probe may be valuable for detection of BE and dysplasia in vivo. In this study, we show that the Raman signal acquired with such a probe, provides the information needed to distinguish between Barrett's and squamous epithelium.

SAMENVATTING

De incidentie van het adenocarcinoom van de slokdarm is de laatste 30 jaar in Westerse landen sterk gestegen (1). Ondanks nieuwe ontwikkelingen in diagnose en behandeling, is de 5-jaars overleving van patiënten met adenocarcinoom van de slokdarm nog immer laag. Er wordt aangenomen dat de meeste adenocarcinomen ontstaan in Barrett's oesofagus (BE). BE kan via een sequentie van laaggradige, en hooggradige dysplasie uiteindelijk maligne ontaarden in een adenocarcinoom (2). De aanwezigheid van Barrett slijmvlies in de slokdarm verhoogt de kans op het krijgen van adenocarcinoom met 30 – 125 maal en patiënten met BE hebben 0,5% per jaar kans op een oesofagus adenocarcinoom (3). BE wordt gekenmerkt door intestinale metaplasie met cilinder epitheel van de mucosa met aanwezigheid van slijmbekercellen (4). BE is een histologische diagnose die wordt gesteld in endoscopisch verkregen biopten van slokdarm mucosa. Voor BE is geen geaccepteerde behandeling voorhanden. Als BE veranderd in hooggradige dysplasie of adenocarcinoom, dan heeft slokdarm resectie de voorkeur, indien dit mogelijk is. Meestal treedt hooggradige dysplasie echter op hogere leeftijd op (5). Daarnaast is bij de meeste patiënten die zich presenteren met een adenocarcinoom voorheen geen BE ontdekt, en overlijden de meeste patiënten met BE niet aan een oesofagus adenocarcinoom (6). Om deze redenen is er behoefte aan een minder invasieve, endoscopische behandeling voor BE met hooggradige dysplasie. Verder zou de aandacht kunnen verschuiven naar een meer preventieve therapie, namelijk ablatie van het gehele premaligne Barrett epitheel.

Fotodynamische therapie (PDT) met 5-aminolevulinezuur (ALA) als fotosensitizer is een relatief nieuwe optie voor endoscopische ablatie van BE. Bij PDT wordt een fotosensitizer systemisch toegediend. Daaropvolgende belichting met laserlicht van de juiste golflengte veroorzaakt een fotochemische reactie waarbij het belichte weefsel wordt vernietigd. ALA is zelf geen fotosensitizer, maar een lichaamseigen intermediair in de haemsynthese. Toediening van ALA leidt tot productie van de lichtgevoelige stof protoporfyrine IX (PpIX). ALA geïnduceerde PpIX productie vindt selectief plaats in tumoren en weefsels die oppervlakken bekleden, zoals de gastrointestinale mucosa (7, 8). De resultaten van ALA-PDT voor BE in de mens zijn nog niet optimaal (9-12). Dysplasie wordt doorgaans verwijderd, maar ablatie van BE is niet radicaal, en cellen, of eilandjes BE blijven doorgaans achter na behandeling. Complete ablatie van het Barrett epitheel wordt bij 19% bereikt na 1 behandeling met ALA-PDT. Na multipele sessies en in combinatie met argon plasma coagulatie verbetert dit tot 82-90% (9). Om de resultaten te verbeteren zou zorgvuldig monitoren van de hoeveelheid toegediend laser licht (dosimetrie), en afname van de PpIX fluorescentie tijdens de belichting waardevolle parameters kunnen zijn. In dit proefschrift wordt de waarde van deze parameters dan ook onderzocht.

In **hoofdstuk 1** wordt een overzicht gegeven van het gebruik van ALA-PDT voor BE. ALA geïnduceerde PpIX concentraties zijn het hoogst in de mucosa, en lager in submucosa en muscularis (7). De productie van PpIX vindt zowel in de normale, als in Barrett mucosa plaats. Deze selectiviteit voor de mucosa maakt ALA een geschikte fotosensitizer voor BE (15). Om de resultaten te optimaliseren moeten aanpassingen van de belichtingsparameters en timing van de belichting verder worden onderzocht.

In **hoofdstuk 3** worden twee diermodellen voor BE beschreven. Het effect van duodenale reflux na aanleggen van een oesofagojejunostomie werd onderzocht in de rat en de opossum (*Monodelphis domestica*). De tractus digestivus van opossums lijkt anatomisch meer op die van de mens dan van de rat. De opossum slokdarm heeft niet-verhoornend plaveiselcelepitheel en submucosale klieren. Bovendien heeft de opossum een galblaas. Twaalf maanden na oesofagojejunostomie hadden alle ratten macroscopisch en microscopisch intestinale metaplasie. Opossums ontwikkelden geen BE, ongeacht of ze een galblaasresectie hadden ondergaan. In

ratten was er een correlatie tussen de duur van de reflux en de lengte van het segment gespecialiseerde intestinale metaplasie. De microscopische anatomie hiervan kwam overeen met humaan Barrett slijmvlies. Wij concluderen dat de rat een geschikt model is om behandelingsmodaliteiten voor BE te bestuderen. Gezien de grote verschillen in anatomie tussen mens en rat is extrapolatie van etiologische en pathogenetische mechanismen controversieel. De afwezigheid van BE en reflux oesofagitis maakt de opossum ongeschikt als proefdiermodel voor BE.

In diverse dierexperimentele en humane studies is gebleken dat gallige reflux een rol speelt bij de ontwikkeling van Barrett oesofagus (16, 17). Echter, de relatieve bijdrage van de primaire versus de secundaire galzuren, gemetaboliseerd door bepaalde bacteriën, is nog niet duidelijk. Bij patiënten met Barrett oesofagus is de concentratie secundaire galzuren verhoogd (18). In **hoofdstuk 4** wordt daarom onderzocht of de ontwikkeling van Barrett oesofagus geassocieerd is met een verandering in de samenstelling van de galzuurpool en of er sprake is van bacteriële overgroei in de dunne darm. In een groep ratten werd een oesofagojejunostomie met gastrectomie verricht. Na 6 maanden werden de lengte van het ontstane segment Barrett oesofagus en de galzuurcompositie in de ductus choledochus gemeten en werd de kolonisatie door bacteriën in het jejunum, ileum, coecum en colon bepaald. In 23 van de 24 ratten ontstond Barrett oesofagus. De aanwezigheid van Barrett oesofagus was geassocieerd met een vijfvoudige toename in concentratie van het secundaire galzuur deoxycholaat (DCA) in de oesofagojejunostomie groep in vergelijking met de controle groep. De lengte van het segment Barrett oesofagus correleerde met de mate van DCA verhoging. Het jejunum en ileum van de ratten met een oesofagojejunostomie bleken gekoloniseerd met de bacteriën *Clostridium perfringens* and *Bacteroides* spp. Concluderend kan worden gesteld dat de ontwikkeling van Barrett oesofagus geassocieerd is met een verandering in galzuursamenstelling en met overgroei van bacteriën in de dunne darm. Deze bacteriën zijn in staat om galzuren te om te zetten in secundaire galzuren.

ALA-PDT VOOR BARRETT OESOFAGUS

In **hoofdstuk 5** werd onderzocht of het mogelijk is in situ dosimetrie te verrichten en PpIX fluorescentie in de normale rattenslokdarm tijdens fotodynamische therapie (PDT) te meten. Met deze endoscopische therapie wordt ablatie van het premaligne

Barrett epitheel beoogd. De reproduceerbaarheid van de resultaten zijn tot op heden nog onvoldoende en daarnaast is het effect vaak niet compleet (19). Bij ALA-PDT, verricht in studieverband bij patiënten met BE worden grote verschillen gezien in de gemeten lichtdosis (fluence) en intensiteit (fluence rate) tussen patiënten en binnen een individu (20). Eerder bleek accurate illuminatie met licht van de juiste golflengte (633 nm), fluence en fluence rate, van groot belang voor het succes van ALA-PDT (15). In de huidige studie werd dosimetrie verricht in de rattenslokdarm, en werden de fluence en fluence rate aangepast tot een fluence van 54 J cm^{-2} en fluence rate van 75 mW cm^{-2}. Daarnaast werd PpIX fluorescentie tijdens de belichting gemeten. Echter, met behulp van deze nauwkeuriger dosimetrie werd de variatie in weefseleffecten van ALA-PDT niet verminderd. Eveneens werden grote verschillen gezien in de kinetiek van PpIX fluorescentie afname (photobleaching), bij dezelfde gemeten belichtingsparameters. Hogere PpIX photobleaching rates correleerden met meer epitheelschade, terwijl lagere PpIX photobleaching rates correleerden met geen respons. De curve van de PpIX fluorescentie tijdens belichting bestond uit 2 fasen, een snelle initiële daling in PpIX fluorescentie gevolgd door een langzamere daling. Non-responders misten de snelle eerste fase en hadden een vlakkere curve over de rest van het PpIX photobleaching traject in de tweede fase. De hoeveelheid en snelheid van PpIX photobleaching tijdens ALA-PDT lijken daarom goede parameters voor de weefselrespons op ALA-PDT.

Dezelfde in situ dosimetrie en PpIX monitoring technieken werden in **hoofdstuk 6** gebruikt voor ALA-PDT bij ratten met Barrett oesofagus. Fluence en fluence rate werden in vivo gestandaardiseerd en PpIX fluorescentie werd tijdens therapie gemeten in de rattenoesofagus. Ook in deze experimenten werden grote verschillen gezien in de kinetiek van PpIX photobleaching tussen de verschillende dieren. Snelle PpIX photobleaching correspondeerde met ablatie van het epitheel, langzame PpIX photobleaching correspondeerde met geen epitheelschade. Met additionele experimenten kon niet worden aangetoond dat deze verschillen berustten op verschillen in weefseloxygenatie of doorbloeding (21). Concluderend bleek in situ dosimetrie en PpIX monitoren mogelijk in de rattenslokdarm, en bleek de kinetiek van PpIX photobleaching een bruikbare parameter om de respons van ALA-PDT te voorspellen.

RAMAN SPECTROSCOPIE

Patiënten met BE worden endoscopisch gecontroleerd, waarbij random biopten uit de slokdarm worden genomen om de aanwezigheid van hooggradige dysplasie of carcinoom op te sporen. Inherent aan een dergelijk controle protocol zijn sampling errors en observer variatie (22, 23), wat een onderzoek naar meer objectieve detectiemethoden noodzakelijk maakt. Raman spectroscopie is een niet invasieve optische spectroscopie techniek die gedetailleerde informatie kan geven over de moleculaire samenstelling van weefsel. Veranderingen in moleculaire samenstelling ten gevolge van pathologische veranderingen kunnen dan ook worden herkend. Om Raman spectroscopie klinisch te kunnen toepassen kunnen dunne, flexibele fiberoptische probes worden gebruikt die door het hulpkanaal van een endoscoop ingebracht kunnen worden. In de studie beschreven in **hoofdstuk 7** is een multivariaat classificeringssysteem ontwikkeld om Barrett oesofagus te kunnen onderscheiden van de normale slokdarm mucosa, gebaseerd op ex vivo Raman spectra van de ratten slokdarm. Dit model levert een discriminant op van de spectra waarmee de spectra optimaal gescheiden kunnen worden. Om de interpretatie van deze discriminant te vergemakkelijken zijn Raman spectra opgenomen van oesofagus epitheel, keratine en spier. Na eliminatie van interfererende achtergrond signalen van de verschillende probes met behulp van een vector correctie procedure, was het mogelijk Barrett mucosa van normale mucosa te onderscheiden met een nauwkeurigheid van meer dan 93%. In de toekomst zou Raman spectroscopie via een flexibele fiberoptische probe gebruikt kunnen worden voor detectie van Barrett oesofagus en dysplasie in vivo. Met dit onderzoek werd aangetoond dat het Raman signaal gedetecteerd met een dergelijke probe voldoende informatie oplevert om onderscheid te maken tussen Barrett en normaal weefsel.

REFERENCES

1. Devesa, S. S., W. J. Blot and J. F. Fraumeni, Jr. (1998) Changing patterns in the incidence of esophageal and gastric carcinoma in the United States. *Cancer.* **83**, 2049-53.

2. Jankowski, J. A., N. A. Wright, S. J. Meltzer, G. Triadafilopoulos, K. Geboes, A. G. Casson, D. Kerr and L. S. Young (1999) Molecular evolution of the metaplasia-dysplasia-adenocarcinoma sequence in the esophagus. *Am J Pathol.* **154**, 965-73.

3. Hage, M., P. D. Siersema, H. van Dekken, E. W. Steyerberg, J. Dees and E. J. Kuipers (2004) Oesophageal cancer incidence and mortality in patients with long-segment Barrett's oesophagus after a mean follow-up of 12.7 years. *Scand J Gastroenterol.* **39**, 1175-9.

4. Offerhaus, G. J., P. Correa, S. van Eeden, K. Geboes, P. Drillenburg, M. Vieth, M. L. van Velthuysen, H. Watanabe, P. Sipponen, F. J. ten Kate, F. T. Bosman, A. Bosma, A. Ristimaki, H. van Dekken, R. Riddell and G. N. Tytgat (2003) Report of an Amsterdam working group on Barrett esophagus. *Virchows Arch.* **443**, 602-8.

5. Boogert, J. v. d., R. v. Hillegersberg, R. W. d. Bruin, H. W. Tilanus and P. D. Siersema (1998) Barrett's oesophagus: pathophysiology, diagnosis, and management. *Scand J Gastroenterol.* **33**, 449-53.

6. Macdonald, C. E., A. C. Wicks and R. J. Playford (2000) Final results from 10 year cohort of patients undergoing surveillance for Barrett's oesophagus: observational study. *Bmj.* **321**, 1252-5.

7. Boogert, J. v. d., A. B. Houtsmuller, F. W. d. Rooij, R. W. d. Bruin, P. D. Siersema and R. v. van Hillegersberg (1999) Kinetics, localization, and mechanism of 5-aminolevulinic acid-induced porphyrin accumulation in normal and Barrett's-like rat esophagus. *Lasers Surg Med.* **24**, 3-13.

8. Hinnen, P., F. W. de Rooij, E. M. Terlouw, A. Edixhoven, H. van Dekken, R. van Hillegersberg, H. W. Tilanus, J. H. Wilson and P. D. Siersema (2000) Porphyrin biosynthesis in human Barrett's oesophagus and adenocarcinoma after ingestion of 5-aminolaevulinic acid. *Br J Cancer.* **83**, 539-43.

9. Hage, M., P. D. Siersema, H. van Dekken, E. W. Steyerberg, J. Haringsma, W. van de Vrie, T. E. Grool, R. L. van Veen, H. J. Sterenborg and E. J. Kuipers (2004) 5-aminolevulinic acid photodynamic therapy versus argon plasma coagulation for ablation of Barrett's oesophagus: a randomised trial. *Gut.* **53**, 785-90.

10. Ackroyd, R., C. J. Kelty, N. J. Brown, T. J. Stephenson, C. J. Stoddard and M. W. Reed (2003) Eradication of dysplastic Barrett's oesophagus using photodynamic therapy: long-term follow-up. *Endoscopy.* **35**, 496-501.

11. Kelty, C. J., R. Ackroyd, N. J. Brown, T. J. Stephenson, C. J. Stoddard and M. W. Reed (2004) Endoscopic ablation of Barrett's oesophagus: a randomized-controlled trial of photodynamic therapy vs. argon plasma coagulation. *Aliment Pharmacol Ther.* **20**, 1289-96.

12. Ackroyd, R., N. J. Brown, M. F. Davis, T. J. Stephenson, S. L. Marcus, C. J. Stoddard, A. G. Johnson and M. W. Reed (2000) Photodynamic therapy for dysplastic Barrett's oesophagus: a prospective, double blind, randomised, placebo controlled trial. *Gut.* **47**, 612-617.

13. Hage, M., P. D. Siersema, K. J. Vissers, E. W. Steyerberg, J. Haringsma, E. J. Kuipers and H. van Dekken (2005) Molecular evaluation of ablative therapy of Barrett's oesophagus. *J Pathol.* **205**, 57-64.

14. Gossner, L., M. Stolte, R. Sroka, K. Rick, A. May, E. G. Hahn and C. Ell (1998) Photodynamic ablation of high-grade dysplasia and early cancer in Barrett's esophagus by means of 5-aminolevulinic acid. *Gastroenterology.* **114**, 448-55.

15. Boogert, J. v. d., R. v. Hillegersberg, H. J. v. Staveren, R. W. d. Bruin, H. v. Dekken, P. D. Siersema and H. W. Tilanus (1999) Timing of illumination is essential for effective and safe photodynamic therapy: a study in the normal rat oesophagus. *Br J Cancer.* **79**, 825-830.

16. Pera, M., M. J. Brito, R. Poulsom, E. Riera, L. Grande, A. Hanby and N. A. Wright (2000) Duodenal-content reflux esophagitis induces the development of glandular metaplasia and adenosquamous carcinoma in rats. *Carcinogenesis.* **21**, 1587-91.

17. Richter, J. E. (2000) Importance of bile reflux in Barrett's esophagus. *Dig Dis.* **18**, 208-16.

18. Nehra, D., P. Howell, C. P. Williams, J. K. Pye and J. Beynon (1999) Toxic bile acids in gastro-oesophageal reflux disease: influence of gastric acidity. *Gut.* **44**, 598-602.

19. Siersema, P. D. (2005) Photodynamic therapy for Barrett's esophagus: not yet ready for the premier league of endoscopic interventions. *Gastrointest Endosc.* **62**, 503-7.

20. Van Veen, R. L., M. C. Aalders, K. L. Pasma, P. D. Siersema, J. Haringsma, W. Van De Vrie, E. E. Gabeler, D. J. Robinson and H. J. Sterenborg (2002) In situ light dosimetry during photodynamic therapy of Barrett's esophagus with 5-aminolevulinic acid. *Lasers Surg Med.* **31**, 299-304.

21. Wang, H. W., M. E. Putt, M. J. Emanuele, D. B. Shin, E. Glatstein, A. G. Yodh and T. M. Busch (2004) Treatment-induced changes in tumor oxygenation predict photodynamic therapy outcome. *Cancer Res.* **64**, 7553-61.

22. Montgomery, E. (2005) Is there a way for pathologists to decrease interobserver variability in the diagnosis of dysplasia? *Arch Pathol Lab Med.* **129**, 174-6.

23. Ormsby, A. H., R. E. Petras, W. H. Henricks, T. W. Rice, L. A. Rybicki, J. E. Richter and J. R. Goldblum (2002) Observer variation in the diagnosis of superficial oesophageal adenocarcinoma. *Gut.* **51**, 671-6.

DANKWOORD

Onderzoek wordt gelukkig niet alleen gedaan. Daarom wil ik graag dit proefschrift besluiten met het bedanken van de mensen die hebben geholpen met het tot stand komen van dit proefschrift en mijn promotie. Behalve samenwerking en hulp bij de diverse experimenten is ook de gezelligheid en morele steun van een aantal mensen onontbeerlijk geweest. Een aantal mensen zou ik graag in het bijzonder willen noemen.

Ron de Bruin, beste co-promotor. Vanaf het begin was je betrokken bij dit onderzoek en het is dan ook een beetje je kindje geweest. Samen hebben we de experimenten bedacht die ons antwoorden zouden moeten geven, maar die natuurlijk ook meer vragen oproepen. Door je ervaring heb je mij geholpen tegenslagen te relativeren en door te zetten. Ook als mens ben je heel compleet, je bent voor mij een van de belangrijke factoren aan de gezelligheid, diepgang en Chinese lunches met het lab geweest.

Professor Tilanus, uw inbreng is altijd een inspiratie geweest. Met behulp van een paar korte zinnen die precies de kern bevatten of een paar bemoedigende woorden, kon ik als jonge arts onderzoeker weer verder. Ik wil u graag bedanken dat u mijn promotor wil zijn, voor uw luisterend oor, commentaar en energie.

Jolanda Kluin, je bent mijn grote voorganger van dit onderzoek naar fotodynamische therapie voor Barrett oesofagus. Je stond samen met Ron en Richard van Hillegersberg aan de basis van dit onderzoek en aangestoken door jullie enthousiasme en nieuwsgierigheid naar bevindingen ben ik aan dit onderzoek begonnen. Daarnaast ben je door je enorme werklust, en efficiëntie mijn voorbeeld geweest, hoewel ik daar natuurlijk niet altijd aan kon voldoen. Hartelijk dank voor je inspiratie en begeleiding.

Geachte commissieleden, Prof. dr. J.H.P. Wilson, ik voel me vereerd dat u in mijn commissie wilde plaatsnemen. Ik hoop wanneer ik weer werkzaam ben in het Erasmus MC bij de Interne Geneeskunde nog heel veel van u te leren.

Prof. dr. M.J. van Gemert, Prof. dr. E.J. Kuipers en Prof. dr. H. Obertop, ik vind het een eer dat u in mijn commissie wil plaats nemen, hartelijk dank daarvoor.

Dr. H.J.C.M. Sterenborg, beste Dick, hartelijk dank dat je in de commissie wilde plaats nemen. Jullie groep is onder jouw leiding gedurende het onderzoek en daarnaast een grote inspiratie voor mij geweest.

Dr. P.D. Siersema, ik begon tegelijk samen met een van jouw arts onderzoekers, Rudy Sital aan het onderzoek. De interesses overlapten elkaar, hetgeen altijd heeft geresulteerd in een prettige samenwerking. Er komt nog een stukje aan!

Tijdens dit onderzoek zijn de bijdragen van de Fotodynamische Therapie-groep erg belangrijk geweest, Dominic Robinson, Riëtte de Bruijn, Angelique van der Ploeg, Robert van Veen en Dick Sterenborg. Zonder jullie zou ik op 15 september niet promoveren. Met Riette en Angelique waren de experimenten geweldig leuk om te doen. And Dominic, I have learnt so much during the preparation of our manuscripts. Hartelijk dank voor jullie gezelligheid tijdens experimenten, wetenschappelijke vorming en inbreng.

Het Raman lab, Tom Bakker Schut, Rolf Wolthuis, Peter Caspers en Gerwin Puppels, jullie lab was naast het onze gelegen, waardoor we elkaar zeer regelmatig ook buiten experimenten om zagen. Als we ergens hoorden lachen, kwam dat vaak bij jullie vandaan, hetgeen veel zegt over de goede sfeer. Hartelijk dank voor de samenwerking, gezelligheid en enorme inzet van Tom bij het tot stand komen van hoofdstuk 7 en de experimenten die erna volgden.

Jelle Haringsma, bedankt voor je enthousiasme en gezelligheid tijdens de klinische PDT. Ik vond het altijd erg leuk om de klinische variant te zien.

Beste mede onderzoekers, collega's op het chirurgisch en MDL lab: Rudy Sital, Sander ten Raa, Dorine Bax, Turkan Terkivatan, Miranda ten Kate, Helma van Grevenstein, Denis Susa, Pim Burger, Amir Mearadji, Niels van der Kaaij, Fred Bonthuis en Sandra van den Engel. Allemaal hartelijk dank voor de gezelligheid op het lab. Beste Rudy, we hebben veel werk samen gedaan, ratten geopereerd en verzorgd. Ik hoop dat het je goed gaat.

Onderzoek is niet mogelijk zonder financiële steun om de experimenten uit te voeren. De Stichting Erasmus Heelkundig Kankeronderzoek wil ik daarom graag bedanken.

Als paranimfen heb ik twee heel bijzondere mensen gevraagd, Saskia Kwee en Riëtte de Bruijn, ik voel me vereerd dat jullie mijn paranimf willen zijn en naast me

staan op 15 september. Lieve Saskia, wij zijn lange tijd huisgenootjes geweest en nu weer! Je kent me daardoor waarschijnlijk beter dan ik mezelf, ik prijs mezelf gelukkig met zo'n goede vriendin. Lieve Riëtte, met jou heb ik met veel plezier de PDT experimenten gedaan, en hebben we enorm gepriegeld met anesthesie, fibers, probes en plakbandjes. Als dat geen band schept! Ik hoop op een gelukkig leven voor jou met je gezin en binnenkort een promotie!

Sander, Saskia, Mattijs, Veerna, Hok, Ilse, Ariën, Damian, Lisette, Tjebbe en Yvette, al sinds de studie vrienden, we hebben samen van alles meegemaakt en elkaar volwassen zien worden. Ik hoop dat deze bijzondere band voor altijd blijft.
Lieve Ronald, bedankt voor alle steun en mooie tijd!
Familie Wormgoor, altijd geïnteresseerd en meelevend, bedankt.
Lieve papa en mama, Victor en familie, dank je wel voor alle onvoorwaardelijke steun en liefde. Er is geen moeder liever en geen vader beter te wensen.
De mensen om mij heen maken het leven mooi. Hartelijk dank voor jullie zelf.

Ingrid Boere

CURRICULUM VITAE

Ingrid Alexandra Boere werd geboren op 15 juni 1976 te Gouda. Het Voorbereidend
Wetenschappelijk Onderwijs volgde zij aan de Samenwerkingsschool te
Waddinxveen. In 1994 startte zij met de studie Geneeskunde aan de Erasmus
Universiteit te Rotterdam. Het afstudeeronderzoek werd verricht op de afdeling
immunologie bij dr. E.P. Prens. In december 2000 behaalde zij het artsexamen (cum
laude). Aansluitend kreeg zij een aanstelling als arts-onderzoeker op het
Laboratorium voor Experimentele Chirurgie, afdeling Heelkunde van het Dijkzigt
Ziekenhuis onder begeleiding van Prof. Dr. H.W. Tilanus, Dr. R.W.F. de Bruin en Dr.
J. Kluin. Hier participeerde zij in de behandeling met klinische fotodynamische
therapie voor Barrett oesofagus en verrichtte zij de onderzoeken zoals beschreven in
dit proefschrift. In 2003 werkte zij als AGNIO op de afdeling Interne Geneeskunde
aan het Erasmus MC en in 2004 startte zij met de opleiding tot internist in het Amphia
Ziekenhuis te Breda (opleiders: Prof. dr. H.A.P. Pols / Dr. J.L.C.M. van Saase en Dr.
C. van Guldener). In 2006 verbleef zij gedurende 8 maanden in het Hadassah
University Hospital te Jeruzalem, Israël, alwaar zij een stage hematologie volgde
(opleider Prof. dr. D. Ben Yehuda). Per september start zij weer in het Erasmus MC
voor het vervolg van de opleiding tot internist.